Received: 9 September 2022 | Revised: 9 February 2023 | Accepted: 14 February 2023

DOI: 10.1111/gcb.16646

Global Change Biology WILEY

REVIEW

From remotely-sensed solar-induced chlorophyll fluorescence to ecosystem structure, function, and service: Part II—Harnessing data

Ying Sun[1] | Jiaming Wen[1] | Lianhong Gu[2] | Joanna Joiner[3] | Christine Y. Chang[4] | Christiaan van der Tol[5] | Albert Porcar-Castell[6] | Troy Magney[7] | Lixin Wang[8] | Leiqiu Hu[9] | Uwe Rascher[10] | Pablo Zarco-Tejada[11] | Christopher B. Barrett[12] | Jiameng Lai[1] | Jimei Han[1] | Zhenqi Luo[1]

[1]School of Integrative Plant Science, Soil and Crop Sciences Section, Cornell University, Ithaca, New York, USA

[2]Environmental Sciences Division and Climate Change Science Institute, Oak Ridge National Laboratory, Oak Ridge, Tennessee, USA

[3]National Aeronautics and Space Administration (NASA) Goddard Space Flight Center (GSFC), Greenbelt, Maryland, USA

[4]US Department of Agriculture, Agricultural Research Service, Adaptive Cropping Systems Laboratory, Beltsville, Maryland, USA

[5]Affiliation Faculty of Geo-Information Science and Earth Observation (ITC), University of Twente, Enschede, The Netherlands

[6]Optics of Photosynthesis Laboratory, Institute for Atmospheric and Earth System Research (INAR)/Forest Sciences, Viikki Plant Science Center (ViPS), University of Helsinki, Helsinki, Finland

[7]Department of Plant Sciences, University of California, Davis, Davis, California, USA

[8]Department of Earth Sciences, Indiana University-Purdue University Indianapolis (IUPUI), Indianapolis, Indiana, USA

[9]Department of Atmospheric and Earth Science, University of Alabama in Huntsville, Huntsville, Alabama, USA

[10]Institute of Bio- and Geosciences, Forschungszentrum Jülich GmbH, Jülich, Germany

[11]School of Agriculture and Food (SAF-FVAS) and Faculty of Engineering and Information Technology (IE-FEIT), University of Melbourne, Melbourne, Victoria, Australia

[12]Charles H. Dyson School of Applied Economics and Management, Cornell University, Ithaca, New York, USA

Correspondence
Ying Sun, School of Integrative Plant Science, Soil and Crop Sciences Section, Cornell University, Ithaca, NY, USA.
Email: ys776@cornell.edu

Funding information
National Aeronautics and Space Administration, Grant/Award Number: 80NSSC20K1263, 80NSSC20K1646, 80NSSC21K0430 and 80NSSC21K1058; National Science Foundation, Grant/Award Number: 1554894 and 1926488; U.S. Department of Agriculture, Grant/Award Number: 1014740; United States Agency for International Development, Grant/Award Number: 7200AA18CA00014

Abstract

Although our observing capabilities of solar-induced chlorophyll fluorescence (SIF) have been growing rapidly, the quality and consistency of SIF datasets are still in an active stage of research and development. As a result, there are considerable inconsistencies among diverse SIF datasets at all scales and the widespread applications of them have led to contradictory findings. The present review is the second of the two companion reviews, and data oriented. It aims to (1) synthesize the variety, scale, and uncertainty of existing SIF datasets, (2) synthesize the diverse applications in the sector of ecology, agriculture, hydrology, climate, and socioeconomics, and (3) clarify how such data inconsistency superimposed with the theoretical complexities laid out in (Sun et al., 2023) may impact process interpretation of various applications and contribute to inconsistent findings. We emphasize that accurate interpretation of the functional relationships between SIF and other ecological indicators is contingent

This paper aims to (1) synthesize the variety, scale, and uncertainty of existing solar-induced chlorophyll fluorescence datasets, (2) synthesize the diverse applications in the sector of ecology, agriculture, hydrology, climate, and socioeconomics, and (3) clarify how such data inconsistency superimposed with the theoretical complexities may impact process interpretation of various applications and contribute to inconsistent findings. We offer our perspectives on innovations needed to help improve informing ecosystem structure, function, and service under climate change.

upon complete understanding of SIF data quality and uncertainty. Biases and uncertainties in SIF observations can significantly confound interpretation of their relationships and how such relationships respond to environmental variations. Built upon our syntheses, we summarize existing gaps and uncertainties in current SIF observations. Further, we offer our perspectives on innovations needed to help improve informing ecosystem structure, function, and service under climate change, including enhancing in-situ SIF observing capability especially in "data desert" regions, improving cross-instrument data standardization and network coordination, and advancing applications by fully harnessing theory and data.

KEYWORDS
carbon cycle, climate change, photosynthesis, precision agriculture, retrievals, SIF, stress monitoring and early warning, vegetation index

1 | INTRODUCTION

The rapid growth in research of solar-induced chlorophyll fluorescence (SIF) remote sensing in the past two decades was primarily initiated by serendipitous advances in SIF observing capabilities from spaceborne platforms since the early 2010s (Frankenberg et al., 2011; Guanter et al., 2007, 2012; Joiner et al., 2011). Spaceborne SIF retrievals in turn have also generated momentum to push for technological advances to observe and even image SIF at much finer spatial and temporal resolutions with airborne and proximal sensing systems (Frankenberg et al., 2018; Grossmann et al., 2018; Gu, Wood, et al., 2019; Rascher et al., 2015; Yang et al., 2015; Zarco-Tejada et al., 2012), resulting in rapid expansion in applications of SIF in diverse research sectors (e.g., ecology, agriculture, hydrology, climate, and socioeconomics). These developments, while exciting, are marred by considerable inconsistencies among diverse SIF datasets and contradictory findings in applying them. These issues, which represent "growing pains", are due not only to scale-related challenges common in Earth system science studies, but also multiple factors specific to SIF measurements/products summarized below:

1. *Lack of specifically designed SIF measurement instrumentation/mission*. So far, all available satellite SIF products are from space missions that were designed to monitor atmospheric trace gasses. Ground-based SIF systems use generic spectroradiometers; most charge-coupled devices of these spectroradiometers are not specifically designed for SIF measurements. This indicates that current SIF systems, both spaceborne and in-situ, are not optimized for SIF monitoring.
2. *Observable versus unobservable but ecophysiologically relevant SIF*. The at-sensor SIF signal that is directly measured does not equal to the total Chl*a*F emission that is directly related to ecophysiological processes. Even when SIF is retrieved accurately at specific wavelengths, it is not certain whether they are equally informative as the total Chl*a*F emission (which is a broadband quantity, that is, integrated over the full spectra of fluorescence emission) that is directly related to photosynthetic electron transport and CO_2 assimilation (Gu, Wood, et al., 2019; Zhang et al., 2019), equations 6–7 in Sun et al., 2023). Furthermore, a substantial portion of the total Chl*a*F emission is reabsorbed/scattered within a canopy and only a fraction escapes from the canopy to be detected by a sensor (section 3.1 in Sun et al., 2023). Unfortunately, the total Chl*a*F emission is currently unobservable.
3. *Correlation versus causal inference*. SIF data availability and applications far outpace the growth in mechanistic understanding of SIF dynamics and their relationships with ecophysiological processes of interest to broad scientific communities. Currently, SIF research activities have been dominated by correlational analyses, while causal effects have been rarely established. This is primarily caused by the unique challenges transferring knowledge from laboratory experiments to actual field conditions under natural environment, from molecular to regional/global scales (Porcar-Castell et al., 2014, 2021), and from the traditional plant physiology to remote sensing communities.

Sun et al. (2023) attempts to provide theoretical guidance to enable mechanistic causal inference in SIF research. It demonstrates, from theoretical perspectives, that (a) Chl*a*F emission is interactively impacted by a myriad of structural and functional processes at the leaf and canopy levels, and (b) how such impacts, when carefully quantified and disentangled, can be used to infer terrestrial ecosystem structure, function, and services. However, the theoretical inferences envisioned in Sun et al. (2023) can only be achieved with the support of high-quality SIF observations at relevant scales/resolutions.

The present paper, as a companion review to Sun et al. (2023), aims to provide clarifications on the "growing pains" in SIF research related to the three issues identified above. It is not our intention to offer definitive solutions to these issues in this review. Rather, our intention is to place the inconsistencies and contradictory findings of past SIF research from the aspect of unique characteristics of available SIF datasets. Further, we attempt to address the forward,

inference, and innovation questions laid out in the first companion review (Sun et al., 2023) from the data perspective.

A few recent synthesis studies have attempted to summarize or intercompare SIF products/measurements from different spaceborne platforms (e.g., Doughty et al., 2022; Parazoo et al., 2019) or from proximal instruments (Aasen et al., 2019; Cendrero-Mateo et al., 2019; Pacheco-Labrador et al., 2019). For in-depth review and detailed discussion of instrument configuration and retrieval methods, we refer readers to these previous reviews. However, it still remains unclear the extent to which discrepancies and/or uncertainties in SIF products/measurements may confound the inference of ecosystem structure, function, and service. Compared to previous reviews, the major contribution of this paper is to provide thorough discussion of (1) how the variety, scale and uncertainty in SIF datasets may impact process interpretation for various applications and contribute to inconsistency across findings, (2) efforts needed to reconcile such inconsistencies from the data perspective, integrated with the theoretical angle (Sun et al., 2023), and (3) existing data gaps in SIF observations and required innovations to advance SIF applications in ecosystem structure, function, and service under climate change.

2 | DATA: VARIETY, SCALE, AND UNCERTAINTY IN SIF MEASUREMENTS

2.1 | Spaceborne SIF retrievals

The first retrievals of SIF were at the far-red wavelengths, achieved regionally with the Medium Resolution Imaging Spectrometer (MERIS; Guanter et al., 2007) and globally with high spectral resolution spectrometer (i.e., <0.1 nm) from the Greenhouse gasses Observing SATellite (GOSAT; Frankenberg et al., 2011; Guanter et al., 2012; Joiner et al., 2011). These retrievals were somewhat limited in terms of spatial resolution or revisit time. The next advance demonstrated that SIF could be retrieved with lower spectral resolution instruments (spectral resolution of ~0.5 nm), such as the Global Ozone Monitoring Experiment 2 (GOME-2) and the SCanning Imaging Absorption SpectroMeter for Atmospheric CHartographY (SCIAMACHY; Joiner et al., 2013; Khosravi et al., 2015; Köhler et al., 2015; Sanders et al., 2016; van Schaik et al., 2020). Since then, higher spatial resolution SIF retrievals have also been produced using the Orbiting Carbon Observatory 2 (OCO-2) and the Chinese Carbon Dioxide Observation Satellite Mission (TanSat) at ~2 km resolution (Doughty et al., 2022; Du et al., 2018; Sun et al., 2018). Most recently, moderate spatial resolution (~5 km) with a daily revisit time was achieved with the TROPOspheric Monitoring Instrument (TROPOMI) onboard Sentinel 5p (Guanter et al., 2015; Köhler, Frankenberg, et al., 2018). Retrieval of red SIF has also been accomplished with GOME-2 and TROPOMI (Joiner et al., 2016; Köhler et al., 2020; Wolanin et al., 2015). For detailed cross-instrument comparison and discussion of the impact of instrument characterization on SIF retrievals, we refer readers to Doughty et al. (2022), Joiner et al. (2020), and Parazoo et al. (2019).

Figure 1 and Table S1a summarize the past, current, and future missions with SIF capabilities along with their instrument characteristics. All of these instruments/missions, with the exception of the Fluorescence Explorer (FLEX; expected launch in 2025, Drusch et al., 2017), were designed for measurements of trace gasses and greenhouse gasses (GHGs). Instruments designed to measure GHGs (GOSAT, OCO-2, TanSat) typically only have spectral coverage in the wavelengths where far-red SIF is emitted. All of the current SIF-capable instruments are in Low Earth Orbit (LEO). Several of the planned instruments in Geostationary Earth Orbit (GEO) will be able to retrieve SIF as well, such as Tropospheric Emissions: Monitoring of Pollution (TEMPO) and the Copernicus Sentinel-4.

2.2 | Value-added global SIF products derived from native spaceborne SIF retrievals

Existing native spaceborne SIF products are restricted to either low spatial resolution, incomplete global coverage, low temporal

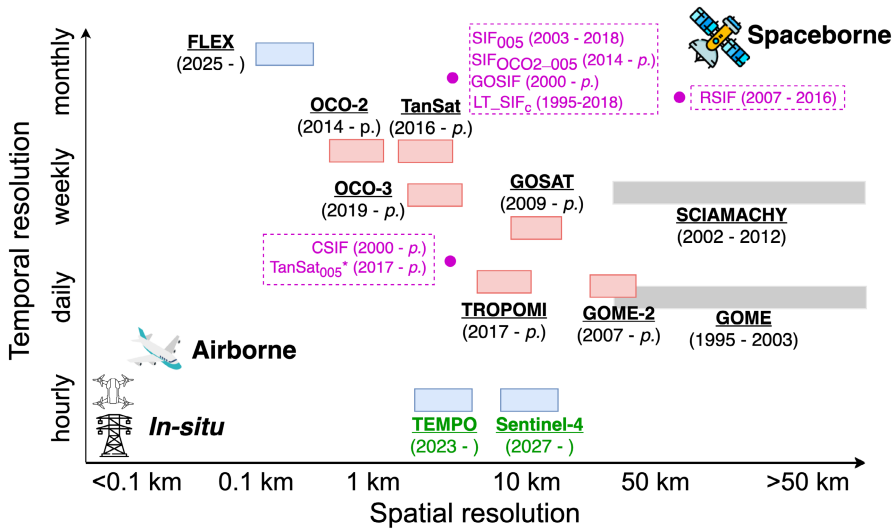

FIGURE 1 Characteristics of the past (grey), current (pink), and future (light blue) missions with solar-induced chlorophyll fluorescence (SIF)-observing capability. Font colors differentiate geostationary (GEO; green) from Low Earth Orbit (LEO; black) missions. Value-added SIF products (purple) are grouped in the dash-line boxes based on their spatial and temporal resolution; the corresponding native SIF retrievals based on which value-added products were developed are provided in Table S1b. 'p.' denotes "present".

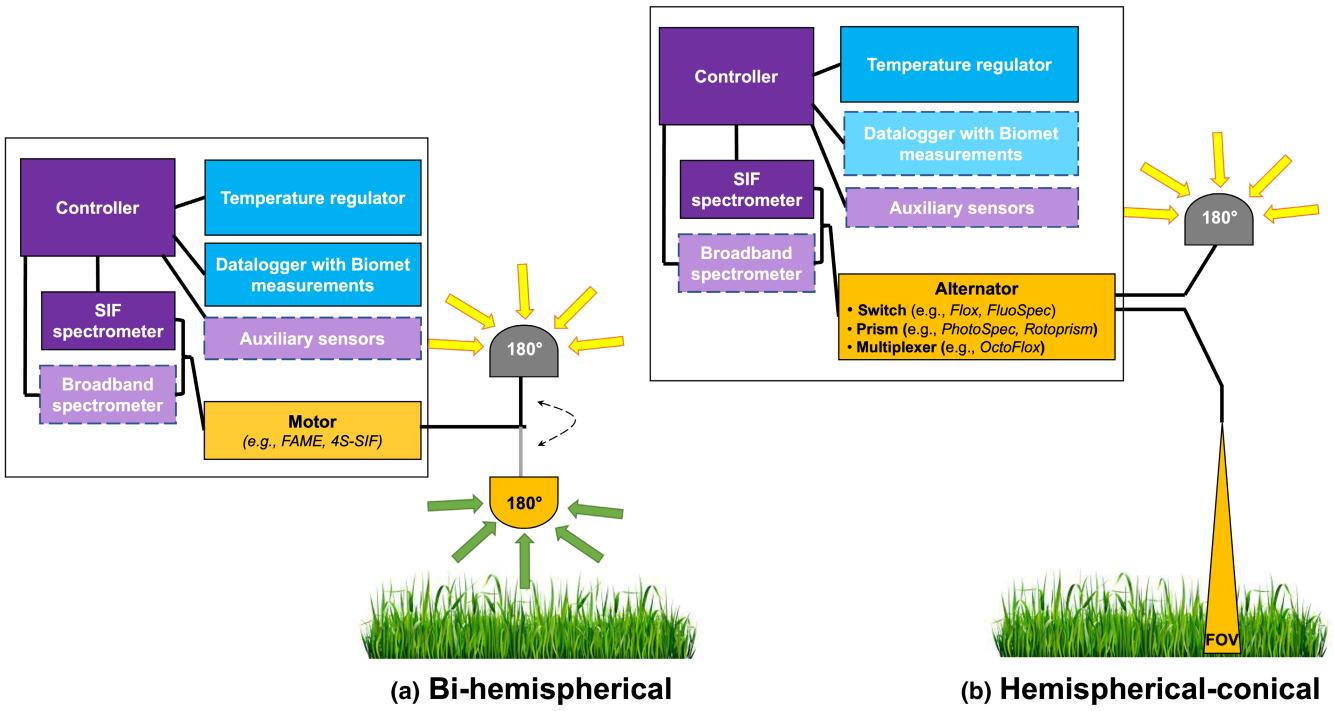

FIGURE 2 A simplified diagram of system configurations for existing non-imaging in-situ SIF systems. (a) Common components of a bi-hemispherical system; (b) common components of a hemispherical-conical system; the bi-directional dashed black arrow indicates the 180° rotation of the fore-optic. Purple components are utilized in both tower and Unmanned Aerial Vehicles (UAV) systems; blue components are currently used only in tower systems. The orange box highlights the key component that differentiate the two types of configurations, exemplified with existing systems (italic) that are mounted on tower and/or UAV. Components with dashed lines and lighter colors are optionally integrated to enhance system applications. The upwelling field of view (FOV) for hemispherical-conical systems varies by system, and typically ranges from ~1° to ~25°. Yellow arrows indicate incoming solar radiation while green arrows indicate incoming reflected radiation from the target canopy. SIF, solar-induced chlorophyll fluorescence.

resolution, short temporal coverage, or a combination of these. For example, Figure 1 reveals a general trade-off between spatial and temporal resolutions of existing native spaceborne SIF products. These limitations impede operational SIF applications, for example, real-time monitoring of vegetation growth in individual farms and forest management, or long-term monitoring of global ecosystem production and carbon budget. To overcome these limitations, a number of "value-added" SIF products have been derived based on native SIF retrievals (summarized in Table S1b). These products include RSIF (Gentine & Alemohammad, 2018), SIF_{005} (Wen et al., 2020), SIF_{oco2_005} (Yu et al., 2019), GOSIF (Li & Xiao, 2019b), CSIF (Zhang, Joiner, Alemohammad, et al., 2018), LT_SIF_c* (Wang, Zhang, et al., 2022), and other fine-resolution SIF products downscaled from GOME-2 (Duveiller et al., 2020; Duveiller & Cescatti, 2016) or TROPOMI (Gensheimer et al., 2022; Turner et al., 2020). These products are derived from different native SIF products, and have disparate spatial and temporal resolutions as well as temporal coverage (Figure 1; Table S1b). Nevertheless, their derivations share a similar strategy. This strategy basically (1) establishes a predictive model with native SIF retrievals (i.e., the model training step), and (2) estimates SIF at finer spatial/temporal resolutions and contiguous spatial coverage utilizing this trained predictive model as well as ancillary datasets available at the same fine spatial/temporal resolutions and spatial coverage (i.e., the model prediction step). Here the predictive model can be either (semi-)process-based (e.g., the light use efficiency LUE-type equation) or derived from machine-learning (ML; e.g., neural networks, regression trees). Detailed discussions on more nuanced differences in technical implementations among these products can be found in Wen et al. (2020). These products have demonstrated overall capability in revealing the spatial and seasonal patterns in native SIF retrievals at the global scale, and have been widely applied to tackle a variety of issues in ecological, agricultural, hydrological, and socioeconomic sectors (Section 3), albeit with varying performance depending on regions or biomes or application types.

2.3 | In-situ SIF measurements and retrievals

Various in-situ SIF systems have been developed to acquire top-of-canopy (TOC) SIF. These systems include both stationary ground tower and mobile airborne systems (e.g., Unmanned Aerial Vehicles, UAV). The former allows continuous, high temporal resolution acquisition, while the latter adds spatial mapping capability. So far, in-situ SIF systems are mostly low-cost non-imaging systems, which broadly fall into two configurations (Figure 2). In the bi-hemispherical configuration, both downwelling and upwelling irradiance are collected using a cosine-corrected fiber (e.g., FAME, which has developed

both tower and UAV versions, Chang, Guanter, et al., 2020; Chang, Zhou, et al., 2020; Gu, Wood, et al., 2019). Recently, a low-cost bi-hemispherical sensor that captures multiple ultra-narrow wavelengths of far-red SIF using photodiodes was developed (4S-SIF, Kim et al., 2022). In the hemispherical-conical configuration, there are alternate acquisitions of hemispherical downwelling irradiance and conical upwelling radiance, either using a switch that alternates incoming ir/radiance measurements between two fixed fibers (e.g., FloX, FluoSpec2, Yang, Shi, et al., 2018) or prisms that rotate acquisition of ir/radiance among different channels to collect dark currents, downwelling and upwelling measurements (e.g., PhotoSpec: Grossmann et al., 2018; rotoprism, Berry & Kornfeld, 2019; Kim et al., 2021). Both configurations now have commercial sources with the bi-hemispherical FAME under production by Campbell Scientific and the hemispherical-conical FloX produced by JB-Hyperspectral GmbH; recently, a multiplexed configuration of the FloX (OctoFlox) with multiple fibers for multiple target acquisition was developed by JB-Hyperspectral. UAV systems of both the bi-hemispherical (Chang, Zhou, et al., 2020) and the hemispherical-conical (switch-based setup) have also been developed (Bendig et al., 2018; MacArthur et al., 2014; Wang, Suomalainen, et al., 2021). For in-depth review of specific instrumentation configurations and sensors, we refer readers to Pacheco-Labrador et al. (2019). In addition to these non-imaging (point-based) SIF systems, a hyperspectral imaging SIF sensor is commercially available from Headwall Photonics (Zarco-Tejada et al., 2013). Selection of an appropriate in-situ SIF system depends upon specific applications (Section 3), and their required resolutions (in time and space) and signal-to-noise ratio, since each configuration comes with different strengths and weaknesses (summarized in Table S2).

Selection of retrieval methods depends upon not only system configuration, but also specifications of the SIF spectrometer utilized and the temporal frequency of acquisition (detailed summary in Table S3). Common SIF retrieval methods are based upon Fraunhofer Line Discrimination (FLD; Plascyk & Gabriel, 1975), Spectral Fitting Method (SFM; Meroni & Colombo, 2006), Singular Vector Decomposition (SVD equivalent to Principal Component Analysis PCA; Guanter et al., 2013), and differential optical absorption spectroscopy (DOAS; Platt & Stutz, 2008). FLD, SFM and DOAS retrieve SIF using single paired up/downwelling spectra, while SVD requires a training set of multiple SIF-free (or downwelling) spectra. The accuracy of SVD improves with higher temporal frequency of acquisition to obtain multiple downwelling spectra under similar sunlight conditions as the upwelling measurement (Chang, Guanter, et al., 2020). FLD, SFM, and SVD can be used to retrieve SIF from the broader telluric O_2 absorption features, while DOAS and SVD can be used to retrieve SIF from narrow solar Fraunhofer lines. Fraunhofer line-based retrievals using DOAS or SVD require a high spectral resolution (e.g., ≤0.3 FWHM) while retrieving SIF from O_2 bands using SFM, FLD or SVD are much less stringent in terms of spectral resolution. Because FLD and SFM use paired spectra, these methods are more prone to error under variable cloudy skies where ambient light conditions can change between acquisition of downwelling and upwelling spectra, which greatly influence the telluric O_2 bands by distorting the edges of the O_2 absorption features. Narrowing the retrieval fitting window can effectively alleviate spectral distortion around the O_2 bands for both SFM and SVD (Chang, Guanter, et al., 2020). Recently, SIF retrievals based on partial least-squares regression (PLS) show lower sensitivity to spectral distortion resulting from atmospheric reabsorption (Naethe et al., 2022). Variable sky conditions do not influence the solar Fraunhofer lines much, but the resulting SIF retrievals can be noisier since the narrow spectral window contains relatively weaker irradiance and thus weaker reflected radiance. For detailed discussion and intercomparisons of these retrieval methods, we refer readers to the works of Cendrero-Mateo et al. (2019) and Chang, Guanter, et al. (2020).

3 | APPLICATIONS

Solar-induced chlorophyll fluorescence research activities in the past two decades have been primarily focused on investigating SIF-gross primary production (GPP) relationships across scales and under different environmental conditions. So far, research findings have shown both consensuses and discrepancies. In this section, we first offer our perspectives on factors that led to such consensuses and discrepancies, from both the theory (Sun et al., 2023) and data aspects (Section 3.1).

Although understanding and teasing out the biological SIF-GPP connections from uncertain datasets is a necessary first step and much work is still needed at this step, broad applications of SIF have started. By harnessing the theoretical understanding and data revolution of SIF, a variety of new research opportunities and possibilities have arisen in ecological, hydrological, agricultural, and socioeconomic applications (a graphical summary in Figure 3). In Sections 3.2–3.8, we attempt to clarify how SIF data uncertainty superimposed with the theoretical complexities laid out in Sun et al. (2023) may impact process interpretation of various applications.

3.1 | Interpretation of SIF measurements, its relationship with GPP, and dependence of their relationships to environmental variations

3.1.1 | The theoretical perspective

Table 1 and Figure 4 summarize consensuses and discrepancies of research findings regarding the SIF-GPP relationship. Here, we employ equations derived in Sun et al. (2023) to theoretically interpret these consensuses and discrepancies. Specifically, equation 10 in Sun et al. (2023; copied below for convenience) reveals the complexity of the SIF-GPP relationship, which critically depends on CO_2 diffusion (controlled by stomatal and mesophyll conductances) and the redox state of PSII (and NPQ, Sun et al., 2023),

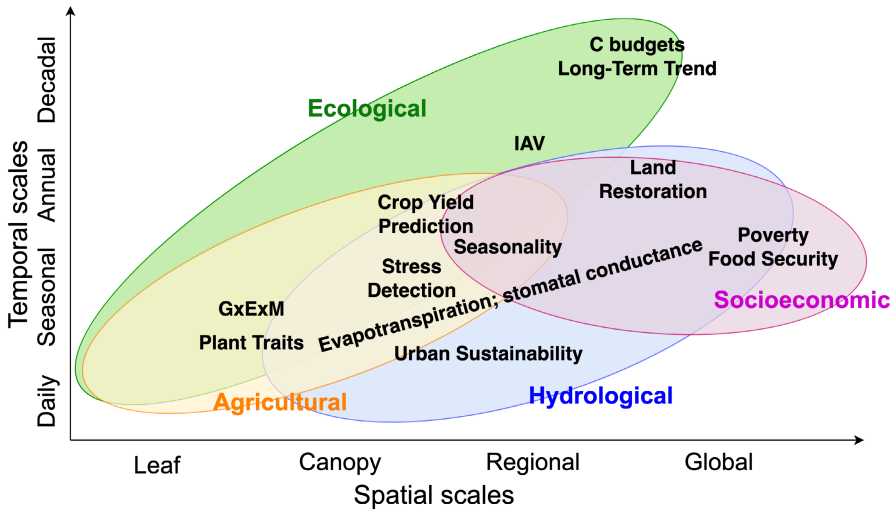

FIGURE 3 Applications of solar-induced chlorophyll fluorescence in sectors of ecological, agricultural, hydrological, and socioeconomic science across temporal and spatial scales. G×E×M, interactions of genetics, environment, and management; IAV, inter-annual variability. Evapotranspiration and stomatal conductance are displayed diagonally because research in these aspects span across the full spectrum of temporal and spatial scales.

$$\mathrm{GPP_T} = \underbrace{\frac{\left(\frac{k_{\lambda_F}}{k_{\mathrm{PAR}}}+1\right)\left[1-e^{-(b+1)k_{\mathrm{PAR}}\mathrm{LAI}}\right]}{\varepsilon_{\uparrow 0}(\lambda_F)\left[1-e^{-\left(k_{\lambda_F}+k_{\mathrm{PAR}}\right)\mathrm{LAI}}\right]}}_{\text{Structure}} \times \underbrace{\frac{\Phi_{\mathrm{PSIIm}}(1+k_{DF})}{1-\Phi_{\mathrm{PSIIm}}}}_{\text{Constant}}$$

$$\times \underbrace{\overbrace{\frac{a\mathrm{PAR}_0^b}{b+1}}^{\text{Redox state}}}_{\text{ChlaF weighting factor}} \times F_{\uparrow}(\lambda_F) \times \begin{cases} \dfrac{C_c-\Gamma^*}{4C_c+8\Gamma^*} & \text{(C3) (a)} \\ \dfrac{1-x}{3} & \text{(C4) (b)} \end{cases}.$$

At seasonal scales and beyond and/or aggregated spatial scales, variations in CO_2 diffusion and the redox state of PSII can be averaged out, and much weaker than variations in the at-sensor SIF, that is, $F_{\uparrow}(\lambda_F)$, resulting in an approximately linear scaling with GPP (denoted as $\mathrm{GPP_T}$, the canopy total GPP). Further, at these scales, variation in leaf area index (LAI) and photosynthetic pigments (i.e., arising from phenological changes or different biome characteristics) is the primary driver of $F_{\uparrow}(\lambda_F)$ dynamics, via impact on both light harvesting and canopy structure (equation 8 in Sun et al., 2023); meanwhile, variation in LAI and photosynthetic pigments also play dominant role in controlling GPP at these scales, and such information is carried largely by $F_{\uparrow}(\lambda_F)$ (although not completely, Sun et al., 2023), resulting in coherent SIF and GPP variations. In contrast, at shorter time scales when LAI and photosynthetic pigments content remain relatively stable, the impact of variations in the redox state (and NPQ) and C_c (CO_2 partial pressure at chloroplast) on GPP is largely due to their instantaneous response to PAR. Moreover, the scattering/reabsorption of Chl*a*F emission (e.g., can be represented by k_{λ_F}, the extinction coefficient of Chl*a*F emission under Beer's law) can also vary instantaneously with sun-canopy-sensor geometry, PAR intensity, and/or other environmental stress. These factors collectively lead to deviation from a linear scaling between SIF and GPP at shorter time scales. Stronger linearity in C4 than C3 plants reported from leaf to global scales is primarily due to the segregation of CO_2 diffusion effects from SIF-GPP coupling in C4 plants. Crops and deciduous forests exhibit stronger SIF-GPP coupling than other biomes (e.g., evergreen broadleaf forests), because their distinct seasonality in LAI drives the co-variation of SIF and GPP, with the impact of CO_2 diffusion and the redox state of PSII being smoothed out (Magney et al., 2020).

Regarding the debate on the existence of biome-universal SIF-GPP scaling, equation 10 in Sun et al. (2023) suggests that any biome-dependent variables (e.g., k_{λ_F}, the vertical extinction coefficient of PAR k_{PAR}, or the redox state of PSII) or parameters (e.g., $\bar{\beta}$ and Γ^*, denoting the canopy-mean relative contribution of pigments associated with PSII and the chloroplastic CO_2 compensation point, respectively) can prevent a biome-universal scaling. However, these individual processes may have a compensatory effect, resulting in an apparent biome-universal scaling. The degree of the compensatory effect depends on time scale, spatial scale, and stress types/conditions, which currently remains a critical knowledge gap and requires dedicated future research.

Equation 10 in Sun et al. (2023) also suggests that SIF-GPP coupling (i.e., often characterized by R^2) and/or scaling (i.e., often characterized by the linear regression slope) can diverge or converge between stress and normal conditions, depending on time and spatial scales under investigation as well as stress intensities and durations. For example, at aggregated temporal–spatial scales and during prolonged drought/heatwaves, SIF and GPP decline can co-occur due to loss of photosynthetic pigments and LAI, and therefore exhibit positive coupling as under normal conditions; in contrast, at local or shorter time scales or during brief stress episodes that are too short to induce any structural changes, SIF and GPP trajectories can decouple due to stomatal/mesophyll regulations on CO_2 diffusion and redistribution of energy dissipation among photochemical quenching (PQ)-NPQ-SIF (Han, Chang, et al., 2022; Martini et al., 2022). Also, the assumed constant parameters (e. g., β, Φ_{PSIIm}, k_{DF}, the latter two denoting the maximal photochemical quantum yield of PSII and the ratio of the rate constant for internal conversion to the rate constant for Chl*a*F emission, respectively) that represent internal properties of plants can also change under stress, which can reshape the SIF-GPP relationship from

TABLE 1 Synthesis of the current consensus and discrepancies among literatures regarding SIF-GPP relationships.

Consensuses	Examples of studies
1. SIF-GPP linearity	
a. SIF-GPP linearity at seasonal scales and beyond for most biomes and/or aggregated spatial scale for most biomes	Li and Xiao (2019a); Magney et al. (2020); Yang et al. (2015)
b. Nonlinearity at shorter time scales (e.g., sub-daily) and/or proximal spatial scale (i.e., leaf or canopy scale)	Damm et al. (2015); Han, Chang, et al. (2022); Kim et al. (2021); Pierrat et al. (2022); Zhang et al. (2016)
c. Tighter linearity in C4 than C3 plants (stronger R^2)	Han, Chang, et al. (2022); Liu, Guan, and Liu (2017); Zhang, Zhang, et al. (2020)
d. Overall stronger R^2 in crops and deciduous forests and relatively weaker R^2 in evergreen forests	Dechant et al. (2022); Gentine and Alemohammad (2018); Zhang, Zhang, et al., 2020
2. Canopy structure versus function	
a. For crops and deciduous forests, canopy structure playing a dominant role in controlling SIF dynamics and SIF-GPP relationship from diurnal to seasonal	Dechant et al. (2020); Koffi et al. (2015); Yang et al. (2015)
b. For evergreen conifers, leaf physiology playing significant role in controlling SIF dynamics and SIF-GPP relationship at the seasonal scale	Magney et al. (2019); Migliavacca et al. (2017); Pierrat et al. (2022)

Discrepancies	Potential causes	Solutions
1. SIF-GPP scaling: biome-specific (Damm et al., 2015; Guanter et al., 2012; Parazoo et al., 2014) versus biome-universal (Li & Xiao, 2022; Li, Xiao, He, et al., 2018) 2. Impact of environmental stress on SIF-GPP relationships: consistent SIF-GPP scaling with normal conditions (Song et al., 2021) versus divergent coupling under stress (Marrs et al., 2020; Martini et al., 2022; Wohlfahrt et al., 2018) 3. Relationship of the quantum yields between SIF and GPP: positive (Yang et al., 2015), negative (Miao et al., 2018), insignificant (Goulas et al., 2017)	A. Environmental conditions: temperature, soil moisture (A. Chen, Mao, Ricciuto, Lu, et al., 2021; A. Chen, Mao, Ricciuto, Xiao, et al., 2021; Y. Song et al., 2021)	a. Moving from correlational to causal b. Accounting for observational bias and uncertainty
	B. Biome characteristics: LAI, $\varepsilon_{\uparrow}$, p, V_{cmax}, leaf angle distribution	a. Theoretically rigorous and practically feasible modeling of individual processes and their interactions b. Measurement innovations at leaf and canopy scales c. Synergy with other techniques
	C. Interactive effects between plant functional and structural variations (Chang et al., 2021)	
	D. SIF and GPP data sources and their uncertainty	Data validation, synthesis, standardization, coordination
	E. Spatial and time scales	Analytical protocol standardization

Note: Cited literatures are only examples of studies that represent each key point here, as including the full list of papers is prohibitive due to space limit.

Abbreviations: GPP, gross primary production; LAI, leaf area index; SIF, solar-induced chlorophyll fluorescence.

normal conditions. For example, Φ_{PSIIm} (the maximal photochemical quantum yields for PSII) is assumed to be conserved across non-stressed plants (Björkman & Demmig, 1987) but can deviate from its assumed constant 0.83 under stress. In addition, the redox reaction (represented by q_{LI}, the fraction of open PSII reaction centers under the lake model) is sensitive to temperature, while equation 10 in Sun et al. (2023) only captured the first-order effect of q_{LI} as a function of PAR (detailed discussion in Sun et al., 2023). This factor can further complicate the SIF-GPP relationship beyond what equation 10 currently suggests.

Further, mixed findings were reported for the relationships of quantum yields between SIF and GPP. This can be explained by $\frac{\Phi_{PSII}}{\Phi_F} = \frac{q_{LI}\Phi_{PSIIm}(1+k_{DF})}{1-\Phi_{PSIIm}}$ (derived as the ratio of equations 16 and 14 in Gu, Han, et al., 2019), which reveals the impact of redox states q_{LI} on the ratio of quantum yields of GPP over SIF. Further complications include the sensitivity of q_{LI} to temperature and water stress (stated above, and detailed discussion in Sun et al., 2023).

3.1.2 | The data perspective

Superimposed on the mechanistic complexities of light and carbon reactions of photosynthesis, biases and uncertainties in observations of SIF and GPP can significantly confound interpretation of their relationships and how such relationships respond to environmental variations. Figure 4 synthesizes the GPP-SIF (standardized to 740 nm) regression slopes from literature, which reveal a striking spread across studies employing different SIF and/or GPP products even for the same biome and spatiotemporal scale. For example, if in-situ GPP (inferred from net ecosystem exchanges [NEE] at eddy covariance EC towers) and spaceborne SIF products (Sections 2.1; Table S1) are utilized for investigation, the GPP-SIF scaling can vary by a factor of three, that is, ~10 for TanSatSIF to ~30 for CSIF, when spatiotemporal scales are controlled across different studies (Figure 4c). Such discrepancies only narrow slightly if SIF products originating from the same spaceborne mission are used, e.g., OCO-2,

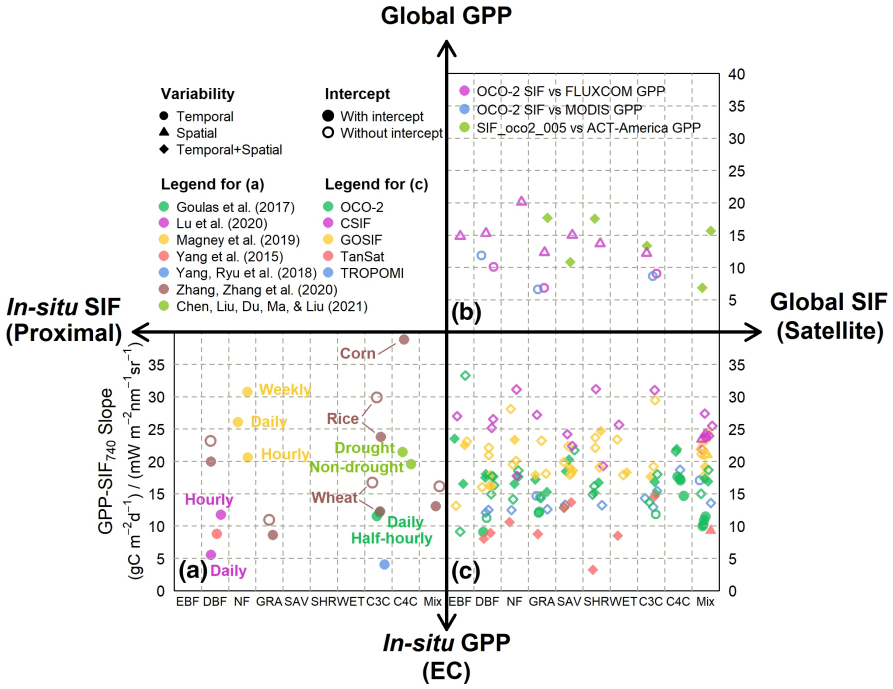

FIGURE 4 Synthesis of gross primary production-solar-induced chlorophyll fluorescence (GPP-SIF) slopes (derived from linear regression) from literature, based on the protocol in Supporting Information 1. Findings are grouped into three categories, depending on data sources of SIF and GPP: right and left quadrants show satellite and in-situ SIF (via proximal sensing), respectively; top and bottom quadrants show global gridded and in-situ GPP (inferred from the net ecosystem exchange NEE at eddy covariance EC towers), respectively. Specifically, (a) slopes from in-situ SIF and in-situ GPP; (b) slopes from satellite SIF and global GPP products; (c) slopes from satellite SIF and in-situ GPP. The units of GPP and SIF are standardized to $gC\,m^{-2}\,day^{-1}$ and $mW\,m^{-2}\,nm^{-1}\,sr^{-1}$, respectively. All SIF values are normalized to 740 nm based on the scaling factors derived from the measured spectra in (Guanter et al., 2013; details in Supporting Information 1). Definition of biome types can be found in Supporting Information 1. The shape of scatters differentiates scales across studies, that is, temporal (diurnal, seasonal, interannual), spatial (across sites or biomes), or temporal and spatial combined. Open and filled symbols indicate whether the intercept is forced to be zero or not, respectively. Colors in (a) differentiate studies with text annotation detailing time scales, crop types or stress conditions in the same study; colors in (b) separate different combinations of SIF and GPP products; colors in (c) differentiate sources of satellite SIF products. Supporting Information 2 synthesizes all literatures selected for this figure based on the protocol in Supporting Information 1.

CSIF, and GOSIF (Figure 4c). Other factors such as the selection of EC sites and temporal period may induce extra variations in the GPP-SIF scaling. Note that most existing studies examined the GPP-SIF slopes utilizing at-sensor SIF; a few recent studies suggested that the total Chl*a*F emission of a canopy (i.e., $F_{eT}(\lambda_F)$), after correcting the escape probability $f_{\Omega\uparrow}^{esc}$, not only present higher coherence with GPP (Lu et al., 2020), but also result in more convergence of GPP-SIF slopes across C3 biomes (Zhang, Zhang, et al., 2020). However, specific formulation of $f_{\Omega\uparrow}^{esc}$ may (on top of the choice of SIF data sources) can also impact the GPP-SIF.

Moreover, the level of biome-specificity in GPP-SIF scaling can be considerably confounded by the choice of SIF products and/or versions (Figure 4c; Parazoo et al., 2019; van Schaik et al., 2020). Further biases/uncertainties in GPP data, for example, global gridded products (e.g., Anav et al., 2015), not only impact the absolute magnitude of GPP-SIF scaling but also possibly contribute to more biome-specificity (Figure 4b).

If both SIF and GPP come from in-situ measurements (Figure 4a), which are usually assumed to be "ground truth", greater disparity can emerge even within the same biome. These disparities arise not only from different time scales and plant species, but also from inconsistencies in SIF retrieval algorithms, instrument configuration, footprint sizes, across studies (synthesized in Section 2.3). Often, users choose system configuration (which largely determines footprint sizes) and retrieval methods depending on the trade-offs of advantages and disadvantages (summarized in Tables S2 and S3) that can optimize SIF measurement for specific applications. For example, bi-hemispherical systems can more closely match the footprint of a typical EC flux system and suffer less from angular effects than hemispherical-conical systems. In contrast, the hemispherical-conical more closely mimics the setup and angular effects of space-borne SIF instruments. Moreover, certain retrieval methods such as SVD and PLS (Chang, Guanter, et al., 2020; Naethe et al., 2022) are relatively more robust to atmospheric conditions and therefore may be more suitable for in-situ SIF systems across diverse platforms (e.g., at different altitudes) and ecosystems. However, the concomitant consequences of inconsistencies in SIF retrieval algorithms, instrument configuration, and footprint size can lead to considerable disparities (especially under variable sky conditions) in SIF magnitude, temporal patterns, and functional relationships among

variables (e.g., GPP-SIF scaling). Therefore, caution is needed when interpreting obtained patterns and intercomparing across studies.

3.2 | Constraining, estimating, and understanding the budgets and variability of the terrestrial carbon cycle

The global terrestrial carbon sink has increased with rising fossil fuel CO_2 emissions since the 1960s (Ballantyne et al., 2012; Ciais et al., 2019), acting as a key negative feedback and mitigating climate change (Arneth et al., 2010; Arora et al., 2013; Friedlingstein et al., 2014; Gregory et al., 2009). A general consensus among multiple independent observations suggests that intensifying terrestrial biosphere activities was dominated by increased GPP. However, global estimates of GPP, its interannual variability (IAV), and long-term trend remain highly uncertain (Ahlström et al., 2015; Bastos et al., 2019; Fernández-Martínez et al., 2017; Forkel et al., 2016; Haverd et al., 2020; Keenan & Riley, 2018; Smith et al., 2016). This represents one of the largest and most uncertain carbon-climate feedbacks for the Earth System Models (ESMs; Arneth et al., 2010). SIF carries the hope of curbing such uncertainties if it can accurately anchor GPP estimates.

3.2.1 | The carbon budgets

The current estimates of global GPP have a remarkable divergence across literature based on different approaches and/or datasets, for example, ~100.2–167.0 $PgC\,year^{-1}$ for the contemporary period (Anav et al., 2015; Jian et al., 2022). Among them, SIF-based GPP estimates exhibit a narrower but still considerable spread, for example, $135.5 \pm 8.8\ PgC\,year^{-1}$ (2000–2017, Li & Xiao, 2019a) versus $167.0 \pm 5.0\ PgC\,year^{-1}$ (for 2015, Norton et al., 2019).

Existing studies employed two broad types of approaches to compute GPP from SIF. The first type of approach is to apply a linear scaling factor to transform SIF to GPP, for example, GOSIF-based GPP products (Li & Xiao, 2019a), and regional GPP in southern Amazon (Parazoo et al., 2013). Such GPP estimates were further synergized with net carbon exchange derived from CO_2 column-average dry air mole fraction (xCO_2), and biomass burning emission derived from carbon monoxide (CO), to infer other components of carbon fluxes, such as ecosystem respiration (R_{eco}; Bowman et al., 2017; Liu, Bowman, et al., 2017). This linear scaling approach is appealing due to its simplicity, but the accuracy of derived GPP can be susceptible to (a) the data quality of SIF products, and (b) the reality of the employed SIF-GPP scaling factor (Section 3.1). More importantly, a major shortcoming of this strategy is the "implicit" circularity involved (Han, Chang, et al., 2022). For example, the SIF-GPP scaling factor is derived from regressing SIF against GPP either from global gridded products or inferred from in-situ NEE of CO_2 measured with EC techniques. Global gridded GPP products are highly uncertain, whereas the latter, commonly treated as the ground "truth", is actually imprecisely partitioned with well documented biases (Keenan et al., 2019; Kira et al., 2021; Wehr et al., 2016). SIF-GPP scaling derived from these GPP datasets was then used to back-calculate GPP, which is essentially circular, and inherits uncertainties in the original GPP. If in-situ GPP is used for deriving the SIF-GPP scaling factor which is subsequently multiplied to satellite SIF to derive a global GPP estimate, additional uncertainties can arise from (1) uneven degree of linearity of SIF related to GPP across biomes (e.g., weaker correlation in tropical evergreen forests, Gentine & Alemohammad, 2018), and (2) uneven representativeness of EC tower distribution across biomes (Schimel et al., 2015). Without knowing the inherent biological SIF-GPP scaling (from uncertain/inconsistent SIF and GPP products), it still remains challenging to derive accurate global GPP estimates via simple linear scaling.

The second type of approach is to assimilate satellite SIF to land surface models (LSMs) or terrestrial biosphere models (TBMs) to constrain simulations of GPP (based on the Farquhar-von Caemmerer-Berry model—FvCB; Farquhar et al., 1980) and net carbon fluxes (Bloom et al., 2020; MacBean et al., 2018; Norton et al., 2019; Parazoo et al., 2014). The accuracy of these estimates depend on (a) the realism of model representations of SIF-q_{LI}-NPQ-GPP and associated parameters (Parazoo et al., 2020; Yang et al., 2021), and (b) SIF data quality (Section 3.1). LSMs/TBMs that include SIF parameterization are generally adopted from Soil-Canopy Observation of Photochemistry and Energy (SCOPE; van der Tol et al., 2014), which has yet to be tested for a broad range of species or dynamic environmental conditions (Martini et al., 2022; Parazoo et al., 2020; Yang et al., 2021). At its core, SCOPE utilized the FvCB biochemical model to compute photosynthesis, which subsequently is used to calculate SIF. The accuracy of the simulated SIF and GPP are contingent upon the realism of NPQ model parameterization (or q_{LI}, discussed above), which is challenging to model due to its complex dynamics (Sun et al., 2023). It also depends on the assumption that alternative electron sinks are non-existent, which is known to be incorrect as plants have a variety of alternative electron sinks (e.g., nitrate reduction, Mehler reactions, von Caemmerer, 2000). Furthermore, the quality of SIF products (Section 3.1) and the realism of $f_{\Omega\uparrow}^{esc}$ proxy or leaf/canopy radiative transfer (Sun et al., 2023) modeling determines the accuracy of the true Chl*a*F emission utilized to constrain LSMs/TBMs.

3.2.2 | Seasonality and phenology

SIF has been applied to study seasonal patterns of GPP, to characterize phenology dynamics, and to reveal the environmental drivers of such dynamics across biomes. Mixed findings were reported for pan-tropical rainforests in the response to seasonal water stress. For example, in the Amazon basin, SIF tends to increase from the early to late dry season (JJA–SON) and peaks in the early wet season (DJF), a pattern generally consistent across different spaceborne SIF products and also MODIS EVI (Doughty et al., 2019; Köhler, Guanter, et al., 2018; Lee et al., 2013; Parazoo et al., 2013). Such patterns

correspond to a greater atmospheric xCO_2 in the dry than the wet season in the seasonally dry forests over the central-to-south Amazon (Parazoo et al., 2013). In tropical Africa, peak SIF appears in the wet season, consistent across spaceborne SIF products; vegetation indices (VIs) may exhibit similar or different seasonal peaks from SIF (Guan et al., 2015; Mengistu et al., 2020).

However, Guan et al. (2015) argued that spatial disparity (i.e., contrast between the Amazon and Congo basins) exists in seasonal SIF (and EVI) dynamics in response to water stress in the pan-tropics, depending on the precipitation regime. Furthermore, Wu et al. (2021) suggested that the degree of synchrony between precipitation and solar radiation determines whether the wet or dry season exhibits higher SIF in tropical Asia. These patterns and interpretation can be future confounded by strong BRDF effect on spaceborne SIF (Köhler, Guanter, et al., 2018), the degree of which also varies across different platforms (Doughty et al., 2019).

Consensus is achieved in characterizing phenological metrics, for example, the start, end, and length of growing season (denoted as SOS, EOS, and GSL respectively) with different SIF products for extra-tropical biomes among literature (e.g., Jeong et al., 2017; Joiner et al., 2014; Magney et al., 2019; Smith et al., 2018; Turner et al., 2020; Walther et al., 2016; Wang, Beringer, et al., 2019). Specifically, both SOS and EOS in SIF closely resembled that of EC GPP, outperforming reflectance-based VIs consistently across a diverse range of biomes, that is, deciduous broadleaf forests (DBF), crops, drylands, and evergreen neefleleaf forests (ENF). Recently, NIRv has been demonstrated to have equivalent or superior capability to SIF in depicting seasonal variations in GPP, primarily for temperate DBF and crops that have distinct seasonal cycles (Dechant et al., 2022). Such capability does not necessarily hold for ENF (Magney et al., 2019; Pierrat et al., 2021, 2022) or dryland ecosystems (Wang, Beringer, et al., 2019; Wang, Biederman, et al., 2022). ENF has relatively muted seasonal variations in VIs due to the presence of chlorophyll content even during the dormant season, but exhibits distinct seasonal changes in GPP and SIF in parallel (Kim et al., 2021; Magney et al., 2019; Pierrat et al., 2022). Phenology of dryland ecosystems (e.g., grassland, savannas, shrublands) is challenging to characterize with VIs, due to their complex composition/shifts of diverse species and rapid environmental fluctuations. For these systems, Wang, Beringer, et al. (2019) found that SIF outperforms NIRv (and other VIs) in depicting the seasonal GPP dynamics, thanks to its muted sensitivity to the background soil, which does not emit SIF but can contaminate VIs.

Attempts have also been made to understand how environmental variations control the variations in GPP phenology metrics utilizing various SIF products (Jeong et al., 2017; Zhang, Commane, et al., 2020; Zhang, Parazoo, et al., 2020). Jeong et al. (2017) found that variations in SOS and EOS of ENF in northern hemisphere mid-latitude are constrained by temperature and PAR, respectively, based on GOSAT and GOME-2 SIF products; while Zhang, Parazoo, et al. (2020) argued for the joint constraints of temperature and precipitation on IAV of EOS for biomes across the globe, depending on which factor is more limiting, based on CSIF. In terms of phenology trend, Wang, Ju, et al. (2019) reported that higher daytime LST and atmospheric CO_2 can jointly lead to earlier onset (i.e., SOS) and delayed senescence (i.e., EOS), using the urban–rural gradient (of OCO-2 SIF) as a natural laboratory to mimic future warming scenarios. Zhang, Commane, et al. (2020) found a weaker EOS trend in SIF than in VIs in northern hemisphere natural biomes, and attributed it to PAR limitations. However, all these efforts implicitly assume that SIF is an accurate proxy of GPP, which can be invalid, as demonstrated by the analytical equations in Sun et al. (2023). Detailed discussion of this issue is provided in section 3.3 of Sun et al. (2023) and Section 3.1 above.

3.2.3 | IAV of terrestrial carbon cycle and its climate feedbacks

The net carbon fluxes between terrestrial ecosystems and atmosphere (and therefore the atmospheric CO_2 growth rate, CGR) exhibit large IAV (Ahlström et al., 2015; Bacastow, 1976; Bousquet et al., 2000), and are strongly regulated by climate variability, for example, El Niño–Southern Oscillation (ENSO; Humphrey et al., 2018; Wang et al., 2016). However, how individual components (e.g., GPP, ecosystem respiration R_{eco}) contribute to the net fluxes and how they distinctively respond to and feedback to climate still remain elusive, despite numerous studies in the past decades (Piao et al., 2020).

SIF has been employed to anchor IAV of GPP. It is promising that SIF outperforms VIs in capturing the IAV of EC GPP in both drylands and ENF ecosystems in the US (Smith et al., 2018; Zuromski et al., 2018). Furthermore, by implicitly assuming SIF is an accurate proxy of GPP, Butterfield et al. (2020) identified two modes of IAV: seasonal compensation (i.e., opposite sign of GPP anomalies between spring and summer, associated with warmer/colder spring and drier/wetter summer) and seasonal amplification (i.e., the same sign of GPP anomalies from spring to summer, associated with persistent soil moisture anomaly). These studies explained a larger IAV of GPP and NEE in the arid western US (dominated by seasonal amplification) than the humid eastern US (typical of seasonal compensation; Byrne et al., 2020). In contrast, Liu et al. (2018) reported that while IAV of NEE is dominated by that of GPP in the western CONUS, R_{eco} plays the dominant role in the humid east.

Recently, SIF has been utilized (with the hope) to elucidate the relative role of soil moisture versus vapor pressure deficit (VPD) in controlling IAV of GPP (Liu et al., 2020; Lu et al., 2022), a long debate in the past decade (Fu et al., 2022; Novick et al., 2016). Li and Xiao (2020) and Liu et al. (2020) reported a dominant role of soil moisture in controlling IAV of SIF over >70% of global vegetated regions, especially in arid and semi-arid regions. In contrast, Lu et al. (2022) showed that the dominant role of soil moisture can greatly attenuate if the influence of PAR and *f*PAR were accounted for. They obtained an overall equal or even more important role of VPD in controlling IAV of SIF over nearly 60% of global vegetated regions, a pattern also supported by EC GPP across the globe (Fu et al., 2022). Disparate patterns also exist within the Amazon basin

(Green et al., 2020), with the wettest region (light-limited) showing positive SIF-VPD response while the tropical savannas and seasonally dry forests (water-limited) exhibiting a negative relationship.

Regarding climate-carbon cycle feedbacks, Green et al. (2017) reported strong positive feedbacks to precipitation in semi-arid and monsoon regions (i.e., greater SIF or GPP leading to higher precipitation), while positive feedbacks to PAR occurred in some moderately wet regions (e.g., eastern US, central Eurasia) and the Mediterranean (i.e., greater SIF or GPP leading to reduced cloud cover and increased PAR).

Similar to the seasonality and phenology characterization with SIF, the major caveats of these efforts are the implicit assumption of the equivalence of SIF and GPP (which is invalid, Sun et al., 2023) and the uncertain and disparate SIF products (Section 3.1). Such caveats can confound the interpretation of the obtained patterns; moving forward, theoretical (Sun et al., 2023) and observing advances (Section 4.2) are needed to refine the research findings synthesized here.

3.2.4 | The long-term trend of GPP

SIF has also been employed to infer the long-term trend of GPP. Both CSIF and GOSIF show a growth in the global mean SIF at a rate of ~0.4% year^{-1} since the start of the 21st century, stronger than other GPP products (i.e., FLUXCOM, BESS, MODIS C6, and WECANN; Li & Xiao, 2019b; Zhang, Joiner, Alemohammad, et al., 2018). Moreover, spatial distribution of such SIF trends and regional hotspots (i.e., growth in southwest China and India, decline in eastern Brazil) are highly consistent with MODIS (C6) EVI (Zhang et al., 2017). Recently, Wang, Zhang, et al. (2020) reported a weakened CO_2 fertilization effect on GPP across the globe, utilizing NIRv (from AVHRR, complemented with CSIF), and attributed it to nitrogen and water limitation. Robustness of such findings can be confounded by the implicit assumption that NIRv and SIF accurately represent GPP dynamics, along with uncertainties in SIF and NIRv datasets and specific analytical approaches (Frankenberg et al., 2021; Sang et al., 2021; Zhu et al., 2021).

3.3 | Advancing precision agriculture

The mechanistic linkage among SIF, electron transport rate (ETR), and GPP has also generated momentum for employing SIF remote sensing as a non-invasive and cost-effective tool to advance precision agriculture towards improving food security. Research efforts range from informing G×E×M (**G**enetic variation by **E**nvironmental variation by agronomic **M**anagement) at the field scale (Belwalkar et al., 2022; Chang, Zhou, et al., 2020; Fu, Meacham-Hensold, et al., 2021; Jia et al., 2021; Zarco-Tejada et al., 2012) to advancing crop monitoring and yield estimation at the regional/global scales (Cai et al., 2018; Guan et al., 2016; Peng et al., 2020; Sloat et al., 2021).

At the field scale, high-throughput phenotyping and agronomic management have been increasingly exploited with remote sensing techniques, primarily focusing on RGB or multi-spectral images (Araus et al., 2018), but recently extending to SIF acquired from ground and UAV platforms as well as piloted aircraft. Promising results have been obtained in utilizing SIF to guide agronomic management. For example, SIF (itself or a SIF-based indicator) outperforms reflectance-based VIs in inferring leaf nitrogen content (LNC) of wheat (Jia et al., 2021; Wang, Suarez, et al., 2021), indicating its potential in improving nitrogen fertilizer management. Moreover, SIF (and/or its quantum yield) has been employed to infer V_{cmax} (and/or J_{max}) across cultivars, indicating the potential of SIF in rapidly screening cultivars with different traits (Camino et al., 2019; Fu, Meacham-Hensold, et al., 2021). In the future, such efforts can be guided by the toy model developed in Sun et al. (2023). For example, any trait variations among cultivars (related to genetic variations) may drive differences in variables (e.g., LAI, leaf angle, pigment content) and parameters (e.g., k_{λ_F}, k_{PAR}, $\overline{\beta}$, and that affecting the redox state) in equations 8–9 of Sun et al. (2023), assuming other conditions are equal.

At regional/global scales, numerous efforts have been made to estimate crop yields utilizing spaceborne SIF products. Earlier studies demonstrated that SIF, once translated to GPP, can be more precisely correlated with yield-based Net Primary Production (NPP) than VIs for corn and soybean (Guan et al., 2016; Guanter et al., 2014). Recent efforts, however, argued that the native coarse-resolution SIF retrievals superimposed with comparatively higher noise may not necessarily lead to superior performance than VIs (which are usually available at finer resolution and lower noise; Cai et al., 2018). Finer resolution SIF may lead to greater yield predictability than VIs, though other factors such as crop types and analytical approach can influence such predictability (He et al., 2020; Peng et al., 2020). However, Sloat et al. (2021) reported an opposite finding, that is, coarse-resolution SIF and NDVI exhibiting similar capability for in-season forecasting (of corn and soybean yield in the US Midwest). Such apparent discrepancies may be a consequence of disparate SIF retrieval approaches (Section 3.1) with varying qualities and different statistical yield estimation methods, and therefore caution is needed to interpret or compare these findings (detailed discussions in Section 3.8). Moreover, crop yield estimation utilizing SIF has almost been exclusively based on statistical approaches. Our developed toy model (Sun et al., 2023) has the potential to serve as a mechanistic model and a scalable approach to transform SIF to GPP and ultimately to crop yield.

3.4 | Enhancing stress monitoring capacity towards informing mitigation and adaptation practices

Both leaf-level Chl*a*F emission and canopy-level SIF observations (red, far-red, or their ratio) are sensitive to diverse abiotic stresses such as water, temperature, and nitrogen content (Ač et al., 2015), even when VIs are asymptomatic to these stresses (Daumard et al., 2010; Martini et al., 2022). Such sensitivity generated excitement for utilizing SIF as a cost-effective tool for monitoring climate stresses (i.e., temperature and droughts are projected to increase in frequency and intensity under climate warming, Seneviratne et al., 2021) and evaluating its agricultural, ecological, and

socioeconomic applications to inform decision-making for climate impact mitigation and/or adaptation (e.g., Jiao et al., 2019; Mishra et al., 2010).

At the regional to global scale, spaceborne SIF has been utilized to explore its capability in revealing the spatiotemporal patterns of drought/heatwave impacts and the underlying mechanisms. The general consensus is that, under severe and/or persistent stress, SIF exhibits a significant drop relative to its climatological mean, a pattern consistent across a number of record-breaking drought and heatwave events over the globe (Qiu et al., 2020; Song et al., 2018; Sun et al., 2015; Wen et al., 2020; Yoshida et al., 2015). The stress sensitivity of SIF (e.g., under drought) could vary spatially, depending on biome-characteristics and hydro-climatic regimes (Jiao et al., 2019). In particular, the tropical Amazon, due to its global significance in regulating the terrestrial carbon and water cycles, and in turn its climate feedbacks (both local and teleconnection), as well as sensitivity to the periodical El Niño-Southern Oscillation (ENSO), has been extensively studied in terms of drought impact. Anomalously lower SIF occurred from the late dry to wet season (Doughty et al., 2021; Koren et al., 2018; Li, Xiao, & He, 2018; Yang, Tian, et al., 2018) during the 2015–2016 El Nino events, but the severity of SIF anomaly had strong spatial heterogeneity and was susceptible to data uncertainties in SIF retrievals (Koren et al., 2018; van Schaik et al., 2020; Zhang, Joiner, Gentine, et al., 2018). The large reduction in SIF suggested a significant drop in GPP during the wet season, which may have contributed to the anomalously higher carbon release during this event (Gloor et al., 2018; Liu, Bowman, et al., 2017).

As SIF has the potential to identify physiological responses to stress that may be muted in VIs, SIF has been utilized in conjunction with reflectance-based *f*PAR to parse the relative contribution of structural versus physiological variations to the overall drought response. So far, the consensus is that, under severe and/or persistent stress, concurrent decline of *f*PAR and the apparent quantum yield of SIF (without correction of $f_{\Omega\uparrow}^{esc}$) are likely to happen, but their relative contribution can be biome-dependent and stress-severity dependent (Sun et al., 2015; Yoshida et al., 2015). Mechanistic explanation of such patterns and causal inference can be guided by equation 8 in Sun et al. (2023) in the future. For example, the contribution of *f*PAR (previously based on the LUE model) can be broken into light harvesting and canopy vertical extinction of PAR and SIF driven by the 3D leaf/canopy structure; the contribution of quantum yield of SIF can be studied separately from the contribution of PSII/PSI stoichiometry and state transition (if such ancillary information is available).

SIF may offer early warning of stress onset. An earlier study observed evidence of a steady decrease in canopy-level SIF under progressive water stress and a rapid rebound following rainfall recovery at a sorghum field, whereas NDVI and chlorophyll content remained unchanged during the same month-long period (Daumard et al., 2010). Other promising findings were reported at the regional scale with spaceborne SIF, which exhibited an earlier drop than VIs during the 2010 heatwave in India's Gangetic plain (L. Song et al., 2018) and identified flash drought in the US with a lead time of 2 weeks to 2 months (Mohammadi et al., 2022). However, other studies allude to limited capacity of SIF in early warning of stress onset resulting from rapid-changing physiological response, prior to any detectable changes in leaf/canopy structure (that can be detected by VIs; Wohlfahrt et al., 2018). For example, Sloat et al. (2021) reported a significantly better yield prediction with NDVI than with spaceborne SIF during droughts in the US Midwest. Further, disparate SIF-GPP responses under water/heat stress were reported (Section 3.1). Wohlfahrt et al. (2018) found a steady decline of GPP in a Mediterranean pine forest during the 2017 heatwave in Israel while a drop in canopy SIF did not emerge until the peak of stress, indicating a decoupling of light reactions and stomatal response under stress, a pattern that coincides with response of leaf-level (Helm et al., 2020; Marrs et al., 2020) and canopy-level SIF measurements (Chen, Liu, Du, Ma, & Liu, 2021) under water stress. In contrast, Martini et al. (2022) revealed an inverse SIF-GPP relationship at the sub-daily scale from both leaf and canopy measurements during the 2019 heatwave in a Mediterranean forest in Europe; such inverse relationship was attributed to NPQ saturation, which caused the excess APAR to be emitted as SIF. Such inverse patterns disappeared when daily mean values were examined, that is, concomitant decline in daily mean SIF and GPP, while NDVI and NIRv stayed stable. Such time scale-dependent SIF response to stress was also evident in Damm et al. (2022), which identified a nonlinear response of far-red SIF (from the airborne HyPlant measurements) to soil moisture deficit in a controlled water experiment for corn, that is, an initial brief increase followed by a subsequent decrease. Unfortunately, such complex SIF-NPQ-GPP dynamics under water/heat stress has not been adequately incorporated by the state-of-the-art mechanistic models, for example, SCOPE (Martini et al., 2022; Wohlfahrt et al., 2018), although De Cannière et al. (2021) reported improved water and carbon fluxes simulations during water stress if SIF was utilized to constrain the water stress functions in these models. Resolving these discrepancies requires improved theoretical understandings of underlying mechanisms (e.g., stress- avoiding or adaptation strategies, Flexas & Medrano, 2002; Rascher et al., 2004) and modeling of such understanding across stress types, severity, and duration (discussion in Sun et al., 2023; Section 3.1.1 above), as well as improved SIF data quality and consistency (Section 4.2).

3.5 | Inferring plant traits

Figure 1 and equation 10 of Sun et al. (2023) depict the theoretical, although convoluted, linkage between SIF and inherent plant traits. The capability of SIF for inferring plant traits has been explored, with target traits so far focusing on: LNC, chlorophyll content, and carboxylation parameters (e.g., V_{cmax}). For example, far-red SIF (and/or its ratio with the red SIF) is able to differentiate nitrogen treatments for both crop and natural species (Migliavacca et al., 2017; Schächtl et al., 2005), primarily driven by the strong sensitivity of far-red SIF to LNC (Ač et al., 2015). Moreover, the ratio of far-red to red SIF (or their normalized indices) is capable of inferring LNC (and in turn the

nitrogen use efficiency NUE) of wheat for both irrigated and rainfed fields (Camino et al., 2018; Jia et al., 2021).

As plant nutrients, especially LNC, are key compounds for chloroplast, photosynthetic pigments, and Rubisco, SIF has also been employed to infer chlorophyll content and V_{cmax}. Promising correlations of chlorophyll content with $\Phi_{FII}(red)/\Phi_{FII}(fr)$ (negative) or with far-red SIF (positive) have been consistently found from observations (Tubuxin et al., 2015) and modeling-based analyses (with SCOPE; Koffi et al., 2015; Verrelst et al., 2015). Regarding inferring V_{cmax} (or J_{max}) with SIF, conflicting results were reported, ranging from weak sensitivity (Koffi et al., 2015; Verrelst et al., 2015) to strong positive correlation (Y. Zhang et al., 2014; all based on ensemble SCOPE simulations), to negative correlation between SIF and V_{cmax} (or J_{max}; P. Fu, Meacham-Hensold, et al., 2021) based on field measurements. Han, Gu, et al. (2022) attempted to elucidate such discrepancies from theoretical perspectives, and revealed that SIF itself is insufficient to reliably infer V_{cmax} (or J_{max}), as their relationship is strongly regulated by the redox state of PSII (i.e., q_{LII}). Consequently, the sign and strength of SIF-V_{cmax} depends on actual environmental conditions that regulate q_{LII} and the actual carboxylation limitation stages (supporting information 5 in Sun et al., 2023). Despite such complex relationships, attempts of retrieving V_{cmax} via inverting process-based models with SIF as one major input have been made at both the field (Camino et al., 2019) and global scales (He et al., 2019). The fidelity of these inferred traits should be carefully evaluated, as SIF dynamics is impacted by a myriad of interacting canopy and functional processes (Sun et al., 2023), and teasing out a single trait requires information of all other processes being adequately anchored (e.g., equation 8 in Sun et al., 2023). In this regard, the analytical framework developed in Sun et al. (2023) can facilitate the trait inference, if harnessing the synergy of SIF with other sensing technology, for example, hyperspectral imaging, Lidar, and thermal, and microwave (Section 4.1).

Recently, SIF at high spatial resolution has been demonstrated as a powerful measure of ecosystem functional diversity, outperforming reflectances (and the derived VIs) and thus foreshadowing its potential for quantifying biodiversity (Tagliabue et al., 2020). This can also be explained by the analytical framework developed in Sun et al. (2023), that is, any structural and/or functional diversity can impact variables and parameters in figure 2 of Sun et al. (2023), and propagate to the observed $F_{\uparrow}(\lambda_F)$.

3.6 | Constraining the dynamics of the hydrological cycle

Motivated by the joint control of stomatal conductance (g_s) on photosynthesis and transpiration, SIF was employed to infer g_s, transpiration, and evapotranspiration (ET; Jonard et al., 2020). For example, X. Lu et al. (2018) found that the canopy-level SIF (especially far-red or a combination of far-red and red) was capable of estimating transpiration via parsimonious statistical scaling at the Harvard Forest, outperforming the classical Penman-Monteith (PM) model, which is more input/parameter-demanding. Expanding to global scales, Maes et al. (2020) showed promising correlation between GOME-2 SIF and transpiration (partitioned from ET measured at EC towers) across diverse biomes, which can be even stronger than the SIF-GPP correlation. Shan et al. (2021) and Zhou et al. (2022) further attempted to estimate transpiration with far-red SIF in a more mechanistic manner, by integrating Fick's law of water diffusion, optimal water use efficiency (WUE) theory, and empirical SIF-GPP scaling, from in-situ and satellite-based measurements, respectively. However, Damm et al. (2021) argued that the apparent promising empirical SIF-transpiration relationship is a consequence of their shared drivers, that is, PAR and LAI, while a robust estimation of transpiration requires not only SIF but also more nuanced considerations of environmental and physiological dynamics. Indeed, the apparent promising correlation between SIF and transpiration is sensitive to multiple assumptions that may break depending on biomes, time scale, stress conditions (Stoy et al., 2019). In particular, a linear SIF-GPP scaling assumption may result in bias in SIF-based estimation of g_s and transpiration. This issue should be resolved in the future by coupling equation 10 in Sun et al. (2023) and a stomatal conductance model.

3.7 | Contribution to socioeconomic impact and sustainability assessment

Beyond conventional applications in the domain of "natural science", satellite SIF has been recently employed as a real-time cost-effective tool for regional-scale socioeconomic evaluation, such as international development, sustainability, and food security. For example, high-resolution SIF products (e.g., SIF_{005}, Wen et al., 2020) were used as a major input for targeting, mapping and monitoring poverty/malnutrition in developing countries (Browne et al., 2021; McBride et al., 2022). These attempts were motivated by SIF's capability in monitoring (and potentially providing early warning, Section 3.4) of climate risks/shocks, which can induce crop and forage failure in rural areas of the developing world where poor households' livelihoods depend disproportionately, directly or indirectly, on crop and livestock productivity.

Another such example is evaluating the impact of the Sustainable Land Management Project (SLMP) in Ethiopia, to date one of the world's most ambitious national-scale land restoration programs, on ecosystem productivity (Constenla-Villoslada et al., 2022). SIF_{005} and GOSIF paired with intensive in-situ surveys revealed the substantial benefits of SLMP, that is, improved drought resilience of GPP in Ethiopia's degraded watersheds. Such national-scale socioeconomic evaluation was previously challenging with conventional survey-based approaches, which are costly and labor-intensive.

One emerging line of SIF application is to evaluate urban sustainability and human health. Cities support more than half of the global population. Urban vegetation supports urban sustainability and is critical for mitigating climate extremes via carbon sequestration and evaporative cooling. For example, Sun et al. (2017) demonstrated the remarkable urban–rural SIF gradients from OCO-2; further, SIF combined with LAI were used to quantify the role of evaporative cooling

in regulating urban heat islands (Paschalis et al., 2021). From a flipped perspective, the urban–rural climate gradient was taken as a natural experiment to study how future climate change/extremes impact on ecosystem health (P. Fu, Hu, et al., 2021; Wang, Ju, et al., 2019).

3.8 | Practical benefits and barriers of remotely sensed SIF over conventional surface reflectance and the derived VIs

One may wonder: Does the *mechanistic advantage* of SIF (i.e., carrying structural and functional information of plants, Sun et al., 2023), combined with its *lower sensitivity to atmospheric contamination* (such as thin clouds and thus alleviating potential data loss, Frankenberg et al., 2012), *reduced susceptibility to background soil* (i.e., non-fluorescing, Wang, Beringer, et al., 2019) and *to saturation under high LAI* relative to the conventional surface reflectance and/or derived VIs, outweigh SIF's practical barriers (e.g., coarser spatial/temporal resolutions and comparatively stronger retrieval noise/bias), and thus lead to practical benefits in real-world applications (e.g., crop yield estimation, socioeconomic impact evaluation, stress early-warning)?

The general consensus so far is a stronger sensitivity of SIF than NDVI to seasonal and IAV across all major biomes, but SIF does not appear to possess substantial comparative advantage over EVI or NIRv, especially for crops and temperate DBF (Badgley et al., 2019; Baldocchi et al., 2020; Dechant et al., 2022). Note that a comparison between SIF and surface reflectance (or VIs) as a proxy of GPP is not valid unless the latter is converted to a flux quantity with an energy unit (e.g., multiplied with irradiance/radiance; G. Wu et al., 2020). Moreover, intensive efforts utilizing hyperspectral imaging spectroscopy to infer plant traits have obtained promising outcomes (Serbin et al., 2016; Wang, Chlus, et al., 2020; Wang, Townsend, & Kruger, 2022; Zarco-Tejada et al., 2021). The practical benefits of SIF relative to hyperspectral reflectance remain to be explored, especially considering that SIF, as a flux variable, is not only affected by plant structural and functional traits (state variables) but also rapid environmental fluctuations, which need to be teased out. On the other hand, SIF may still carry greater scalability in inferring GPP (and other associated functions and traits) across biomes than NIRv, given its mechanistic linkage with ETR and GPP (equations 9 and 10 in Sun et al., 2023), despite the biome-specific or universal debate on the SIF-GPP scaling. Moreover, the practical advantage of SIF over NIRv may be more apparent under stress conditions (Damm et al., 2022; Martini et al., 2022), and when the growing season progresses towards senescence especially for conifers (Raczka et al., 2019). We should acknowledge that NIRv is still sensitive to the reflectance of soil, snow, wood and cirrus clouds, which is unrelated to SIF. This may make the relationship between NIRv and SIF biome-specific. In order to answer the above question, future research is critically needed to investigate more biomes (especially in tropical rainforests and boreal ecosystems in the northern high-latitudes where the largest uncertainties in carbon sink/source changes are located) and more dynamic environments (e.g., climate extremes and natural/anthropogenic disturbance).

4 | INNOVATIONS

> *Given the numerous discrepancies among current literature across the spectrum of applications (Section 3), does SIF help resolve existing knowledge gaps or add extra complexities and uncertainty?*

To answer this question, innovations are needed to fill existing theoretical and data gaps that currently challenge real-world applications (Figure 5). Sun et al. (2023) offers perspectives on research priorities and potential solutions to theoretical knowledge gaps. This paper focuses on discussing data gaps (Section 4.1), research innovations needed in observations (Section 4.2) and applications (Section 4.3).

4.1 | Data gaps

4.1.1 | Bias in "ground-truth" GPP and transpiration

Present studies all consider GPP fluxes partitioned from NEE of CO_2 (measured at EC towers) with the standard night- or day-time (NT or DT) based approaches (Lasslop et al., 2010; Reichstein et al., 2005) as the ground-truth, and use it to establish the empirical SIF-GPP scaling, or evaluate SIF product quality using the degree of their linearity as metrics. However, NT and DT are known to contain biases, the extent of which also change across the seasonal course and environmental variations (Keenan et al., 2019; Kira et al., 2021; Wehr et al., 2016). Similarly, transpiration fluxes at EC towers, usually taken as the in-situ gold standard for validation, are not directly measured but partitioned from the total ET, which involve common assumptions of transpiration/ET ratio approaching to unity and the optimal theory of WUE (Stoy et al., 2019). Under circumstances when these assumptions are violated (which can be common, Stoy et al., 2019), transpiration estimated from SIF can suffer from bias. Data uncertainties in GPP and transpiration fluxes are under-appreciated at present.

4.1.2 | SIF retrieval bias and noise

The SIF-GPP relationships (Figure 4) and all other applications obtained so far can be greatly confounded by bias and noise in SIF measurements/retrievals, for both spaceborne (Parazoo et al., 2019) and in-situ (Aasen et al., 2019; Cendrero-Mateo et al., 2019; Chang, Guanter, et al., 2020; Marrs et al., 2021; Pacheco-Labrador et al., 2019) platforms. Discrepancies among studies across applications identified in Section 3 may arise partly from these data artifacts.

Spaceborne SIF products can differ significantly across SIF retrieval algorithms, fitting spectral window, footprint size, overpass

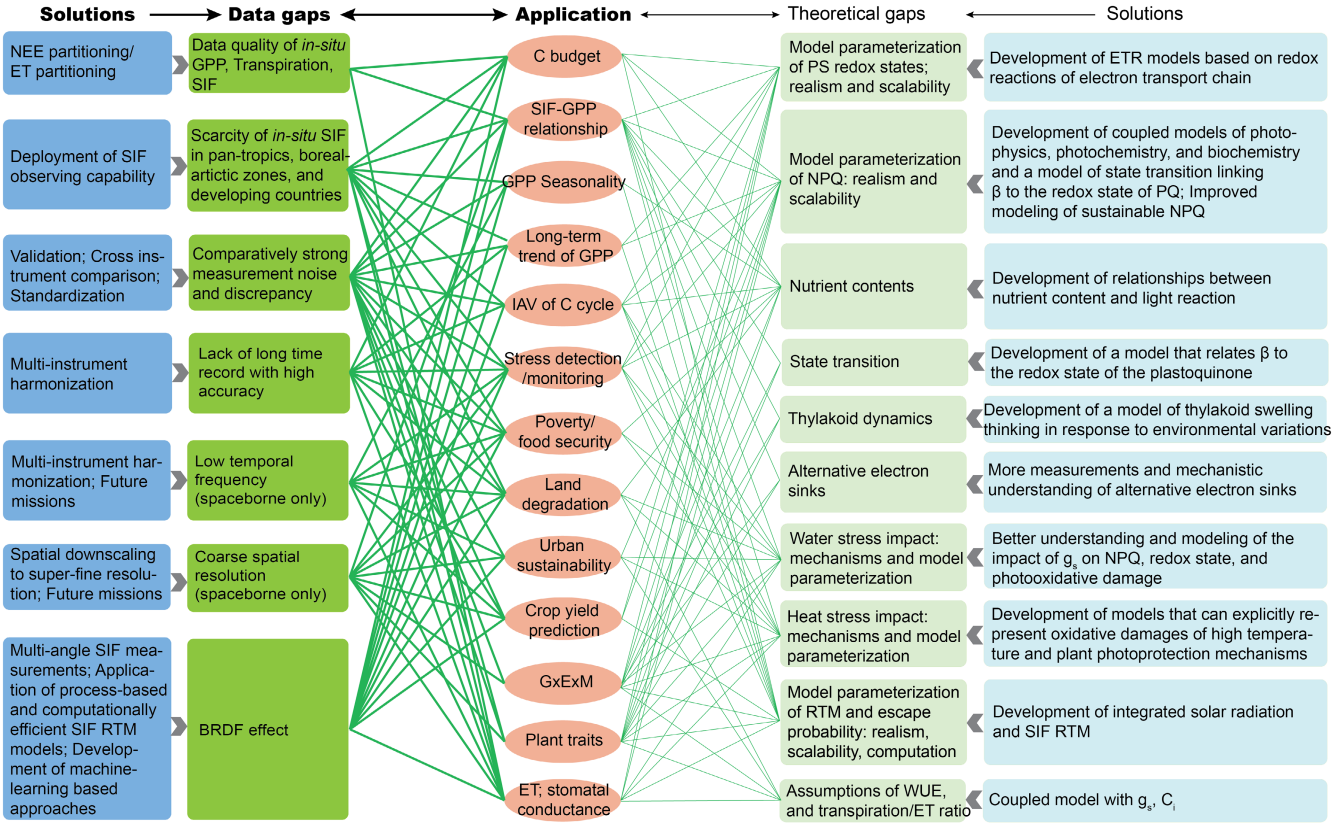

FIGURE 5 Existing theoretical and data gaps through the lens of applications, and potential solutions moving forward. This paper focuses on the theoretical side (the left columns highlighted in dark color) of this diagram. BRDF, Bidirectional Reflectance Distribution Function; ET, evapotranspiration; G×E×M, interactions of genetics, environment, and management; GPP, gross primary production; IAV, interannual variability; NEE, net ecosystem exchange; NPQ, non-photochemical quenching; PS, photosystem; RTM, radiative transfer model; SIF, solar-induced chlorophyll fluorescence; WUE, water use efficiency.

time, BRDF (Bidirectional Reflectance Distribution Function) effect, which can be further confounded by instrumental degradation and other calibration issues (Joiner et al., 2013; Oshio et al., 2019; Parazoo et al., 2019; Zhang, Joiner, Gentine, et al., 2018). For example, negative GOME-2 SIF anomalies can be an artifact of or amplified by its secular decline due to instrument degradation (Song et al., 2018; Yang, Tian, et al., 2018). The effects of clouds on moderate to low spatial resolution satellite data also have to be considered, although SIF retrievals with relatively good accuracy can be achieved under thin clouds and aerosol (Frankenberg et al., 2012). Validation of spaceborne retrievals has been a major challenge, particularly for instruments with larger footprints, where the representativeness error for comparison with in-situ instruments can be large.

Accuracy and precision of in-situ (and also airborne) SIF are sensitive to instrument configuration, calibration protocols, retrieval methods, and atmospheric conditions, as well as ambient environment (e.g., temperature, humidity) that can impact instrument stability (Aasen et al., 2019; Cendrero-Mateo et al., 2019; Chang, Guanter, et al., 2020; Chang, Zhou, et al., 2020; Marrs et al., 2021; Pacheco-Labrador et al., 2019).

Such uncertainties in SIF retrievals can propagate to the quantum yield of SIF, which is usually computed as the ratio of SIF against APAR (with or without correction of $f_{\Omega\uparrow}^{esc}$). As both the numerator and denominator are measurements/retrievals that contain noise/bias, the derived quantum yield of SIF could carry these uncertainties that may be further exaggerated by the division. Consequently, the quantum yield of SIF may not necessarily reflect true biological variations.

4.1.3 | Low temporal frequency

Most spaceborne SIF retrievals have relatively low temporal frequency (Table S1), which is inadequate to characterize the intra-seasonal variation of plant activities. This can inhibit SIF's full potential for phenology characterization (e.g., dryland ecosystems that have fast-changing dynamics and complex species composition/abundance), prediction of crop yield (as it is highly sensitive to agronomic management that can be irregular depending on weather fluctuations, and stress during grain filling that is short-duration), and monitoring/early-warning of fast-onset stresses. These applications may require at least sub-weekly temporal resolutions. For example, TROPOMI SIF has greatly improved revisit time, and demonstrated such benefits in depicting the complex seasonal trajectory of California's complex mixture of ecosystems (Turner et al., 2020).

4.1.4 | Lack of long-time record

The major roadblocks to applying spaceborne SIF to study the long-term trend and IAV of the terrestrial carbon cycle is lack of a SIF record that is both sufficiently long and of trustworthy quality. For example, native SIF retrievals from GOME-2 have the longest time coverage (Table S1), but suffer from inherent instrument degradation/orbital drift (i.e., post August 2013), which could lead to a spurious negative trend (van Schaik et al., 2020); GOSAT SIF is available for over 10 years but has sparse spatial sampling.

4.1.5 | Coarse spatial resolution and/or sparse spatial sampling

Current native spaceborne SIF retrievals are at low spatial resolutions and/or spatially discontinuous (Table S1). Value-added SIF products have relatively finer spatial resolution with global contiguous coverage (Table S1), but have not yet been sufficiently validated with independent in-situ or airborne SIF at high-resolution. Moreover, they can be susceptible to (a) biases/noise inherited from native SIF retrievals; (b) the training algorithm; (c) uncertainties in selected predictor variables. These limitations hamper the potential of SIF in truly benefiting crop monitoring and yield prediction, poverty and malnutrition targeting, or urban sustainability, which all require resolving complex and heterogeneous landscapes. For example, existing SIF-based attempts exclusively focus on developed countries where agricultural landscapes and management practices are more homogeneous and high-quality ground-truthing data (for calibrating yield estimation models) are more readily available. However, in heterogeneous landscapes (such as developing countries where farm size is typically small), present SIF products (both native and value-added products) are unable to resolve individual crop types or fields (Kira & Sun, 2020), making them of limited use to inform decision-making at the field-scale (e.g., fertilizer or irrigation). Moreover, none of the existing spaceborne SIF products can be reliably matched with in-situ socioeconomic surveys (e.g., poverty metrics, children malnutrition) due to their sparse data acquisition, randomized spatial offsets of socioeconomic data to protect respondents' privacy, or some combination. Consequently, it remains unclear whether SIF possesses substantial competitive advantages over conventional VIs for these operational applications, as the latter is technologically much more mature and available at super fine resolutions (e.g., sub-meter).

4.1.6 | Scarcity of in-situ SIF measurements

Despite the growth of in-situ SIF observing systems in the northern hemisphere mid-latitude, especially in agricultural regions, such systems are sparse in the pan-tropics and arctic/boreal regions as well as developing countries (e.g., Africa; see figure 4 of Parazoo et al., 2019), a situation similar to the uneven global distribution of the EC flux measurements (Schimel et al., 2015).

4.2 | Observational innovations

4.2.1 | Satellite missions and airborne campaigns

Validation and cross-instrument standardization

High SIF data accuracy/precision is foundational to meaningful downstream applications. Parazoo et al. (2019) demonstrated that agreement among spaceborne SIF retrievals can be achieved if overpass time, fitting windows, and viewing angles are standardized. Dedicated efforts have also been made to apply standardized retrieval algorithms consistently to GOME, SCIAMACHY, and GOME-2/MetOp-A (and also corrected the artificial trend in GOME-2 SIF). Such cross-instrument comparison and standardization should continue in the future (e.g., extending to other spaceborne instruments, as well as airborne measurements), to further improve the retrieval accuracy/precision of spaceborne SIF products. In addition, validation of spaceborne SIF retrievals (as well as value-added products and airborne measurements) with in-situ SIF is critical, but remains a major research gap. Challenges preventing effectiveness of such efforts include scale mismatch, inconsistency in instrument configuration and retrieval approaches, BRDF effect, and so forth but can be addressed if utilizing trustworthy radiative transfer model (RTM) simulations (section 3.1 and table 1 in Sun et al., 2023) as a bridge to reproduce both in-situ and spaceborne/airborne SIF in parallel under their respective instrument setup and landscape scenarios.

Multi-instrument harmonization

So far value-added SIF products (e.g., based on ML approaches) date back to 1995, but their reliability still requires further investigation, given the above-stated quality issues in native SIF retrievals, which the value-added SIF products are trained against. Also, temporal extrapolation has been employed to cover periods prior to the availability of native SIF products, but may result in bias as the true SIF signal falls outside the "observed" range/distribution of the training period. One alternative approach to extend the timespan is to harmonize SIF from different instruments with some overlaps (Parazoo et al., 2019; Wang, Zhang, et al., 2022; Wen et al., 2020), for example, GOME (1995–2003), SCIAMACHY (2003–2012), GOME-2/MetOp-A (2007–2018; Joiner et al., 2019, 2021), and MetOp-B/C (2012–present; Table S1). Caution is needed as quality of such harmonized products is contingent upon consistency of the native products across different instruments.

Pushing higher-frequency sampling

A new frontier in spaceborne SIF will be realized with the first measurements from geostationary (GEO) platforms on an approximately hourly basis. These observations, from Tropospheric Emissions: Monitoring Pollution (TEMPO) and Sentinel-4, may provide a

glimpse into diurnal variability in plant function at a regional scale (Figure 6). While the suite of current instruments in LEO covers a wide range of hours due to their large swaths and slightly inclined orbits, recovering information on the diurnal variations in plant physiology was found to be problematic owing to the difficulty in accounting for the large variations due to sun-viewing geometry (Joiner et al., 2020). GEO observations, in contrast, will have a fixed geometry day-to-day for a given point on Earth and a given time of day. Both SIF and reflectance have complicated diurnal variations owing to changes of sun-viewing geometries throughout a day, making it difficult to decouple structural and physiological effects on SIF (Chang et al., 2021). Averaging at fixed times of day and fixed locations, where the GEO satellite geometry is identical day to day may lead to the ability to detect temporal anomalies in the SIF signal at different times of day. Here, it would not be necessary to adjust for the structural effects that may impact the signal over the course of a day; rather these effects on SIF would be assumed to remain relatively stable over short time periods. The anomalous signals due to stress could then be studied at different times of day as indicated in Figure 6.

Harnessing the synergy of SIF with hyperspectral imaging, Lidar, and thermal, and microwave remote sensing

In principle, SIF carries plant physiological information beyond plant biophysical properties that hyperspectral reflectance can help infer and leaf/canopy structures that lidar (or VIs) can characterize (figure 2 in Sun et al., 2023). On the flip side, SIF is a mixed signal of all these factors, making it necessary to disentangle them. This is particularly critical for applications where a pool of plant traits is required in applications such as plant phenotyping (Belwalkar et al., 2022), precision agronomic management (Wang, Suarez, et al., 2021), and disease detection (Poblete et al., 2021; Zarco-Tejada et al., 2018). One innovation is to harness the complementary strengths among SIF, hyperspectral reflectance, and lidar to disentangle contributions from physiological variations, leaf biophysical traits (e.g., chlorophyll, carotenoids, xanthophylls and anthocyanin content), and canopy structure (e.g., LAI, leaf inclination angle, canopy height, and crown volume; Porcar-Castell et al., 2021; Schimel & Schneider, 2019; Stavros et al., 2017). For example, an optimal instrument would measure radiance in the visible and NIR range to derive hyperspectral reflectances and SIF simultaneously, and thus ensure the same sun-viewing geometry between them. Most SIF-capable instruments currently flying in-orbit do not have such capability. Moreover, utilizing synergies with thermal and/or microwave-based measurements (i.e., Land Surface Temperature LST, soil moisture) when possible can also help disentangle contributions from physiology versus leaf-canopy structure under biotic or abiotic stress. Harnessing these diverse and complementary remote sensing techniques can also help infer ecosystem efficiency terms, such as light use efficiency (LUE), water use efficiencies (LUE), carbon use efficiencies (CUE), and nitrogen use efficiency (NUE), which cannot be measured directly but carry functional information of ecosystem dynamics (Schimel & Schneider, 2019; Stavros et al., 2017). To facilitate such synergy, the key here is to integrate different types of measurements from the "hardware" side as much as possible (e.g., a single multi-functional instrument, or different instruments onboard the same platform), which is more beneficial than from the "software" side (e.g., correction of sun-viewing geometry, irradiance calibration, or footprint mismatch via post-processing). Meanwhile, theoretical modeling is much needed to guide the integration of different data streams (e.g., equations 8–10, and figure 2 in Sun et al., 2023) and maximize their information content while mitigating their individual measurement uncertainties. For example, LAI and pigment contents that determine light harvesting in equation 8 of Sun et al. (2023) could be anchored (to some degree) by Lidar and hyperspectral measurements, and hence SIF can be used to infer other physiological quantities. On the other hand, these diverse measurements can help reveal the degree to which and conditions under which certain assumptions hold in deriving the analytical equations of Sun et al. (2023), and hence identify quantities/variables that should be prioritized for either more data collection, process understanding, or sophisticated modeling (laid out in figure 5 in Sun et al., 2023).

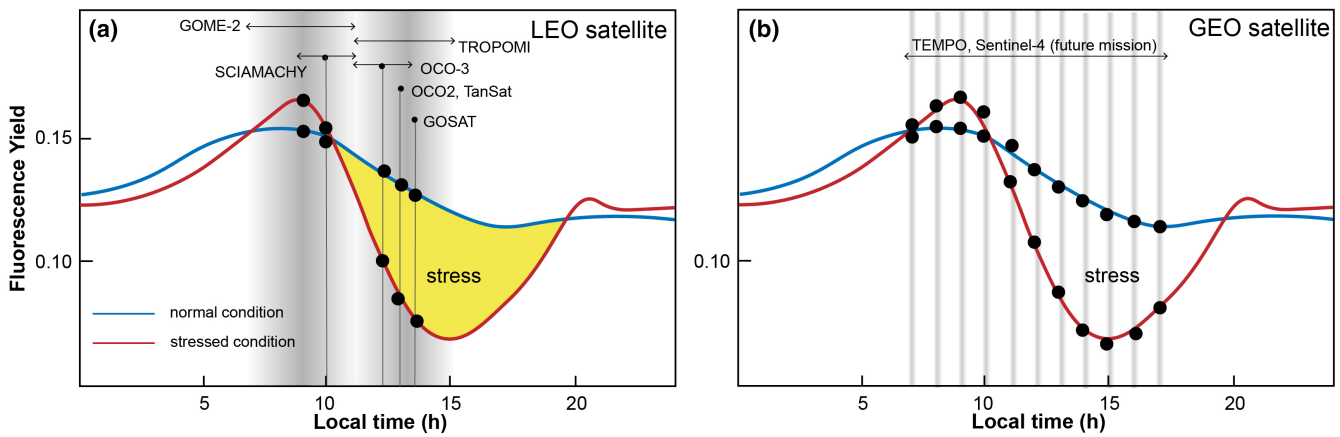

FIGURE 6 Diagram of resolving diurnal cycle of spaceborne solar-induced chlorophyll fluorescence for the past and future from (a) Low Earth Orbit (LEO) and (b) geostationary (GEO) platforms.

4.2.2 | Canopy-scale observations

Standardization of instrument configuration, calibration, and retrieval methods

The diversity of available in-situ systems and retrieval methods for canopy SIF currently presents a challenge for large-scale syntheses that have proven fruitful in other ecological networks (i.e., Fluxnet), as SIF observation so far has no standardization of procedure, calibration, or system design across sites and principal investigators (PIs). Such standardization is critical for establishing an effective global SIF network, ensuring comparability across SIF measurements (Aasen et al., 2019; Albert et al., 2023; Cendrero-Mateo et al., 2019; Marrs et al., 2021; Pacheco-Labrador et al., 2019), and validating spaceborne SIF retrievals. To facilitate this endeavor, differences among system configurations and retrieval methods for the same canopy target must be carefully quantified and corrected. This can be done with concurrent bi-hemispherical and hemispherical-conical systems, ideally mounted on both stationary tower and mobile UAV platforms. Continuous high-frequency point measurements at fixed locations of a stationary tower and spatial mapping (within the tower footprint) with flexible resolution/altitude control of a mobile UAV offer complementary information towards quantifying (a) spatial heterogeneity within a tower footprint, (b) impact of atmospheric conditions on SIF retrievals. In the meantime, intercomparison of different instrument configuration and retrieval methods must be conducted over a wide range of biomes and sky conditions (Chang et al., 2021; Chang, Zhou, et al., 2020). Further, each system should simultaneously observe a minimum set of meteorological variables (e.g., radiation, temperature, humidity, and wind speed) that can facilitate designing practical solutions for correcting differences of SIF retrievals across system configurations.

Improving in-situ SIF observing capability in "data desert" regions

The information contained in SIF complements that observed by EC systems. Thus more SIF observations should be conducted at well-established flux sites such as AmeriFlux or Fluxnet, perhaps using integrated SIF-EC systems (Gu, Wood, et al., 2019). In particular, more in-situ SIF instruments are needed in "data desert" regions, for example, tropical rainforests and northern hemisphere high-latitudes where the most discrepancies among literature and largest uncertainties in carbon fluxes/storages as well as strength of carbon-climate feedbacks (Schimel et al., 2015) are both located. Also, dryland ecosystems, although important in regulating IAV of the global carbon cycle, are underrepresented by in-situ SIF (and EC) measurements (Schimel & Schneider, 2019). Deploying more SIF observing systems in these areas will assist satellite SIF retrievals (e.g., validation and spatial scaling) for constraining regional carbon mapping/budgets. Moreover, improving in-situ SIF observing capability in areas with high socioeconomic vulnerability is also highly beneficial (discussion in Section 3.7).

Development of high-resolution SIF-specific spectroradiometers

A critical need of observational innovation is the development of high-resolution spectroradiometers that are designed specifically for observing SIF. Scientists have been working with companies to design spectroradiometers tailored for SIF research (e.g., Ocean Optics QE-Pro), while others have used off the shelf spectrometers (e.g., ASD Field Spec). These spectrometers contain a great number of charges coupled devices (CCDs) that collect charges at wavelengths that are not usable for SIF retrieval. These unusable CCDs increase the cost, contribute to heat generation which decreases spectroradiometer sensitivity, and limit the number of CCDs that can be used in a spectroradiometer for retrieving SIF at single wavelengths. Future development of SIF-specific spectroradiometers should focus on Fraunhofer lines and oxygen absorption bands which are highly resolved with a limited number of CCDs in neighboring bands to provide reference wavelengths. Similar to point measurements, SIF imaging systems will also be useful but will need to undergo strict retrieval processes and reflectance correction (Frankenberg et al., 2012). A close collaboration between the SIF science community and industry is needed to develop SIF-specific spectroradiometers.

4.2.3 | Leaf scale observations

At the canopy level, the true values of neither SIF nor GPP can be directly measured and known. Therefore, it is at the leaf level that the relationship between SIF and photosynthesis can be theoretically established and verified. Currently, no commercially available instruments can be used to measure total Chl*a*F emission from a leaf, which includes adaxial and abaxial emissions and re-absorption. Current commercially available fluorometers output fluorescence quantum yield (typically across all wavelengths >700 nm) in arbitrary units, which must be ratioed to a reference (e.g., maximal or minimal fluorescence, Baker, 2008) in any calculations. These measurements cannot be used directly as total Chl*a*F emission (i.e., in the unit of $mol\,m^{-2}\,s^{-1}$). There is an urgent need for fluorometers that can measure total Chl*a*F emission from a leaf directly (Magney et al., 2017; Meeker et al., 2021; Van Wittenberghe et al., 2019, 2021). This includes both broadband and spectral fluorescence from both the adaxial and abaxial sides. Ideally, these emission measurements should be accompanied with transmittance measurements of λ_F, perhaps with incidence from both adaxial and abaxial sides. These transmittance measurements can be used to estimate the fraction of total Chl*a*F emission that is being self-absorbed with a leaf RTM, for example, equation S25 of Sun et al. (2023) derived with Beer's Law.

Ideally, the true Chl*a*F emission measurements at the leaf level should be jointly conducted with conventional PAM fluorometry and gas exchange measurements (Magney et al., 2017; Meeker et al., 2021). With these measurements, mechanistic Chl*a*F emission models can be tested and theoretical SIF-photosynthesis relationships can be verified. Breakthroughs in this much-needed innovation

cannot be made without close collaboration between the scientific community and industry.

4.2.4 | Bridging the scaling gap: From leaf to canopy, to ecosystems, and to the globe

Built upon innovations at individual scales discussed above, efforts are also much needed to bridge the "scaling" gap from leaf to canopy, ecosystems, and globe, a paramount issue not only to SIF but almost to every variable in the Earth system science context. For example, it is challenging to couple SIF acquiring instruments at different scales, due to their vastly different footprints composed of dynamic/heterogeneous vegetation structures/functions (Sun et al., 2023). Specific to leaf-to-canopy scaling, vertical profiling of the joint spectral SIF, PAM fluorometry, and gas exchange measurements (Section 4.2.3) along with a hemispherical-conical system over a plant canopy will be ideal to resolve these issues. Further, concurrent stationary tower and mobile UAV measurements (Chang et al., 2021) will offer quantitative information on spatial heterogeneity within a tower footprint, towards bridging the gap from individual canopy to the ecosystem scale. Most often, the relationship between SIF and GPP (or with other variables) had to be examined with mismatched footprints. To resolve such scale mismatch, emerging efforts attempt to couple the OctoFlox SIF system and LI-7000 gas analyzers (acquiring carbon and water fluxes) for crop measurements in enclosures with precise temperature and CO_2 control. This allows a much closer footprint (~1–2 m^2) than any setup currently achievable with EC towers. In the meantime, the theory-driven model remains an important tool to bridge the scaling gap, as model simulations can be conducted at any temporal and spatial scale while measurements can only be made at discrete and disparate scales. If measurements made at different scales can all be reproduced by model simulations, confidence can be gained in these models. For example, the theoretical framework developed in Sun et al. (2023) can be applied and tested for such purposes.

4.3 | Application innovations

To advance our current understanding of SIF dynamics and expand its utility to infer ecosystem structure, function, and service, we offer perspectives on potential application innovations.

4.3.1 | Innovations in ecological applications

Quest for the "true" GPP across time and space

The culprit of the challenges in pinning down the true GPP and its variability in space and time is the infeasibility of directly measuring this flux beyond a single leaf. In the quest to identify "true" GPP at the canopy scale and beyond, SIF should be utilized in a way that can stay away from the current known uncertainties, moving beyond simple correlational analyses between SIF and existing GPP estimates that are well documented to have bias at many different scales. Two potential pathways to tackle this core problem: *What is the true GPP, at the canopy and global scale respectively?*

A. NEE partitioning. At the canopy scale, the commonly referred "gold standard" GPP at EC towers, is not a direct observable, but rather indirectly inferred from the directly measurable NEE with EC techniques (Lasslop et al., 2010; Reichstein et al., 2005). SIF could be employed in a way that truly escapes from existing known uncertainties. For example, it could be directly used to partition NEE, if functional relationships can be integrated with SIF to anchor GPP (e.g., the toy model developed in Sun et al., 2023). Initial exploration has been made for a single biome (e.g., C4) during a single growing season (Kira et al., 2021) but much larger-scale coordinated efforts are needed to expand such exploration, that is, for more biomes/sites with SIF-observing capabilities. Such strategies would allow for true GPP inference and avoid the current "circular" and "uncertain" approaches (Section 3.1). In the meantime, we should always be vigilant to measurement quality/noise, and cross-site calibration/standardizations, which are key to ensure faithful GPP estimation (Section 4.1).

B. Integration of SIF, OCS, and $\delta^{13}CO_2$. Over the past decades, multiple photosynthetic tracers, including SIF, carbonyl sulfide (OCS), and $\delta^{13}CO_2$ isotopes, were identified and utilized to constrain GPP fluxes (Campbell et al., 2017; Graven et al., 2020). Specifically, OCS is an atmospheric trace gas that diffuses from the atmosphere to photosynthetic enzymes along a shared pathway with CO_2. It is consumed by plants (Berry et al., 2013; Campbell et al., 2008; Montzka et al., 2007; Seibt et al., 2010; Whelan et al., 2018; Wohlfahrt et al., 2012), and at regional scales is closely correlated with GPP (Campbell et al., 2017; Hilton et al., 2017). ^{13}C isotope has long been used to study photosynthetic metabolism and its environmental response (Farquhar et al., 1989), taking advantage of the unique feature of isotopic discrimination of photosynthesis, that is, selective uptake of $^{12}CO_2$ over $^{13}CO_2$. The long-term measurements of atmospheric $\delta^{13}CO_2$ have also been used to provide unique insights on the growth trend of global GPP and WUE along with the underlying drivers (Graven et al., 2020; Keeling et al., 2017). The shared strength of these independent tracers is their capability to directly infer photosynthesis without involving uncertainties in separating ecosystem respiration. However, progress toward this end has only been made within their respective communities; their joint power for constraining predictive understanding of GPP has never been explored or realized. Future research efforts should leverage their unique and complementary strengths as photosynthetic tracers. Towards this end, a theory-driven model that can mechanistically represent/connect these three tracers is foundational to harnessing their synergy. For example, coupling the analytical equation(s) (e.g., equations 8 and 10) in Sun et al. (2023) with an OCS model (Berry et al., 2013; Kooijmans et al., 2021) can be a starting endeavor.

Pigment content

Pigment contents are sensitive to various environmental stresses. Large scale monitoring of pigment contents represents one of the most promising applications of SIF remote sensing for climate change and ecosystem research. As Chl*a*F is emitted by excited chlorophyll molecules, a natural application of SIF would be to use it to monitor chlorophyll content. Equation 8 in Sun et al. (2023) shows that SIF could be approximately proportional to the pigment content of the canopy if LAI and PAR are controlled. To our knowledge, this approach has not been tested, but may be more direct and sensitive than reflectance/transmittance-based approaches, as it has a theoretic basis and can be derived in a mechanistic way, as opposed to the conventional approach such as statistical regression (Wang, Townsend, & Kruger, 2022).

4.3.2 | Innovations in hydrological applications

ET partitioning

Evapotranspiration is a keystone climate variable that links the water cycle, energy balance, and carbon cycle (Fisher et al., 2017; Katul et al., 2012; Monteith, 1965; Wang & Dickinson, 2012; Wong et al., 1979). Its trajectory under changing climate, however, is highly uncertain (Gedney et al., 2006; Mao et al., 2015; Piao et al., 2007; Zeng et al., 2017). One primary reason for such uncertainty is a lack of understanding of how ET is partitioned into its constituent fluxes—transpiration (T) and evaporation (E)—across a wide range of bio-climatic conditions, because these components are differentially impacted by changing temperature, CO_2, and hydrologic regimes (Fisher et al., 2017; Lawrence et al., 2007; Miralles et al., 2016; Wang & Dickinson, 2012). Studies have reported a large divergence of global T:ET ratio (Coenders-Gerrits et al., 2014; Fatichi & Pappas, 2017; Wang et al., 2014; Wei et al., 2017), indicating a severe lack of understanding of the dynamics of ET partitioning and its underlying controlling factors. This level of uncertainty impairs the ability to predict both *future ET budgets* (due to the differential sensitivity of E and T to environmental forcings) as well as *how ET will dampen or amplify climate feedbacks* (Fisher et al., 2017). It will also inhibit our ability to *optimize sustainable water allocations for food production* in a changing climate to meet the demands of a growing population (Foley et al., 2011).

A major source of difficulty to partition the observed ET (at the canopy scale), which is typically measured with EC techniques, into the desired E and T is due to a lack of constraining information. This issue is, in many ways, similar to the classical problem of NEE partitioning (Section 4.3.1). Existing efforts utilizing SIF to constrain transpiration is highly empirical (Section 3.6), and involves many assumptions (Stoy et al., 2019; discussed in Sun et al., 2023). Currently, there are no studies explicitly utilizing SIF to partition ET in a mechanistic way, and also bypassing the key assumptions. A promising approach is to couple the light-reaction based GPP estimation derived from SIF (e.g., equation 10 in Sun et al., 2023), with g_s models and energy balance models, in order to dynamically close the system of equations. In this regard, thermal remote sensing would be also helpful to constrain the energy balance model (e.g., leaf/canopy temperature; Anderson et al., 1997), while concurrent SIF can anchor GPP, both in a mechanistic way. ET partitioning can be further combined with NEE partitioning above, to fully take advantage of the constraining power of shared information contained in ET and NEE fluxes and in the meantime preserving the authentic functional relationships among constituent components and their respective sensitivity to environmental forcings.

Stress monitoring and early warning

To unleash the potential of SIF in assisting operational stress monitoring and early warning systems for informing stakeholders and policy-making, it is crucial to have real-time SIF observations at high temporal frequency (e.g., sub-daily) and fine spatial resolution. The diurnal SIF capability from GEO satellites, for example, TEMPO (Section 4.2.1), holds potential to reveal both the short-term physiological dynamics and long-term impacts. Exploration along this line can already be started with platforms like OCO-3 or synthetic simulations with observing system simulation experiments (OSSEs)-type systems (Somkuti et al., 2021). To concurrently alleviate the issues of coarse spatial resolution (which is the case for geostationary satellite), data fusion with other types of spaceborne observations available at fine resolutions (e.g., reflectance, thermal, radar) with state-of-the-art ML techniques (Gensheimer et al., 2022) are worth research exploration. Elucidating the mechanisms in response to stress, especially co-occurring events, requires effective synergy of different sensing techniques (e.g., SIF, thermal, hyperspectral, lidar) along with mechanistic models/understanding.

4.3.3 | Innovations in agricultural and forestry management applications

Agriculture and forest management must rapidly adapt to face challenges including extreme climate events, shifting prevalence of diseases and pests, changes in water availability and temperatures. Two main and complementary avenues of agricultural and forest management research focus on climate adaptation and mitigation. The adaptation strategy focuses on identifying or developing plant species and cultivars, as well as management practices, which are better suited for future climate conditions through a better understanding of G×E×M interaction in phenotyping studies. The mitigation strategy focuses on developing and improving regional or site-specific plant and environmental monitoring systems which can alert when and how to adjust management practice, for example, by knowledge guided fertilization, optimized pesticide and herbicide use and irrigation schemes. SIF could be an advantageous tool for both adaptation and mitigation strategies, due to the critical nature and sensitivity of photosynthesis for plant health and productivity.

Climate change adaptation

While fluorescence-based phenotyping approaches are already widely included in laboratory, greenhouse and field trials (Murchie

et al., 2018), airborne-based hyperspectral scanners capable of assessing plant traits including SIF for operational stress detection in the context of plant phenotyping only recently emerged (Belwalkar et al., 2022). For example, Belwalkar et al. (2022) demonstrated that hyperspectral airborne imaging spectrometers of 5–6 nm FWHM can quantify the spatial variability of SIF linked to nutrient deficiencies towards improving plant phenotyping. Airborne systems capable of SIF retrieval are well-adapted for precision agriculture applications but often lack spatial resolution for the relatively small plots of field phenotyping (Krämer et al., 2021). UAV-based SIF sensors (imaging and non-imaging) are currently being developed with the goal to close this technological gap and it can be expected that such UAV-based SIF approaches will become available for a wider use in field phenotyping science (Bendig et al., 2018; Chang, Zhou, et al., 2020; MacArthur et al., 2014; Quirós-Vargas et al., 2020; Wang, Suomalainen, et al., 2021).

On the other hand, active fluorescence techniques are often lacking high throughput capabilities for large field-phenotyping experiments. Recently laser-based scanning fluorescence systems have been shown to potentially overcome this limitation of throughput, but thus far only a very limited number of studies using active fluorescence approaches are available (Keller et al., 2022; Zendonadi Dos Santos et al., 2021). Developing SIF-capable phenotyping systems may allow for rapid screening of genotypes with high photosynthetic capacity under different environmental and/or management conditions in statistically relevant settings. In the future, such efforts can be further coupled with the analytical modeling framework in Sun et al. (2023) to uncover the biological (both plant structure and function) drivers.

Climate change mitigation

The rapidly exploding availability of ground and satellite measurements for crops and forests is currently revolutionizing management practice by enabling the farmer and forest manager to detect both abiotic and biotic stresses earlier than conventional approaches. Here, SIF may play a unique role in identifying early signs of vegetation stress, before classical measurement techniques (reflectance- or thermal-based approaches) become sensitive (Damm et al., 2022). Studies have demonstrated the potential of SIF for monitoring of water stress in fruit orchards (Zarco-Tejada et al., 2016), potato (Xu et al., 2021), heat stress in wheat (Song et al., 2020), and disease in olive orchards (Poblete et al., 2020; Zarco-Tejada et al., 2018) and oak forests (Hernández-Clemente et al., 2017). SIF may also play a unique role in early detection and improving the specificity of disease detection by complementing hyper- and multispectral methods (Mahlein et al., 2019). For example, SIF has also been demonstrated critical in the early detection of pathogen-induced stress due to the reduction in photosynthesis along with the degradation and reduction of the concentration of plant pigments such as anthocyanins, xanthophylls, chlorophyll and carotenoids quantified using airborne imaging spectroscopy (Zarco-Tejada et al., 2018). In such a study, SIF was the fifth ranked plant trait used in the ML model to detect all levels of infection, but ranked first at the initial (pre-visual) versus advanced pathogen infection stages. This indicates that SIF is modulated by the infection level, and is important to differentiate between biotic- and abiotic-induced stress (Zarco-Tejada et al., 2021). Moreover, the sensitivity of SIF to pathogen-induced stress in vascular diseases was shown across plants infected with *Verticillium dahliae* and *Xylella fastidiosa* using airborne imaging spectroscopy (Poblete et al., 2021).

4.3.4 | Innovations in socioeconomic and sustainability applications

Socioeconomic assessment and intervention

The core promise that SIF offers is a scalable measure in time and space, binded in its functional and quantifiable relationship with productivity, unlike VIs. A "scalable" approach is highly desired as it would not require much in-situ data for model recalibration, which can be cost- or logistically-prohibitive to obtain especially in regions with poor communications, low-quality transportation infrastructure or suffering from active conflicts (Browne et al., 2021). The potential "scalability" of the SIF-based approach to link between GPP and agricultural production, rangeland health, and carbon sequestration (and also carbon accounting/trading) make SIF a highly promising Earth Observation (EO) technique to aid poverty targeting/intervention, agricultural index insurance design, conservation finance metrics, and carbon-neutral goals. Advances in these applications also open up important new opportunities to extend SIF application to broader policy questions, from addressing food insecurity and rural poverty in the Global South, to monitoring forest degradation for conservation finance, and to identifying infectious disease hotspots based on inferred ecosystem structure and function.

Urban sustainability

Maintaining and enhancing urban ecosystem health is a critical step towards sustainable urban development under a changing climate. A degraded urban ecosystem combined with a rapid urban expansion can decrease NPP (Liu et al., 2019). The spatial or temporal anomalies of SIF in complex urban landscapes can potentially assist understanding the feedbacks between urban vegetation and the microclimate under urban environmental stresses (e.g., drought and heat extremes). However, depicting such variations from much weaker background urban SIF signals (due to relatively low coverage of vegetation) requires more precise retrievals from satellite platforms. This also requires isolation of the urban vegetative SIF signals from building interference, which can impact the illumination-viewing geometry in tall building districts. An initial attempt (Paschalis et al., 2021) used the simple urban–rural contrasts among cities to characterize the spatial variability of evaporative cooling using SIF but was limited by its coarse spatial resolution. Growing spatial resolutions with improved SIF retrieval algorithms over heterogeneous landscapes can offer new research opportunities on intra-urban variability of urban vegetation health and the

consequent capability in mitigating heat and air pollution, which is vital in human living environments. SIF measurement that can reveal biological processes in all forms of urban greenery is much needed for effective management and long-term development of sustainable community-level urban infrastructures in the context of climate change and environmental justice.

5 | CONCLUSIONS

This review synthesizes progress in SIF observations/instrumentation while highlighting diverse applications of SIF datasets in ecology, agriculture, hydrology, climate, and socioeconomics research domains. This synthesis identifies inconsistent/contradictory findings in SIF literature, provides clarifications on these issues, and offers insights, from the data perspective integrated with the theoretical perspective, on innovations needed to fill knowledge gaps in utilizing SIF to inform ecosystem structure, function, and service under climate change. Key points this review aims to deliver are:

- *Data uncertainty*: Accurate interpretation of the functional relationships between SIF and other ecological indicators is contingent upon complete understanding of the SIF data quality and uncertainty. Biases and uncertainties in SIF observations can significantly confound interpretation of their relationships and how such relationships respond to environmental variations. Controlling data uncertainties requires coordinated efforts of SIF-specific instrumentation design, uncertainty quantification, tracing, and documentation. For example, despite the many merging value-added SIF products, their accuracy and credibility require further investigation, given the many yet-to-be-resolved uncertainties in native SIF retrievals (against which value-added SIF products were trained) and well-documented low transferability of ML algorithms in time and space.
- *Data network coordination and synthesis*: To promote the mechanistic understanding of SIF and its relationship with other ecological indicators across biomes and hydroclimatic regimes, a dedicated effort is needed to establish a global network with in-situ and airborne SIF instruments, with standardized protocols to minimize discrepancies resulting from instrument configuration/setup, retrieval methods, atmospheric contamination, sun-canopy-viewing geometries, and so forth.
- *Improving in-situ SIF observing capability in "data desert" regions*: More in-situ SIF observations are needed in regions with the largest uncertainties in carbon-climate feedbacks or with high socioeconomic vulnerability.
- *Data fusion and harmonization*: There is a need to maximize the synergy among different SIF products, and among SIF, thermal, lidar, and hyperspectral, and microwave measurements. Standardization is needed to minimize challenges in SIF post-processing such as cross-instrument calibration, overpass time, instrument degradation, footprint mismatch, and so forth.

ACKNOWLEDGMENTS

YS, JW, JL, and ZL acknowledge support from NSF Macrosystem Biology (Award 1926488), NASA-CMS (80NSSC21K1058), NASA-FINESST (80NSSC20K1646), NASA MEaSures project, USDA-NIFA Hatch Fund (1014740), and the Cornell Initiative for Digital Agriculture Research Innovation Fund. CYC acknowledges support from USDA, Agricultural Research Service. JL acknowledges the Saltonstall Fellowship from the Soil and Crop Science Section at Cornell University. LH acknowledges support from NASA-IDS (80NSSC20K1263) and NASA-HAQAST (80NSSC21K0430). JJ is supported by NASA through the Arctic-Boreal Vulnerability Experiment (ABoVE) science team. LW acknowledges partial support from NSF Division of Earth Sciences (EAR-1554894). YS, JW, LH, and CBB also acknowledge support from USAID Feed the Future program (7200AA18CA00014). TSM acknowledges the Macrosystems Biology and NEON-Enabled Science program at NSF (award 1926090). ORNL is managed by UT-Battelle, LLC, for DOE under contract DE-AC05-00OR22725. We acknowledge Kathleen Kanaley for proofreading.

CONFLICT OF INTEREST STATEMENT

The authors have no conflict of interest to disclose.

DATA AVAILABILITY STATEMENT

The data that support the findings of this study are synthesized from published literatures. The synthesized data is published as supplementary data.

ORCID

Ying Sun https://orcid.org/0000-0002-9819-1241
Lianhong Gu https://orcid.org/0000-0001-5756-8738

REFERENCES

Aasen, H., Van Wittenberghe, S., Medina, N. S., Damm, A., Goulas, Y., Wieneke, S., Hueni, A., Malenovský, Z., Alonso, L., Pacheco-Labrador, J., Cendrero-Mateo, M. P., Tomelleri, E., Burkart, A., Cogliati, S., Rascher, U., & Arthur, A. M. (2019). Sun-induced chlorophyll fluorescence II: Review of passive measurement setups, protocols, and their application at the leaf to canopy level. *Remote Sensing*, *11*(8), 927 10.3390/RS11080927

Ač, A., Malenovský, Z., Olejníčková, J., Gallo, A., Rascher, U., & Mohammed, G. (2015). Meta-analysis assessing potential of steady-state chlorophyll fluorescence for remote sensing detection of plant water, temperature and nitrogen stress. *Remote Sensing of Environment*, *168*, 420–436. https://doi.org/10.1016/j.rse.2015.07.022

Ahlström, A., Raupach, M. R., Schurgers, G., Smith, B., Arneth, A., Jung, M., Reichstein, M., Canadell, J. G., Friedlingstein, P., Jain, A. K., & Kato, E. (2015). The dominant role of semi-arid ecosystems in the trend and variability of the land CO_2 sink. *Science*, *248*(6237), 895–899. https://doi.org/10.1126/science.aaa1668

Albert, L. P., Cushman, K. C., Zong, Y., Allen, D. W., Alonso, L., & Kellner, J. R. (2023). Sensitivity of solar-induced fluorescence to spectral stray light in high resolution imaging spectroscopy. *Remote Sensing of Environment*, *285*, 113313. https://doi.org/10.1016/j.rse.2022.113313

Anav, A., Friedlingstein, P., Beer, C., Ciais, P., Harper, A., Jones, C., Murray-Tortarolo, G., Papale, D., Parazoo, N. C., Peylin, P., Piao, S., Sitch, S., Viovy, N., Wiltshire, A., & Zhao, M. (2015). Spatiotemporal

patterns of terrestrial gross primary production: A review. *Reviews of Geophysics*, *53*(3), 785–818. https://doi.org/10.1002/2015RG000483

Anderson, M. C., Norman, J. M., Diak, G. R., Kustas, W. P., & Mecikalski, J. R. (1997). A two-source time-integrated model for estimating surface fluxes using thermal infrared remote sensing. *Remote Sensing of Environment*, *60*(2), 195–216.

Araus, J. L., Kefauver, S. C., Zaman-Allah, M., Olsen, M. S., & Cairns, J. E. (2018). Translating high-throughput phenotyping into genetic gain. *Trends in Plant Science*, *23*(5), 451–466. https://doi.org/10.1016/j.tplants.2018.02.001

Arneth, A., Harrison, S. P., Zaehle, S., Tsigaridis, K., Menon, S., Bartlein, P. J., Feichter, J., Korhola, A., Kulmala, M., O'Donnell, D., Schurgers, G., Sorvari, S., & Vesala, T. (2010). Terrestrial biogeochemical feedbacks in the climate system. *Nature Geoscience*, *3*(8), 525–532. https://doi.org/10.1038/ngeo905

Arora, V. K., Boer, G. J., Friedlingstein, P., Eby, M., Jones, C. D., Christian, J. R., Bonan, G., Bopp, L., Brovkin, V., Cadule, P., Hajima, T., Ilyina, T., Lindsay, K., Tjiputra, J. F., & Wu, T. (2013). Carbon–concentration and carbon–climate feedbacks in CMIP5 Earth System Models. *Journal of Climate*, *26*(15), 5289–5314. https://doi.org/10.1175/jcli-d-12-00494.1

Bacastow, R. B. (1976). Modulation of atmospheric carbon dioxide by the southern oscillation. *Nature*, *261*(5556), 116–118. https://doi.org/10.1038/261116a0

Badgley, G., Anderegg, L., Berry, J., & Field, C. (2019). Terrestrial gross primary production: Using NIRv to scale from site to globe. *Global Change Biology*, *25*, 3731–3740. https://doi.org/10.1111/gcb.14729

Baldocchi, D. D., Ryu, Y., Dechant, B., Eichelmann, E., Hemes, K., Ma, S., Sanchez, C. R., Shortt, R., Szutu, D., Valach, A., Verfaillie, J., Badgley, G., Zeng, Y., & Berry, J. A. (2020). Outgoing near-infrared radiation from vegetation scales with canopy photosynthesis across a Spectrum of function, structure, physiological capacity, and weather. *Journal of Geophysical Research: Biogeosciences*, *125*(7). https://doi.org/10.1029/2019jg005534

Baker, N. R. (2008). Chlorophyll fluorescence: A probe of photosynthesis in vivo. *Annual Review of Plant Biology*, *59*(1), 89–113.

Ballantyne, A. P., Alden, C. B., Miller, J. B., Tans, P. P., & White, J. W. C. (2012). Increase in observed net carbon dioxide uptake by land and oceans during the past 50 years. *Nature*, *488*(7409), 70–72. https://doi.org/10.1038/nature11299

Bastos, A., Ciais, P., Chevallier, F., Rödenbeck, C., Ballantyne, A. P., Maignan, F., Yin, Y., Fernández-Martínez, M., Friedlingstein, P., Peñuelas, J., & Piao, S. L. (2019). Contrasting effects of CO_2 fertilization, land-use change and warming on seasonal amplitude of northern hemisphere CO_2 exchange. *Atmospheric Chemistry and Physics*, *19*, 12361–12375. https://doi.org/10.5194/acp-19-12361-2019

Belwalkar, A., Poblete, T., Longmire, A., Hornero, A., Hernandez-Clemente, R., & Zarco-Tejada, P. J. (2022). Evaluation of SIF retrievals from narrow-band and sub-nanometer airborne hyperspectral imagers flown in tandem: Modelling and validation in the context of plant phenotyping. *Remote Sensing of Environment*, *273*, 112986. https://doi.org/10.1016/J.RSE.2022.112986

Bendig, J., Gautam, D., Malenovský, Z., & Lucieer, A. (2018). *Influence of cosine corrector and UAS platform dynamics on airborne spectral irradiance measurements*. International Geoscience and Remote Sensing Symposium (IGARSS), 2018-July, 8822–8825 https://doi.org/10.1109/IGARSS.2018.8518864

Berry, J., & Kornfeld, A. (2019). *Collaborative research on ecophysiological controls on Amazonian precipitation seasonality and variability*. https://doi.org/10.2172/1570388

Berry, J., Wolf, A., Elliott Campbell, J., Baker, I., Blake, N., Blake, D., Scott Denning, A., Randy Kawa, S., Montzka, S. A., Seibt, U., Stimler, K., Yakir, D., & Zhu, Z. (2013). A coupled model of the global cycles of carbonyl sulfide and CO_2: A possible new window on the carbon cycle. *Journal of Geophysical Research: Biogeosciences*, *118*(2), 842–852. https://doi.org/10.1002/jgrg.20068

Björkman, O., & Demmig, B. (1987). Photon yield of O_2 evolution and chlorophyll fluorescence characteristics at 77 K among vascular plants of diverse origins. *Planta*, *170*, 489–504. https://doi.org/10.1007/BF00402983

Bloom, A. A., Anthony Bloom, A., Bowman, K. W., Liu, J., Konings, A. G., Worden, J. R., Parazoo, N. C., Meyer, V., Reager, J. T., Worden, H. M., Jiang, Z., Quetin, G. R., Luke Smallman, T., Exbrayat, J.-F., Yin, Y., Saatchi, S. S., Williams, M., & Schimel, D. S. (2020). Lagged effects regulate the inter-annual variability of the tropical carbon balance. *Biogeosciences*, *17*(24), 6393–6422. https://doi.org/10.5194/bg-17-6393-2020

Bousquet, P., Peylin, P., Ciais, P., Le Quéré, C., Friedlingstein, P., & Tans, P. P. (2000). Regional changes in carbon dioxide fluxes of land and oceans since 1980. *Science*, *290*(5495), 1342–1347. https://doi.org/10.1126/science.290.5495.1342

Bowman, K. W., Liu, J., Bloom, A. A., Parazoo, N. C., Lee, M., Jiang, Z., Menemenlis, D., Gierach, M. M., Collatz, G. J., Gurney, K. R., & Wunch, D. (2017). Global and Brazilian carbon response to El Niño Modoki 2011–2010. *Earth and Space Science*, *4*(10), 637–660. https://doi.org/10.1002/2016ea000204

Browne, C., Matteson, D. S., McBride, L., Hu, L., Liu, Y., Sun, Y., Wen, J., & Barrett, C. B. (2021). Multivariate random forest prediction of poverty and malnutrition prevalence. *PLoS One*, *16*(9), e0255519. https://doi.org/10.1371/journal.pone.0255519

Butterfield, Z., Buermann, W., & Keppel-Aleks, G. (2020). Satellite observations reveal seasonal redistribution of northern ecosystem productivity in response to interannual climate variability. *Remote Sensing of Environment*, *242*, 111755. https://doi.org/10.1016/j.rse.2020.111755

Byrne, B., Liu, J., Bloom, A. A., Bowman, K. W., Butterfield, Z., Joiner, J., Keenan, T. F., Keppel-Aleks, G., Parazoo, N. C., & Yin, Y. (2020). Contrasting regional carbon cycle responses to seasonal climate anomalies across the east-West divide of temperate North America. *Global Biogeochemical Cycles*, *34*(11), e2020GB006598. https://doi.org/10.1029/2020GB006598

Cai, Y., Guan, K., Peng, J., Wang, S., Seifert, C., Wardlow, B., & Li, Z. (2018). A high-performance and in-season classification system of field-level crop types using time-series Landsat data and a machine learning approach. *Remote Sensing of Environment*, *210*, 35–47. https://doi.org/10.1016/J.RSE.2018.02.045

Camino, C., González-Dugo, V., Hernández, P., Sillero, J. C., & Zarco-Tejada, P. J. (2018). Improved nitrogen retrievals with airborne-derived fluorescence and plant traits quantified from VNIR-SWIR hyperspectral imagery in the context of precision agriculture. *International Journal of Applied Earth Observation and Geoinformation*, *70*, 105–117. https://doi.org/10.1016/j.jag.2018.04.013

Camino, C., Gonzalez-Dugo, V., Hernandez, P., & Zarco-Tejada, P. J. (2019). Radiative transfer Vcmax estimation from hyperspectral imagery and SIF retrievals to assess photosynthetic performance in rainfed and irrigated plant phenotyping trials. *Remote Sensing of Environment*, *231*, 111186. https://doi.org/10.1016/j.rse.2019.05.005

Campbell, J. E., Berry, J. A., Seibt, U., Smith, S. J., Montzka, S. A., Launois, T., Belviso, S., Bopp, L., & Laine, M. (2017). Large historical growth in global terrestrial gross primary production. *Nature*, *544*(7648), 84–87.

Campbell, J. E., Carmichael, G. R., Chai, T., Mena-Carrasco, M., Tang, Y., Blake, D. R., Blake, N. J., Vay, S. A., Collatz, G. J., Baker, I., Berry, J. A., Montzka, S. A., Sweeney, C., Schnoor, J. L., & Stanier, C. O. (2008). Photosynthetic control of atmospheric carbonyl sulfide during the growing season. *Science*, *322*(5904), 1085–1088.

Cendrero-Mateo, M. P., Wieneke, S., Damm, A., Alonso, L., Pinto, F., Moreno, J., Guanter, L., Celesti, M., Rossini, M., Sabater, N., Cogliati,

S., Julitta, T., Rascher, U., Goulas, Y., Aasen, H., Pacheco-Labrador, J., & Mac Arthur, A. (2019). Sun-induced chlorophyll fluorescence III: Benchmarking retrieval methods and sensor characteristics for proximal sensing. *Remote Sensing*, *11*(8), 962. https://doi.org/10.3390/rs11080962

Chang, C. Y., Guanter, L., Frankenberg, C., Köhler, P., Gu, L., Magney, T. S., Grossmann, K., & Sun, Y. (2020). Systematic assessment of retrieval methods for canopy far-red solar-induced chlorophyll fluorescence using high-frequency automated field spectroscopy. *Journal of Geophysical Research—Biogeosciences*, *125*(7). https://doi.org/10.1029/2019jg005533

Chang, C. Y., Wen, J., Han, J., Kira, O., LeVonne, J., Melkonian, J., Riha, S. J., Skovira, J., Ng, S., Gu, L., Wood, J. D., Näthe, P., & Sun, Y. (2021). Unpacking the drivers of diurnal dynamics of sun-induced chlorophyll fluorescence (SIF): Canopy structure, plant physiology, instrument configuration and retrieval methods. *Remote Sensing of Environment*, *265*, 112672. https://doi.org/10.1016/j.rse.2021.112672

Chang, C. Y., Zhou, R., Kira, O., Marri, S., Skovira, J., Gu, L., & Sun, Y. (2020). An unmanned aerial system (UAS) for concurrent measurements of solar-induced chlorophyll fluorescence and hyperspectral reflectance toward improving crop monitoring. *Agricultural and Forest Meteorology*, *294*, 108145. https://doi.org/10.1016/j.agrformet.2020.108145

Chen, A., Mao, J., Ricciuto, D., Lu, D., Xiao, J., Li, X., Thornton, P. E., & Knapp, A. K. (2021). Seasonal changes in GPP/SIF ratios and their climatic determinants across the northern hemisphere. *Global Change Biology*, *27*(20), 5186–5197. https://doi.org/10.1111/gcb.15775

Chen, A., Mao, J., Ricciuto, D., Xiao, J., Frankenberg, C., Li, X., Thornton, P. E., Gu, L., & Knapp, A. K. (2021). Moisture availability mediates the relationship between terrestrial gross primary production and solar-induced chlorophyll fluorescence: Insights from global-scale variations. *Global Change Biology*, *27*(6), 1144–1156. https://doi.org/10.1111/gcb.15373

Chen, J., Liu, X., Du, S., Ma, Y., & Liu, L. (2021). Effects of drought on the relationship between photosynthesis and chlorophyll fluorescence for maize. *IEEE Journal of Selected Topics in Applied Earth Observations and Remote Sensing*, *14*, 11148–11161. https://doi.org/10.1109/JSTARS.2021.3123111

Ciais, P., Tan, J., Wang, X., Roedenbeck, C., Chevallier, F., Piao, S.-L., Moriarty, R., Broquet, G., Le Quéré, C., Canadell, J. G., Peng, S., Poulter, B., Liu, Z., & Tans, P. (2019). Five decades of northern land carbon uptake revealed by the interhemispheric CO gradient. *Nature*, *568*(7751), 221–225. https://doi.org/10.1038/s41586-019-1078-6

Coenders-Gerrits, A. M. J., Van der Ent, R. J., Bogaard, T. A., Wang-Erlandsson, L., Hrachowitz, M., & Savenije, H. H. G. (2014). Uncertainties in transpiration estimates. *Nature*, *506*(7487), E1–E2.

Constenla-Villoslada, S., Liu, Y., Wen, J., Sun, Y., & Chonabayashi, S. (2022). Large-scale land restoration improved drought resilience in Ethiopia's degraded watersheds. *Nature Sustainability*, *5*(6), 488–497. https://doi.org/10.1038/s41893-022-00861-4

Damm, A., Cogliati, S., Colombo, R., Fritsche, L., Genangeli, A., Genesio, L., Hanus, J., Peressotti, A., Rademske, P., Rascher, U., Schuettemeyer, D., Siegmann, B., Sturm, J., & Miglietta, F. (2022). Response times of remote sensing measured sun-induced chlorophyll fluorescence, surface temperature and vegetation indices to evolving soil water limitation in a crop canopy. *Remote Sensing of Environment*, *273*, 112957. https://doi.org/10.1016/j.rse.2022.112957

Damm, A., Guanter, L., Paul-Limoges, E., van der Tol, C., Hueni, A., Buchmann, N., Eugster, W., Ammann, C., & Schaepman, M. E. (2015). Far-red sun-induced chlorophyll fluorescence shows ecosystem-specific relationships to gross primary production: An assessment based on observational and modeling approaches. *Remote Sensing of Environment*, *166*, 91–105.

Damm, A., Haghighi, E., Paul-Limoges, E., & van der Tol, C. (2021). On the seasonal relation of sun-induced chlorophyll fluorescence and transpiration in a temperate mixed forest. *Agricultural and Forest Meteorology*, *304–305*, 108386. https://doi.org/10.1016/j.agrformet.2021.108386

Daumard, F., Champagne, S., Fournier, A., Goulas, Y., Ounis, A., Hanocq, J.-F., & Moya, I. (2010). A Field platform for continuous measurement of canopy fluorescence. *IEEE Transactions on Geoscience and Remote Sensing*, *48*(9), 3358–3368. https://doi.org/10.1109/TGRS.2010.2046420

De Cannière, S., Herbst, M., Vereecken, H., Defourny, P., & Jonard, F. (2021). Constraining water limitation of photosynthesis in a crop growth model with sun-induced chlorophyll fluorescence. *Remote Sensing of Environment*, *267*, 112722. https://doi.org/10.1016/j.rse.2021.112722

Dechant, B., Ryu, Y., Badgley, G., Köhler, P., Rascher, U., Migliavacca, M., Zhang, Y., Tagliabue, G., Guan, K., Rossini, M., Goulas, Y., Zeng, Y., Frankenberg, C., & Berry, J. (2022). NIRvP: A robust structural proxy for sun-induced chlorophyll fluorescence and photosynthesis across scales. *Remote Sensing of Environment*, *268*, 112763. https://doi.org/10.31223/x5zs35

Dechant, B., Ryu, Y., Badgley, G., Zeng, Y., Berry, J. A., Zhang, Y., Goulas, Y., Li, Z., Zhang, Q., Kang, M., Li, J., & Moya, I. (2020). Canopy structure explains the relationship between photosynthesis and sun-induced chlorophyll fluorescence in crops. *Remote Sensing of Environment*, *241*, 111733. https://doi.org/10.1016/j.rse.2020.111733

Doughty, R., Köhler, P., Frankenberg, C., Magney, T. S., Xiao, X., Qin, Y., Wu, X., & Moore, B., 3rd. (2019). TROPOMI reveals dry-season increase of solar-induced chlorophyll fluorescence in the Amazon forest. *Proceedings of the National Academy of Sciences of the United States of America*, *116*(44), 22393–22398. https://doi.org/10.1073/pnas.1908157116

Doughty, R., Kurosu, T. P., Parazoo, N., Köhler, P., Wang, Y., Sun, Y., & Frankenberg, C. (2022). Global GOSAT, OCO-2, and OCO-3 solar-induced chlorophyll fluorescence datasets. *Earth System Science Data*, *14*(4), 1513–1529. https://doi.org/10.5194/essd-14-1513-2022

Doughty, R., Xiao, X., Qin, Y., Wu, X., Zhang, Y., & Moore, B. (2021). Small anomalies in dry-season greenness and chlorophyll fluorescence for Amazon moist tropical forests during El Niño and La Niña. *Remote Sensing of Environment*, *253*, 112196. https://doi.org/10.1016/j.rse.2020.112196

Drusch, M., Moreno, J., Del Bello, U., Franco, R., Goulas, Y., Huth, A., Kraft, S., Middleton, E. M., Miglietta, F., Mohammed, G., Nedbal, L., Rascher, U., Schuttemeyer, D., & Verhoef, W. (2017). The fluorescence explorer mission concept—ESA's Earth explorer 8. *IEEE Transactions on Geoscience and Remote Sensing*, *55*(3), 1273–1284. https://doi.org/10.1109/TGRS.2016.2621820

Du, S., Liu, L., Liu, X., Zhang, X., Zhang, X., Bi, Y., & Zhang, L. (2018). Retrieval of global terrestrial solar-induced chlorophyll fluorescence from TanSat satellite. *Science bulletin of the Faculty of Agriculture, Kyushu University*, *63*(22), 1502–1512. https://doi.org/10.1016/j.scib.2018.10.003

Duveiller, G., & Cescatti, A. (2016). Spatially downscaling sun-induced chlorophyll fluorescence leads to an improved temporal correlation with gross primary productivity. *Remote Sensing of Environment*, *182*, 72–89. https://doi.org/10.1016/j.rse.2016.04.027

Duveiller, G., Filipponi, F., Walther, S., Köhler, P., Frankenberg, C., Guanter, L., & Cescatti, A. (2020). A spatially downscaled sun-induced fluorescence global product for enhanced monitoring of vegetation productivity. *Earth System Science Data*, *12*(2), 1101–1116. https://doi.org/10.5194/essd-12-1101-2020

Farquhar, G. D., Ehleringer, J. R., & Hubick, K. T. (1989). Carbon isotope discrimination and photosynthesis. *Annual Review of Plant Physiology and Plant Molecular Biology*, *40*(1), 503–537. https://doi.org/10.1146/annurev.pp.40.060189.002443

Farquhar, G. D., von Caemmerer, S., & Berry, J. A. (1980). A biochemical-model of photosynthetic CO_2 assimilation in leaves of C-3 species. *Planta*, *149*, 78–90.

Fatichi, S., & Pappas, C. (2017). Constrained variability of modeled T: ET ratio across biomes. *Geophysical Research Letters*, *44*(13), 6795–6803.

Fernández-Martínez, M., Vicca, S., Janssens, I. A., Ciais, P., Obersteiner, M., Bartrons, M., Sardans, J., Verger, A., Canadell, J. G., Chevallier, F., Wang, X., Bernhofer, C., Curtis, P. S., Gianelle, D., Grünwald, T., Heinesch, B., Ibrom, A., Knohl, A., Laurila, T., … Peñuelas, J. (2017). Atmospheric deposition, CO_2, and change in the land carbon sink. *Scientific Reports*, *7*(1), 9632. https://doi.org/10.1038/s41598-017-08755-8

Fisher, J. B., Melton, F., Middleton, E., Hain, C., Anderson, M., Allen, R., Mccabe, M. F., Hook, S., Baldocchi, D., Townsend, P. A., Kilic, A., Tu, K., Miralles, D. D., Perret, J., Lagouarde, J.-P., Waliser, D., Purdy, A. J., French, A., Schimel, D., … Wood, E. F. (2017). The future of evapotranspiration: Global requirements for ecosystemfunctioning, carbon and climate feedbacks, agriculturalmanagement, and water resources. *Water Resources Research*, *53*(4), 2618–2626. https://doi.org/10.1002/2016WR020175.Received

Flexas, J., & Medrano, H. (2002). Drought-inhibition of photosynthesis in C3 plants: Stomatal and non-stomatal limitations revisited. *Annals of Botany*, *89*(2), 183–189. https://doi.org/10.1093/AOB/MCF027

Foley, J. A., Ramankutty, N., Brauman, K. A., Cassidy, E. S., Gerber, J. S., Johnston, M., Mueller, N. D., O'Connell, C., Ray, D. K., West, P. C., Balzer, C., Bennett, E. M., Carpenter, S. R., Hill, J., Monfreda, C., Polasky, S., Rockström, J., Sheehan, J., Siebert, S., … Zaks, D. P. M. (2011). Solutions for a cultivated planet. *Nature*, *478*(7369), 337–342. https://doi.org/10.1038/nature10452

Forkel, M., Carvalhais, N., Rödenbeck, C., Keeling, R., Heimann, M., Thonicke, K., Zaehle, S., & Reichstein, M. (2016). Enhanced seasonal CO_2 exchange caused by amplified plant productivity in northern ecosystems. *Science*, *351*(6274), 696–699. https://doi.org/10.1126/science.aac4971

Frankenberg, C., Fisher, J. B., Worden, J., Badgley, G., Saatchi, S. S., Lee, J.-E., Toon, G. C., Butz, A., Jung, M., Kuze, A., & Yokota, T. (2011). New global observations of the terrestrial carbon cycle from GOSAT: Patterns of plant fluorescence with gross primary productivity. *Geophysical Research Letters*, *38*(17). https://doi.org/10.1029/2011GL048738

Frankenberg, C., Köhler, P., Magney, T. S., Geier, S., Lawson, P., Schwochert, M., McDuffie, J., Drewry, D. T., Pavlick, R., & Kuhnert, A. (2018). The chlorophyll fluorescence imaging spectrometer (CFIS), mapping far red fluorescence from aircraft. *Remote Sensing of Environment*, *217*, 523–536. https://doi.org/10.1016/j.rse.2018.08.032

Frankenberg, C., O'Dell, C., Guanter, L., & McDuffie, J. (2012). Remote sensing of near-infrared chlorophyll fluorescence from space in scattering atmospheres: Implications for its retrieval and interferences with atmospheric CO_2 retrievals. *Atmospheric Measurement Techniques*, *5*(8), 2081–2094.

Frankenberg, C., Yin, Y., Byrne, B., He, L., & Gentine, P. (2021). Comment on "recent global decline of CO_2 fertilization effects on vegetation photosynthesis.". *Science*, *373*(6562), eabg2947. https://doi.org/10.1126/science.abg2947

Friedlingstein, P., Meinshausen, M., Arora, V. K., Jones, C. D., Anav, A., Liddicoat, S. K., & Knutti, R. (2014). Uncertainties in CMIP5 climate projections due to carbon cycle feedbacks. *Journal of Climate*, *27*(2), 511–526. https://doi.org/10.1175/jcli-d-12-00579.1

Fu, P., Hu, L., Ainsworth, E. A., Tai, X., Myint, S. W., Zhan, W., Blakely, B. J., & Bernacchi, C. J. (2021). Enhanced drought resistance of vegetation growth in cities due to urban heat, CO_2 domes and O_3 troughs. *Environmental Research Letters*, *16*(12), 124052.

Fu, P., Meacham-Hensold, K., Siebers, M. H., & Bernacchi, C. J. (2021). The inverse relationship between solar-induced fluorescence yield and photosynthetic capacity: Benefits for field phenotyping. *Journal of Experimental Botany*, *72*(4), 1295–1306. https://doi.org/10.1093/jxb/eraa537

Fu, Z., Ciais, P., Prentice, I. C., Gentine, P., Makowski, D., Bastos, A., Luo, X., Green, J. K., Stoy, P. C., Yang, H., & Hajima, T. (2022). Atmospheric dryness reduces photosynthesis along a large range of soil water deficits. *Nature Communications*, *13*(1), 1–10. https://doi.org/10.1038/s41467-022-28652-7

Gedney, N., Cox, P. M., Betts, R. A., Boucher, O., Huntingford, C., & Stott, P. A. (2006). Detection of a direct carbon dioxide effect in continental river runoff records. *Nature*, *439*(7078), 835–838.

Gensheimer, J., Turner, A. J., Köhler, P., Frankenberg, C., & Chen, J. (2022). A convolutional neural network for spatial downscaling of satellite-based solar-induced chlorophyll fluorescence (SIFnet). *Biogeosciences*, *19*(6), 1777–1793. https://doi.org/10.5194/bg-19-1777-2022

Gentine, P., & Alemohammad, S. H. (2018). Reconstructed solar-induced fluorescence: A machine learning vegetation product based on MODIS surface reflectance to reproduce GOME-2 solar-induced fluorescence. *Geophysical Research Letters*, *45*(7), 3136–3146. https://doi.org/10.1002/2017GL076294

Gloor, E., Wilson, C., Chipperfield, M. P., Chevallier, F., Buermann, W., Boesch, H., Parker, R., Somkuti, P., Gatti, L. V., Correia, C., Domingues, L. G., Peters, W., Miller, J., Deeter, M. N., & Sullivan, M. J. P. (2018). Tropical land carbon cycle responses to 2015/16 El Niño as recorded by atmospheric greenhouse gas and remote sensing data. *Philosophical Transactions of the Royal Society of London. Series B, Biological Sciences*, *373*(1760), 20170302. https://doi.org/10.1098/rstb.2017.0302

Goulas, Y., Fournier, A., Daumard, F., Champagne, S., Ounis, A., Marloie, O., & Moya, I. (2017). Gross primary production of a wheat canopy relates stronger to far red than to red solar-induced chlorophyll fluorescence. *Remote Sensing*, *9*(1), 97. https://doi.org/10.3390/RS9010097

Graven, H., Keeling, R. F., & Rogelj, J. (2020). Changes to carbon isotopes in atmospheric CO_2 over the industrial era and into the future. *Global Biogeochemical Cycles*, *34*(11), e2019GB006170. https://doi.org/10.1029/2019GB006170

Green, J. K., Berry, J., Ciais, P., Zhang, Y., & Gentine, P. (2020). Amazon rainforest photosynthesis increases in response to atmospheric dryness. *Science Advances*, *6*(47). https://doi.org/10.1126/sciadv.abb7232

Green, J. K., Konings, A. G., Alemohammad, S. H., Berry, J., Entekhabi, D., Kolassa, J., Lee, J.-E., & Gentine, P. (2017). Regionally strong feedbacks between the atmosphere and terrestrial biosphere. *Nature Geoscience*, *10*(6), 410–414. https://doi.org/10.1038/ngeo2957

Gregory, J. M., Jones, C. D., Cadule, P., & Friedlingstein, P. (2009). Quantifying carbon cycle feedbacks. *Journal of Climate*, *22*(19), 5232–5250. https://doi.org/10.1175/2009jcli2949.1

Grossmann, K., Frankenberg, C., Magney, T. S., Hurlock, S. C., Seibt, U., & Stutz, J. (2018). PhotoSpec: A new instrument to measure spatially distributed red and far-red solar-induced chlorophyll fluorescence. *Remote Sensing of Environment*, *216*, 311–327. https://doi.org/10.1016/j.rse.2018.07.002

Gu, L., Han, J., Wood, J. D., Chang, C. Y.-Y., & Sun, Y. (2019). Sun-induced Chl fluorescence and its importance for biophysical modeling of photosynthesis based on light reactions. *New Phytologist*, *223*(3), 1179–1191. https://doi.org/10.1111/nph.15796

Gu, L., Wood, J. D., Chang, C. Y.-Y., Sun, Y., & Riggs, J. S. (2019). Advancing terrestrial ecosystem science with a novel automated measurement system for Sun-induced chlorophyll fluorescence for integration with Eddy covariance flux networks. *Journal of Geophysical Research: Biogeosciences*, *124*(1), 127–146. https://doi.org/10.1029/2018JG004742

Guan, K., Berry, J. A., Zhang, Y., Joiner, J., Guanter, L., Badgley, G., & Lobell, D. B. (2016). Improving the monitoring of crop productivity

using spaceborne solar-induced fluorescence. *Global Change Biology*, *22*(2), 716–726. https://doi.org/10.1111/gcb.13136

Guan, K., Pan, M., Li, H., Wolf, A., Wu, J., Medvigy, D., Caylor, K. K., Sheffield, J., Wood, E. F., Malhi, Y., Liang, M., Kimball, J. S., Saleska, S. R., Berry, J., Joiner, J., & Lyapustin, A. I. (2015). Photosynthetic seasonality of global tropical forests constrained by hydroclimate. *Nature Geoscience*, *8*(4), 284–289. https://doi.org/10.1038/ngeo2382

Guanter, L., Aben, I., Tol, P., Krijger, J. M., Hollstein, A., Köhler, P., Damm, A., Joiner, J., Frankenberg, C., & Landgraf, J. (2015). Potential of the TROPOspheric monitoring instrument (TROPOMI) onboard the Sentinel-5 precursor for the monitoring of terrestrial chlorophyll fluorescence. *Atmospheric Measurement Techniques*, *8*(3), 1337–1352. https://doi.org/10.5194/amt-8-1337-2015

Guanter, L., Alonso, L., Gómez-Chova, L., Amorós-López, J., Vila, J., & Moreno, J. (2007). Estimation of solar-induced vegetation fluorescence from space measurements. *Geophysical Research Letters*, *34*(8). https://doi.org/10.1029/2007GL029289

Guanter, L., Frankenberg, C., Dudhia, A., Lewis, P. E., Gómez-Dans, J., Kuze, A., Suto, H., & Grainger, R. G. (2012). Retrieval and global assessment of terrestrial chlorophyll fluorescence from GOSAT space measurements. *Remote Sensing of Environment*, *121*, 236–251. https://doi.org/10.1016/j.rse.2012.02.006

Guanter, L., Rossini, M., Colombo, R., Meroni, M., Frankenberg, C., Lee, J.-E., & Joiner, J. (2013). Using field spectroscopy to assess the potential of statistical approaches for the retrieval of sun-induced chlorophyll fluorescence from ground and space. *Remote Sensing of Environment*, *133*, 52–61. https://doi.org/10.1016/j.rse.2013.01.017

Guanter, L., Zhang, Y., Jung, M., Joiner, J., Voigt, M., Berry, J. A., Frankenberg, C., Huete, A. R., Zarco-Tejada, P., Lee, J.-E., Moran, M. S., Ponce-Campos, G., Beer, C., Camps-Valls, G., Buchmann, N., Gianelle, D., Klumpp, K., Cescatti, A., Baker, J. M., & Griffis, T. J. (2014). Global and time-resolved monitoring of crop photosynthesis with chlorophyll fluorescence. *Proceedings of the National Academy of Sciences of the United States of America*, *111*(14), E1327–E1333. https://doi.org/10.1073/pnas.1320008111

Han, J., Chang, C. Y. Y., Gu, L., Zhang, Y., Meeker, E. W., Magney, T. S., Walker, A. P., Wen, J., Kira, O., McNaull, S., & Sun, Y. (2022). The physiological basis for estimating photosynthesis from Chla fluorescence. *New Phytologist*, *234*(4), 1206–1219. https://doi.org/10.1111/NPH.18045

Han, J., Gu, L., Wen, J., & Sun, Y. (2022). Inference of photosynthetic capacity parameters from chlorophyll a fluorescence is affected by redox state of PSII reaction centers. *Plant, Cell & Environment*, *45*(4), 1298–1314. https://doi.org/10.1111/pce.14271

Haverd, V., Smith, B., Canadell, J. G., Cuntz, M., Mikaloff-Fletcher, S., Farquhar, G., Woodgate, W., Briggs, P. R., & Trudinger, C. M. (2020). Higher than expected CO_2 fertilization inferred from leaf to global observations. *Global Change Biology*, *26*, 2390–2402. https://doi.org/10.1111/gcb.14950

He, L., Chen, J. M., Liu, J., Zheng, T., Wang, R., Joiner, J., Chou, S., Chen, B., Liu, Y., Liu, R., & Rogers, C. (2019). Diverse photosynthetic capacity of global ecosystems mapped by satellite chlorophyll fluorescence measurements. *Remote Sensing of Environment*, *232*, 111344. https://doi.org/10.1016/j.rse.2019.111344

He, L., Magney, T., Dutta, D., Yin, Y., Köhler, P., Grossmann, K., Stutz, J., Dold, C., Hatfield, J., Guan, K., Peng, B., & Frankenberg, C. (2020). From the ground to space: Using solar-induced chlorophyll fluorescence to estimate crop productivity. *Geophysical Research Letters*, *47*(7). https://doi.org/10.1029/2020gl087474

Helm, L. T., Shi, H., Lerdau, M. T., & Yang, X. (2020). Solar-induced chlorophyll fluorescence and short-term photosynthetic response to drought. *Ecological Applications*, *30*(5), e02101. https://doi.org/10.1002/eap.2101

Hernández-Clemente, R., North, P. R. J., Hornero, A., & Zarco-Tejada, P. J. (2017). Assessing the effects of forest health on sun-induced chlorophyll fluorescence using the FluorFLIGHT 3-D radiative transfer model to account for forest structure. *Remote Sensing of Environment*, *193*, 165–179. https://doi.org/10.1016/J.RSE.2017.02.012

Hilton, T. W., Whelan, M. E., Zumkehr, A., Kulkarni, S., Berry, J. A., Baker, I. T., Montzka, S. A., Sweeney, C., Miller, B. R., & Elliott Campbell, J. (2017). Peak growing season gross uptake of carbon in North America is largest in the Midwest USA. *Nature Climate Change*, *7*, 450–454. https://doi.org/10.1038/NCLIMATE3272

Humphrey, V., Zscheischler, J., Ciais, P., Gudmundsson, L., Sitch, S., & Seneviratne, S. I. (2018). Sensitivity of atmospheric CO_2 growth rate to observed changes in terrestrial water storage. *Nature*, *560*(7720), 628–631. https://doi.org/10.1038/s41586-018-0424-4

Jeong, S.-J., Schimel, D., Frankenberg, C., Drewry, D. T., Fisher, J. B., Verma, M., Berry, J. A., Lee, J.-E., & Joiner, J. (2017). Application of satellite solar-induced chlorophyll fluorescence to understanding large-scale variations in vegetation phenology and function over northern high latitude forests. *Remote Sensing of Environment*, *190*, 178–187. https://doi.org/10.1016/J.RSE.2016.11.021

Jia, M., Colombo, R., Rossini, M., Celesti, M., Zhu, J., Cogliati, S., Cheng, T., Tian, Y., Zhu, Y., Cao, W., & Yao, X. (2021). Estimation of leaf nitrogen content and photosynthetic nitrogen use efficiency in wheat using sun-induced chlorophyll fluorescence at the leaf and canopy scales. *European Journal of Agronomy*, *122*, 126192. https://doi.org/10.1016/j.eja.2020.126192

Jian, J., Bailey, V., Dorheim, K., Konings, A. G., Hao, D., Shiklomanov, A. N., Snyder, A., Steele, M., Teramoto, M., Vargas, R., & Bond-Lamberty, B. (2022). Historically inconsistent productivity and respiration fluxes in the global terrestrial carbon cycle. *Nature Communications*, *13*(1), 1733. https://doi.org/10.1038/s41467-022-29391-5

Jiao, W., Chang, Q., & Wang, L. (2019). The sensitivity of satellite solar-induced chlorophyll fluorescence to meteorological drought. *Earths Future*, *7*(5), 558–573. https://doi.org/10.1029/2018ef001087

Joiner, J., Guanter, L., Lindstrot, R., Voigt, M., Vasilkov, A. P., Middleton, E. M., Huemmrich, K. F., Yoshida, Y., & Frankenberg, C. (2013). Global monitoring of terrestrial chlorophyll fluorescence from moderate-spectral-resolution near-infrared satellite measurements: Methodology, simulations, and application to GOME-2. *Atmospheric Measurement Techniques*, *6*(10), 2803–2823. https://doi.org/10.5194/amt-6-2803-2013

Joiner, J., Yoshida, Y., Guanter, L., & Middleton, E. M. (2016). New methods for retrieval of chlorophyll red fluorescence from hyper-spectral satellite instruments: Simulations and application to GOME-2 and SCIAMACHY. *Atmospheric Measurement Techniques Discussions*, *9*, 3939–3867.

Joiner, J., Yoshida, Y., Köehler, P., Campbell, P., Frankenberg, C., van der Tol, C., Yang, P., Parazoo, N., Guanter, L., & Sun, Y. (2020). Systematic orbital geometry-dependent variations in satellite solar-induced fluorescence (SIF) retrievals. *Remote Sensing*, *12*(15), 2346. https://doi.org/10.3390/rs12152346

Joiner, J., Yoshida, Y., Koehler, P., Frankenberg, C., & Parazoo, N. C. (2019). SIF-ESDRL2 Daily Solar-Induced Fluorescence (SIF) from ERS-2 GOME, 1995–2003 [NetCDF]. https://doi.org/10.3334/ORNLDAAC/1758

Joiner, J., Yoshida, Y., Koehler, P., Frankenberg, C., & Parazoo, N. C. (2021). SIF-ESDRL2 Solar-Induced Fluorescence (SIF) from SCIAMACHY, 2003–2012 [NetCDF]. https://doi.org/10.3334/ORNLDAAC/1871

Joiner, J., Yoshida, Y., Vasilkov, A. P., Schaefer, K., Jung, M., Guanter, L., Zhang, Y., Garrity, S., Middleton, E. M., Huemmrich, K. F., Gu, L., & Belelli Marchesini, L. (2014). The seasonal cycle of satellite chlorophyll fluorescence observations and its relationship to vegetation phenology and ecosystemon exchange. *Remote*

Sensing of Environment, *152*, 375–391. https://doi.org/10.1016/j.rse.2014.06.022

Joiner, J., Yoshida, Y., Vasilkov, A. P., Yoshida, Y., Corp, L. A., & Middleton, E. M. (2011). First observations of global and seasonal terrestrial chlorophyll fluorescence from space. *Biogeosciences*, *8*(3), 637–651. https://doi.org/10.5194/bg-8-637-2011

Jonard, F., De Cannière, S., Brüggemann, N., Gentine, P., Short Gianotti, D. J., Lobet, G., Miralles, D. G., Montzka, C., Pagán, B. R., Rascher, U., & Vereecken, H. (2020). Value of sun-induced chlorophyll fluorescence for quantifying hydrological states and fluxes: Current status and challenges. *Agricultural and Forest Meteorology*, *291*, 108088. https://doi.org/10.1016/j.agrformet.2020.108088

Katul, G. G., Oren, R., Manzoni, S., Higgins, C., & Parlange, M. B. (2012). Evapotranspiration: A process driving mass transport and energy exchange in the soil-plant-atmosphere-climate system. *Reviews of Geophysics*, *50*(3), RG3002. https://doi.org/10.1029/2011RG000366

Keeling, R. F., Graven, H. D., Welp, L. R., Resplandy, L., Bi, J., Piper, S. C., Sun, Y., Bollenbacher, A., & Meijer, H. A. J. (2017). Atmospheric evidence for a global secular increase in carbon isotopic discrimination of land photosynthesis. *Proceedings of the National Academy of Sciences of the United States of America*, *114*(39), 10361–10366.

Keenan, T. F., Migliavacca, M., Papale, D., Baldocchi, D., Reichstein, M., Torn, M., & Wutzler, T. (2019). Widespread inhibition of daytime ecosystem respiration. *Nature Ecology and Evolution*, *3*(3), 407–415. https://doi.org/10.1038/s41559-019-0809-2

Keenan, T. F., & Riley, W. J. (2018). Greening of the land surface in the world's cold regions consistent with recent warming. *Nature Climate Change*, *8*, 825–828. https://doi.org/10.1038/s41558-018-0258-y

Keller, B., Zimmermann, L., Rascher, U., Matsubara, S., Steier, A., & Muller, O. (2022). Toward predicting photosynthetic efficiency and biomass gain in crop genotypes over a field season. *Plant Physiology*, *188*(1), 301–317. https://doi.org/10.1093/plphys/kiab483

Khosravi, N., Vountas, M., Rozanov, V. V., Bracher, A., Wolanin, A., & Burrows, J. P. (2015). Retrieval of terrestrial plant fluorescence based on the In-filling of far-red Fraunhofer lines using SCIAMACHY observations. *Frontiers in Environmental Science*, *3*. https://doi.org/10.3389/fenvs.2015.00078

Kim, J., Ryu, Y., & Dechant, B. (2022). Development of a filter-based near-surface remote sensing system to retrieve far-red sun-induced chlorophyll fluorescence. *Remote Sensing of Environment*, *283*, 113311. https://doi.org/10.1016/j.rse.2022.113311

Kim, J., Ryu, Y., Dechant, B., Lee, H., Kim, H. S., Kornfeld, A., & Berry, J. A. (2021). Solar-induced chlorophyll fluorescence is non-linearly related to canopy photosynthesis in a temperate evergreen needleleaf forest during the fall transition. *Remote Sensing of Environment*, *258*, 112362. https://doi.org/10.1016/j.rse.2021.112362

Kira, O., Y-Y. Chang, Gu, L., Wen, J., Hong, Z., & Sun, Y. (2021). Partitioning net ecosystem exchange (NEE) of CO_2 using solar-induced chlorophyll fluorescence (SIF). *Geophysical Research Letters*, *48*(4). https://doi.org/10.1029/2020gl091247

Kira, O., & Sun, Y. (2020). Extraction of sub-pixel C3/C4 emissions of solar-induced chlorophyll fluorescence (SIF) using artificial neural network. In *ISPRS journal of photogrammetry and remote sensing* (Vol. *161*, pp. 135–146). https://doi.org/10.1016/j.isprsjprs.2020.01.017

Koffi, E. N., Rayner, P. J., Norton, A. J., Frankenberg, C., & Scholze, M. (2015). Investigating the usefulness of satellite-derived fluorescence data in inferring gross primary productivity within the carbon cycle data assimilation system. *Biogeosciences*, *12*(13), 4067–4084. https://doi.org/10.5194/bg-12-4067-2015

Köhler, P., Behrenfeld, M. J., Landgraf, J., Joiner, J., Magney, T. S., & Frankenberg, C. (2020). Global retrievals of solar-induced chlorophyll fluorescence at red wavelengths with TROPOMI. *Geophysical Research Letters*, *47*(15), e2020GL087541. https://doi.org/10.1029/2020GL087541

Köhler, P., Frankenberg, C., Magney, T. S., Guanter, L., Joiner, J., & Landgraf, J. (2018). Global retrievals of solar-induced chlorophyll fluorescence with TROPOMI: First results and Intersensor comparison to OCO-2. *Geophysical Research Letters*, *45*, 10456–10463. https://doi.org/10.1029/2018GL079031

Köhler, P., Guanter, L., & Joiner, J. (2015). A linear method for the retrieval of sun-induced chlorophyll fluorescence from GOME-2 and SCIAMACHY data. *Atmospheric Measurement Techniques*, *8*(6), 2589–2608. https://doi.org/10.5194/amt-8-2589-2015

Köhler, P., Guanter, L., Kobayashi, H., Walther, S., & Yang, W. (2018). Assessing the potential of sun-induced fluorescence and the canopy scattering coefficient to track large-scale vegetation dynamics in Amazon forests. *Remote Sensing of Environment*, *204*, 769–785. https://doi.org/10.1016/J.RSE.2017.09.025

Kooijmans, L. M. J., Cho, A., Ma, J., Kaushik, A., Haynes, K. D., Baker, I., Luijkx, I. T., Groenink, M., Peters, W., Miller, J. B., Berry, J. A., Ogée, J., Meredith, L. K., Sun, W., Kohonen, K.-M., Vesala, T., Mammarella, I., Chen, H., Spielmann, F. M., … Krol, M. (2021). Evaluation of carbonyl sulfide biosphere exchange in the simple biosphere model (SiB4). *Biogeosciences*, *18*(24), 6547–6565. https://doi.org/10.5194/bg-18-6547-2021

Koren, G., van Schaik, E., Araújo, A. C., Boersma, K. F., Gärtner, A., Killaars, L., Kooreman, M. L., Kruijt, B., van der Laan-Luijkx, I. T., von Randow, C., Smith, N. E., & Peters, W. (2018). Widespread reduction in sun-induced fluorescence from the Amazon during the 2015/2016 El Niño. *Philosophical Transactions of the Royal Society B: Biological Sciences*, *373*(1760), 20170408.

Krämer, J., Siegmann, B., Kraska, T., Muller, O., & Rascher, U. (2021). The potential of spatial aggregation to extract remotely sensed sun-induced fluorescence (SIF) of small-sized experimental plots for applications in crop phenotyping. *International Journal of Applied Earth Observation and Geoinformation*, *104*, 102565. https://doi.org/10.1016/j.jag.2021.102565

Lasslop, G., Reichstein, M., Papale, D., Richardson, A. D., Arneth, A., Barr, A., Stoy, P., & Wohlfahrt, G. (2010). Separation of net ecosystem exchange into assimilation and respiration using a light response curve approach: Critical issues and global evaluation. *Global Change Biology*, *16*(1), 187–208.

Lawrence, D. M., Thornton, P. E., Oleson, K. W., & Bonan, G. B. (2007). The partitioning of evapotranspiration into transpiration, soil evaporation, and canopy evaporation in a GCM: Impacts on land–atmosphere interaction. *Journal of Hydrometeorology*, *8*(4), 862–880.

Lee, J.-E., Frankenberg, C., van der Tol, C., Berry, J. A., Guanter, L., Boyce, C. K., Fisher, J. B., Morrow, E., Worden, J. R., Asefi, S., Badgley, G., & Saatchi, S. (2013). Forest productivity and water stress in Amazonia: Observations from GOSAT chlorophyll fluorescence. *Proceedings of the Royal Society B: Biological Sciences*, *280*(1761), 20130171. https://doi.org/10.1098/rspb.2013.0171

Li, X., & Xiao, J. (2019a). Mapping photosynthesis solely from solar-induced chlorophyll fluorescence: A global, fine-resolution dataset of gross primary production Derived from OCO-2. *Remote Sensing*, *11*(21), 2563. https://doi.org/10.3390/rs11212563

Li, X., & Xiao, J. (2019b). A global, 0.05-degree product of solar-induced chlorophyll fluorescence Derived from OCO-2, MODIS, and reanalysis data. *Remote Sensing*, *11*(5), 517. https://doi.org/10.3390/rs11050517

Li, X., & Xiao, J. (2020). Global climatic controls on interannual variability of ecosystem productivity: Similarities and differences inferred from solar-induced chlorophyll fluorescence and enhanced vegetation index. *Agricultural and Forest Meteorology*, *288–289*, 108018. https://doi.org/10.1016/j.agrformet.2020.108018

Li, X., & Xiao, J. (2022). TROPOMI observations allow for robust exploration of the relationship between solar-induced chlorophyll fluorescence and terrestrial gross primary production. *Remote*

Sensing of Environment, *268*, 112748. https://doi.org/10.1016/j.rse.2021.112748

Li, X., Xiao, J., & He, B. (2018). Higher absorbed solar radiation partly offset the negative effects of water stress on the photosynthesis of Amazon forests during the 2015 drought. *Environmental Research Letters*, *13*(4), 44005. https://doi.org/10.1088/1748-9326/aab0b1

Li, X., Xiao, J., He, B., Altaf Arain, M., Beringer, J., Desai, A. R., Emmel, C., Hollinger, D. Y., Krasnova, A., Mammarella, I., Noe, S. M., Ortiz, P. S., Rey-Sanchez, A. C., Rocha, A. V., & Varlagin, A. (2018). Solar-induced chlorophyll fluorescence is strongly correlated with terrestrial photosynthesis for a wide variety of biomes: First global analysis based on OCO-2 and flux tower observations. *Global Change Biology*, *24*(9), 3990–4008. https://doi.org/10.1111/gcb.14297

Liu, J., Bowman, K. W., Schimel, D. S., Parazoo, N. C., Jiang, Z., Lee, M., Bloom, A. A., Wunch, D., Frankenberg, C., & Sun, Y. (2017). Contrasting carbon cycle responses of the tropical continents to the 2015–2016 El Niño. *Science*, *358*(6360), eaam5690.

Liu, L., Guan, L., & Liu, X. (2017). Directly estimating diurnal changes in GPP for C3 and C4 crops using far-red sun-induced chlorophyll fluorescence. *Agricultural and Forest Meteorology*, *232*, 1–9. https://doi.org/10.1016/j.agrformet.2016.06.014

Liu, L., Gudmundsson, L., Hauser, M., Qin, D., Li, S., & Seneviratne, S. I. (2020). Soil moisture dominates dryness stress on ecosystem production globally. *Nature Communications*, *11*(1), 4892. https://doi.org/10.1038/s41467-020-18631-1

Liu, Z., Ballantyne, A. P., Poulter, B., Anderegg, W. R. L., Li, W., Bastos, A., & Ciais, P. (2018). Precipitation thresholds regulate net carbon exchange at the continental scale. *Nature Communications*, *9*(1), 3596. https://doi.org/10.1038/s41467-018-05948-1

Liu, Z., Ding, M., He, C., Li, J., & Wu, J. (2019). The impairment of environmental sustainability due to rapid urbanization in the dryland region of northern China. *Landscape and Urban Planning*, *187*, 165–180. https://doi.org/10.1016/j.landurbplan.2018.10.020

Lu, H., Qin, Z., Lin, S., Chen, X., Chen, B., He, B., Wei, J., & Yuan, W. (2022). Large influence of atmospheric vapor pressure deficit on ecosystem production efficiency. *Nature Communications*, *13*(1), 1653. https://doi.org/10.1038/s41467-022-29009-w

Lu, X., Liu, Z., An, S., Miralles, D. G., Maes, W., Liu, Y., & Tang, J. (2018). Potential of solar-induced chlorophyll fluorescence to estimate transpiration in a temperate forest. *Agricultural and Forest Meteorology*, *252*, 75–87.

Lu, X., Liu, Z., Zhao, F., & Tang, J. (2020). Comparison of total emitted solar-induced chlorophyll fluorescence (SIF) and top-of-canopy (TOC) SIF in estimating photosynthesis. *Remote Sensing of Environment*, *251*, 112083. https://doi.org/10.1016/j.rse.2020.112083

MacArthur, A., Robinson, I., Rossini, M., Davis, N., & MacDonald, K. (2014). *A dual-field-of-view spectrometer system for reflectance and fluorescence measurements (Piccolo Doppio) and correction of etaloning*. In Proceedings of the fifth international workshop on remote sensing of vegetation fluorescence, European Space Agency, Fifth International Workshop on Remote Sensing of Vegetation Fluorescence.

MacBean, N., Maignan, F., Bacour, C., Lewis, P., Peylin, P., Guanter, L., Köhler, P., Gómez-Dans, J., & Disney, M. (2018). Strong constraint on modelled global carbon uptake using solar-induced chlorophyll fluorescence data. *Scientific Reports*, *8*, 1973. https://doi.org/10.1038/s41598-018-20024-w

Maes, W. H., Pagán, B. R., Martens, B., Gentine, P., Guanter, L., Steppe, K., Verhoest, N. E. C., Dorigo, W., Li, X., Xiao, J., & Miralles, D. G. (2020). Sun-induced fluorescence closely linked to ecosystem transpiration as evidenced by satellite data and radiative transfer models. *Remote Sensing of Environment*, *249*, 112030. https://doi.org/10.1016/j.rse.2020.112030

Magney, T. S., Barnes, M. L., & Yang, X. (2020). On the covariation of chlorophyll fluorescence and photosynthesis across scales. *Geophysical Research Letters*, *47*(23), e2020GL091098. https://doi.org/10.1029/2020GL091098

Magney, T. S., Bowling, D. R., Logan, B. A., Grossmann, K., Stutz, J., Blanken, P. D., Burns, S. P., Cheng, R., Garcia, M. A., Köhler, P., Lopez, S., Parazoo, N. C., Raczka, B., Schimel, D., & Frankenberg, C. (2019). Mechanistic evidence for tracking the seasonality of photosynthesis with solar-induced fluorescence. *Proceedings of the National Academy of Sciences of the United States of America*, *116*(24), 11640–11645. https://doi.org/10.1073/pnas.1900278116

Magney, T. S., Frankenberg, C., Fisher, J. B., Sun, Y., North, G. B., Davis, T. S., Kornfeld, A., & Siebke, K. (2017). Connecting active to passive fluorescence with photosynthesis: A method for evaluating remote sensing measurements of Chl fluorescence. *New Phytologist*, *215*, 1594–1608. https://doi.org/10.1111/nph.14662

Mahlein, A. K., Kuska, M. T., Thomas, S., Wahabzada, M., Behmann, J., Rascher, U., & Kersting, K. (2019). Quantitative and qualitative phenotyping of disease resistance of crops by hyperspectral sensors: Seamless interlocking of phytopathology, sensors, and machine learning is needed! *Current Opinion in Plant Biology*, *50*, 156–162. https://doi.org/10.1016/J.PBI.2019.06.007

Mao, J., Fu, W., Shi, X., Ricciuto, D. M., Fisher, J. B., Dickinson, R. E., Wei, Y., Shem, W., Piao, S., & Wang, K. (2015). Disentangling climatic and anthropogenic controls on global terrestrial evapotranspiration trends. *Environmental Research Letters*, *10*(9), 94008.

Marrs, J. K., Jones, T. S., Allen, D. W., & Hutyra, L. R. (2021). Instrumentation sensitivities for tower-based solar-induced fluorescence measurements. *Remote Sensing of Environment*, *259*, 112413. https://doi.org/10.1016/j.rse.2021.112413

Marrs, J. K., Reblin, J. S., Logan, B. A., Allen, D. W., Reinmann, A. B., Bombard, D. M., Tabachnik, D., & Hutyra, L. R. (2020). Solar-induced fluorescence does not track photosynthetic carbon assimilation following induced stomatal closure. *Geophysical Research Letters*, *47*(15), e02101. https://doi.org/10.1029/2020GL087956

Martini, D., Sakowska, K., Wohlfahrt, G., Pacheco-Labrador, J., van der Tol, C., Porcar-Castell, A., Magney, T. S., Carrara, A., Colombo, R., El-Madany, T. S., Gonzalez-Cascon, R., Martín, M. P., Julitta, T., Moreno, G., Rascher, U., Reichstein, M., Rossini, M., & Migliavacca, M. (2022). Heatwave breaks down the linearity between sun-induced fluorescence and gross primary production. *The New Phytologist*, *233*(6), 2415–2428. https://doi.org/10.1111/nph.17920

McBride, L., Barrett, C. B., Browne, C., Hu, L., Liu, Y., Matteson, D. S., Sun, Y., & Wen, J. (2022). Predicting poverty and malnutrition for targeting, mapping, monitoring, and early warning. *Applied Economic Perspectives and Policy*, *44*(2), 879–892. https://doi.org/10.1002/aepp.13175

Meeker, E. W., Magney, T. S., Bambach, N., Momayyezi, M., & McElrone, A. J. (2021). Modification of a gas exchange system to measure active and passive chlorophyll fluorescence simultaneously under field conditions. *AoB Plants*, *13*(1), laa066. https://doi.org/10.1093/aobpla/plaa066

Mengistu, A. G., Tsidu, G. M., Koren, G., Kooreman, M. L., Folkert Boersma, K., Tagesson, T., Ardö, J., Nouvellon, Y., & Peters, W. (2020). Sun-induced fluorescence and near infrared reflectance of vegetation track the seasonal dynamics of gross primary production over Africa. *Biogeosciences*. https://doi.org/10.5194/bg-2020-242

Meroni, M., & Colombo, R. (2006). Leaf level detection of solar induced chlorophyll fluorescence by means of a subnanometer resolution spectroradiometer. *Remote Sensing of Environment*, *103*(4), 438–448. https://doi.org/10.1016/j.rse.2006.03.016

Miao, G., Guan, K., Yang, X., Bernacchi, C. J., Berry, J. A., DeLucia, E. H., Wu, J., Moore, C. E., Meacham, K., & Cai, Y. (2018). Sun-induced chlorophyll fluorescence, photosynthesis, and light use efficiency of a soybean Field from seasonally continuous measurements. *Journal of Geophysical Research: Biogeosciences*, *123*(2), 610–623.

Migliavacca, M., Perez-Priego, O., Rossini, M., El-Madany, T. S., Moreno, G., van der Tol, C., Rascher, U., Berninger, A., Bessenbacher,

V., Burkart, A., Carrara, A., Fava, F., Guan, J. H., Hammer, T. W., Henkel, K., Juarez-Alcalde, E., Julitta, T., Kolle, O., Martín, M. P., … Reichstein, M. (2017). Plant functional traits and canopy structure control the relationship between photosynthetic CO_2 uptake and far-red sun-induced fluorescence in a Mediterranean grassland under different nutrient availability. *New Phytologist*, *214*(3), 1078–1091. https://doi.org/10.1111/nph.14437

Miralles, D. G., Jiménez, C., Jung, M., Michel, D., Ershadi, A., McCabe, M. F., Hirschi, M., Martens, B., Dolman, A. J., & Fisher, J. B. (2016). The WACMOS-ET project-part 2: Evaluation of global terrestrial evaporation data sets. *Hydrology and Earth System Sciences*, *20*(2), 823–842.

Mishra, V., Cherkauer, K. A., & Shukla, S. (2010). Assessment of drought due to historic climate variability and projected future climate change in the Midwestern United States. *Journal of Hydrometeorology*, *11*(1), 46–68. https://doi.org/10.1175/2009JHM1156.1

Mohammadi, K., Jiang, Y., & Wang, G. (2022). Flash drought early warning based on the trajectory of solar-induced chlorophyll fluorescence. *Proceedings of the National Academy of Sciences of the United States of America*, *119*(32), e2202767119. https://doi.org/10.1073/pnas.2202767119

Monteith, J. L. (1965). Evaporation and environment. *Symposia of the Society for Experimental Biology*, *19*, 205–234.

Montzka, S. A., Calvert, P., Hall, B. D., Elkins, J. W., Conway, T. J., Tans, P. P., & Sweeney, C. S. (2007). On the global distribution, seasonality, and budget of atmospheric carbonyl sulfide (COS) and some similarities to CO_2. *Journal of Geophysical Research Atmospheres*, *112*(9). https://doi.org/10.1029/2006JD007665

Murchie, E. H., Kefauver, S., Araus, J. L., Muller, O., Rascher, U., Flood, P. J., & Lawson, T. (2018). Measuring the dynamic photosynthome. *Annals of Botany*, *122*(2), 207–220. https://doi.org/10.1093/aob/mcy087

Naethe, P., Julitta, T., Chang, C. Y.-Y., Burkart, A., Migliavacca, M., Guanter, L., & Rascher, U. (2022). A precise method unaffected by atmospheric reabsorption for ground-based retrieval of red and far-red sun-induced chlorophyll fluorescence. *Agricultural and Forest Meteorology*, *325*, 109152. https://doi.org/10.1016/j.agrformet.2022.109152

Norton, A. J., Rayner, P. J., Koffi, E. N., Scholze, M., Silver, J. D., & Wang, Y.-P. (2019). Estimating global gross primary productivity using chlorophyll fluorescence and a data assimilation system with the BETHY-SCOPE model. *Biogeosciences*, *16*(15), 3069–3093. https://doi.org/10.5194/bg-16-3069-2019

Novick, K. A., Ficklin, D. L., Stoy, P. C., Williams, C. A., Bohrer, G., Oishi, A. C., Papuga, S. A., Blanken, P. D., Noormets, A., Sulman, B. N., Scott, R. L., Wang, L., & Phillips, R. P. (2016). The increasing importance of atmospheric demand for ecosystem water and carbon fluxes. *Nature Climate Change*, *6*(11), 1023–1027. https://doi.org/10.1038/nclimate3114

Oshio, H., Yoshida, Y., & Matsunaga, T. (2019). On the zero-level offset in the GOSAT TANSO-FTS O_2 a band and the quality of solar-induced chlorophyll fluorescence (SIF): Comparison of SIF between GOSAT and OCO-2. *Atmospheric Measurement Techniques*, *12*(12), 6721–6735. https://doi.org/10.5194/amt-12-6721-2019

Pacheco-Labrador, J., Hueni, A., Mihai, L., Sakowska, K., Julitta, T., Kuusk, J., Sporea, D., Alonso, L., Burkart, A., Cendrero-Mateo, M. P., Aasen, H., Goulas, Y., & Arthur, A. (2019). Sun-induced chlorophyll fluorescence I: Instrumental considerations for proximal Spectroradiometers. *Remote Sensing*, *11*(8), 960. https://doi.org/10.3390/rs11080960

Parazoo, N. C., Bowman, K., Fisher, J. B., Frankenberg, C., Jones, D. B. A., Cescatti, A., Pérez-Priego, Ó., Wohlfahrt, G., & Montagnani, L. (2014). Terrestrial gross primary production inferred from satellite fluorescence and vegetation models. *Global Change Biology*, *20*(10), 3103–3121.

Parazoo, N. C., Bowman, K., Frankenberg, C., Lee, J. E., Fisher, J. B., Worden, J., Jones, D. B. A., Berry, J., Collatz, G. J., Baker, I. T., Jung, M., Liu, J., Osterman, G., O'Dell, C., Sparks, A., Butz, A., Guerlet, S., Yoshida, Y., Chen, H., & Gerbig, C. (2013). Interpreting seasonal changes in the carbon balance of southern Amazonia using measurements of XCO_2 and chlorophyll fluorescence from GOSAT. *Geophysical Research Letters*, *40*(11), 2829–2833. https://doi.org/10.1002/grl.50452

Parazoo, N. C., Frankenberg, C., Köhler, P., Joiner, J., Yoshida, Y., Magney, T., Sun, Y., & Yadav, V. (2019). Towards a harmonized long-term Spaceborne record of far-red solar-induced fluorescence. *Journal of Geophysical Research: Biogeosciences*, *124*, 2518–2539. https://doi.org/10.1029/2019JG005289

Parazoo, N. C., Magney, T., Norton, A., Raczka, B., Bacour, C., Maignan, F., Baker, I., Zhang, Y., Qiu, B., Shi, M., MacBean, N., Bowling, D. R., Burns, S. P., Blanken, P. D., Stutz, J., Grossmann, K., & Frankenberg, C. (2020). Wide discrepancies in the magnitude and direction of modeled solar-induced chlorophyll fluorescence in response to light conditions. *Biogeosciences*, *17*(13), 3733–3755. https://doi.org/10.5194/bg-17-3733-2020

Paschalis, A., Chakraborty, T. C., Fatichi, S., Meili, N., & Manoli, G. (2021). Urban forests as Main regulator of the evaporative cooling effect in cities. *AGU Advances*, *2*(2). https://doi.org/10.1029/2020av000303

Peng, B., Guan, K., Zhou, W., Jiang, C., Frankenberg, C., Sun, Y., He, L., & Köhler, P. (2020). Assessing the benefit of satellite-based solar-induced chlorophyll fluorescence in crop yield prediction. *International Journal of Applied Earth Observation and Geoinformation*, *90*, 102126. https://doi.org/10.1016/j.jag.2020.102126

Piao, S., Friedlingstein, P., Ciais, P., de Noblet-Ducoudré, N., Labat, D., & Zaehle, S. (2007). Changes in climate and land use have a larger direct impact than rising CO_2 on global river runoff trends. *Proceedings of the National Academy of Sciences of the United States of America*, *104*(39), 15242–15247.

Piao, S., Wang, X., Wang, K., Li, X., Bastos, A., Canadell, J. G., Ciais, P., Friedlingstein, P., & Sitch, S. (2020). Interannual variation of terrestrial carbon cycle: Issues and perspectives. *Global Change Biology*, *26*(1), 300–318. https://doi.org/10.1111/gcb.14884

Pierrat, Z., Magney, T., Parazoo, N. C., Grossmann, K., Bowling, D. R., Seibt, U., Johnson, B., Helgason, W., Barr, A., Bortnik, J., Norton, A., Maguire, A., Frankenberg, C., & Stutz, J. (2022). Diurnal and seasonal dynamics of solar-induced chlorophyll fluorescence, vegetation indices, and gross primary productivity in the boreal forest. *Journal of Geophysical Research—Biogeosciences*, *127*(2). https://doi.org/10.1029/2021jg006588

Pierrat, Z., Nehemy, M. F., Roy, A., Magney, T., Parazoo, N. C., Laroque, C., Pappas, C., Sonnentag, O., Grossmann, K., Bowling, D. R., Seibt, U., Ramirez, A., Johnson, B., Helgason, W., Barr, A., & Stutz, J. (2021). Tower-based remote sensing reveals mechanisms behind a two-phased spring transition in a mixed-species boreal forest. *Journal of Geophysical Research: Biogeosciences*, *126*(5), e2020JG006191. https://doi.org/10.1029/2020JG006191

Plascyk, J. A., & Gabriel, F. C. (1975). The Fraunhofer line discriminator MKII an airborne instrument for precise and standardized ecological luminescence measurement. *IEEE Transactions on Instrumentation and Measurement*, *24*(4), 306–313.

Platt, U., & Stutz, J. (2008). *Differential absorption spectroscopy BT—Differential optical absorption spectroscopy: Principles and applications*. Springer. https://doi.org/10.1007/978-3-540-75776-4_6

Poblete, T., Camino, C., Beck, P. S. A., Hornero, A., Kattenborn, T., Saponari, M., Boscia, D., Navas-Cortes, J. A., & Zarco-Tejada, P. J. (2020). Detection of *Xylella fastidiosa* infection symptoms with airborne multispectral and thermal imagery: Assessing bandset reduction performance from hyperspectral analysis. *ISPRS Journal of Photogrammetry and Remote Sensing*, *162*, 27–40. https://doi.org/10.1016/j.isprsjprs.2020.02.010

Poblete, T., Navas-Cortes, J. A., Camino, C., Calderon, R., Hornero, A., Gonzalez-Dugo, V., Landa, B. B., & Zarco-Tejada, P. J. (2021). Discriminating *Xylella fastidiosa* from *Verticillium dahliae* infections

in olive trees using thermal- and hyperspectral-based plant traits. *ISPRS Journal of Photogrammetry and Remote Sensing*, *179*, 133–144. https://doi.org/10.1016/j.isprsjprs.2021.07.014

Porcar-Castell, A., Malenovský, Z., Magney, T., Van Wittenberghe, S., Fernández-Marín, B., Maignan, F., Zhang, Y., Maseyk, K., Atherton, J., Albert, L. P., Robson, T. M., Zhao, F., Garcia-Plazaola, J. I., Ensminger, I., Rajewicz, P. A., Grebe, S., Tikkanen, M., Kellner, J. R., Ihalainen, J. A., … Logan, B. (2021). Chlorophyll a fluorescence illuminates a path connecting plant molecular biology to earth-system science. *Nature Plants*, *7*(8), 998–1009. https://doi.org/10.1038/s41477-021-00980-4

Porcar-Castell, A., Tyystjärvi, E., Atherton, J., Van Der Tol, C., Flexas, J., Pfündel, E. E., Moreno, J., Frankenberg, C., & Berry, J. A. (2014). Linking chlorophyll a fluorescence to photosynthesis for remote sensing applications: Mechanisms and challenges. *Journal of Experimental Botany*, *65*, 4065–4095. https://doi.org/10.1093/jxb/eru191

Qiu, B., Ge, J., Guo, W., Pitman, A. J., & Mu, M. (2020). Responses of Australian dryland vegetation to the 2019 heat wave at a subdaily scale. *Geophysical Research Letters*, *47*(4), e2019GL086569. https://doi.org/10.1029/2019GL086569

Quirós-Vargas, J., Romanelli, T. L., Rascher, U., & Agüero, J. (2020). Sustainability performance through technology adoption: A case study of land leveling in a Paddy Field. *Agronomy*, *10*(11), 1681. https://doi.org/10.3390/agronomy10111681

Raczka, B., Porcar-Castell, A., Magney, T., Lee, J. E., Köhler, P., Frankenberg, C., Grossmann, K., Logan, B. A., Stutz, J., Blanken, P. D., Burns, S. P., Duarte, H., Yang, X., Lin, J. C., & Bowling, D. R. (2019). Sustained nonphotochemical quenching shapes the seasonal pattern of solar-induced fluorescence at a high-elevation Evergreen Forest. *Journal of Geophysical Research: Biogeosciences*, *124*(7), 2005–2020. https://doi.org/10.1029/2018JG004883

Rascher, U., Alonso, L., Burkart, A., Cilia, C., Cogliati, S., Colombo, R., Damm, A., Drusch, M., Guanter, L., Hanus, J., Hyvärinen, T., Julitta, T., Jussila, J., Kataja, K., Kokkalis, P., Kraft, S., Kraska, T., Matveeva, M., Moreno, J., … Zemek, F. (2015). Sun-induced fluorescence—A new probe of photosynthesis: First maps from the imaging spectrometer *HyPlant*. *Global Change Biology*, *21*(12), 4673–4684. https://doi.org/10.1111/gcb.13017

Rascher, U., Bobich, E. G., Lin, G. H., Walter, A., Morris, T., Naumann, M., Nichol, C. J., Pierce, D., Bil, K., Kudeyarov, V., & Berry, J. A. (2004). Functional diversity of photosynthesis during drought in a model tropical rainforest—The contributions of leaf area, photosynthetic electron transport and stomatal conductance to reduction in net ecosystem carbon exchange. *Plant, Cell and Environment*, *27*(10), 1239–1256. https://doi.org/10.1111/j.1365-3040.2004.01231.x

Reichstein, M., Falge, E., Baldocchi, D., Papale, D., Aubinet, M., Berbigier, P., Bernhofer, C., Buchmann, N., Gilmanov, T., Granier, A., Grünwald, T., Havránková, K., Ilvesniemi, H., Janous, D., Knohl, A., Laurila, T., Lohila, A., Loustau, D., Matteucci, G., … Valentini, R. (2005). On the separation of net ecosystem exchange into assimilation and ecosystem respiration: Review and improved algorithm. *Global Change Biology*, *11*, 1424–1439. https://doi.org/10.1111/j.1365-2486.2005.001002.x

Sanders, A. F. J., Verstraeten, W. W., Kooreman, M. L., van Leth, T. C., Beringer, J., & Joiner, J. (2016). Spaceborne Sun-induced vegetation fluorescence time series from 2007 to 2015 evaluated with Australian flux tower measurements. *Remote Sensing*, *8*, 895. https://doi.org/10.3390/rs8110895

Sang, Y., Huang, L., Wang, X., Keenan, T. F., Wang, C., & He, Y. (2021). Comment on "recent global decline of CO_2 fertilization effects on vegetation photosynthesis.". *Science*, *373*(6562), eabg4420. https://doi.org/10.1126/science.abg4420

Schächtl, J., Huber, G., Maidl, F.-X., Sticksel, E., Schulz, J., & Haschberger, P. (2005). Laser-induced chlorophyll fluorescence measurements for detecting the nitrogen status of wheat (*Triticum aestivum* L.) canopies. *Precision Agriculture*, *6*(2), 143–156. https://doi.org/10.1007/s11119-004-1031-y

Schimel, D., Pavlick, R., Fisher, J. B., Asner, G. P., Saatchi, S., Townsend, P., Miller, C., Frankenberg, C., Hibbard, K., & Cox, P. (2015). Observing terrestrial ecosystems and the carbon cycle from space. *Global Change Biology*, *21*(5), 1762–1776.

Schimel, D., & Schneider, F. D. (2019). Flux towers in the sky: Global ecology from space. *New Phytologist*, *224*(2), 570–584. https://doi.org/10.1111/nph.15934

Seibt, U., Kesselmeier, J., Sandoval-Soto, L., Kuhn, U., & Berry, J. A. (2010). A kinetic analysis of leaf uptake of COS and its relation to transpiration, photosynthesis and carbon isotope fractionation. *Biogeosciences*, *7*(1), 333–341. https://doi.org/10.5194/bg-7-333-2010

Seneviratne, S. I., Zhang, X., Adnan, M., Badi, W., Dereczynski, C., Di Luca, A., Ghosh, S., Iskandar, I., Kossin, J., Lewis, S., Otto, F., Pinto, I., Satoh, M., Vicente-Serrano, S. M., Wehner, M., & Zhou, B. (2021). *Weather and climate extreme events in a changing climate*. In Climate change 2021: The physical science basis. Contribution of Working Group I to the sixth assessment report of the Intergovernmental Panel on Climate Change https://doi.org/10.1017/9781009157896.013

Serbin, S. P., Singh, A., McNeil, B. E., Kingdon, C. C., & Townsend, P. A. (2016). Spectroscopic determination of leaf morphological and biochemical traits for northern temperate and boreal tree species. *Ecological Applications*, *24*(7), 1651–1669. https://doi.org/10.1890/13-2110.1

Shan, N., Zhang, Y., Chen, J. M., Ju, W., Migliavacca, M., Peñuelas, J., Yang, X., Zhang, Z., Nelson, J. A., & Goulas, Y. (2021). A model for estimating transpiration from remotely sensed solar-induced chlorophyll fluorescence. *Remote Sensing of Environment*, *252*, 112134. https://doi.org/10.1016/j.rse.2020.112134

Sloat, L. L., Lin, M., Butler, E. E., Johnson, D., Holbrook, N. M., Huybers, P. J., Lee, J.-E., & Mueller, N. D. (2021). Evaluating the benefits of chlorophyll fluorescence for in-season crop productivity forecasting. *Remote Sensing of Environment*, *260*, 112478. https://doi.org/10.1016/j.rse.2021.112478

Smith, W. K., Biederman, J. A., Scott, R. L., Moore, D. J. P., He, M., Kimball, J. S., Yan, D., Hudson, A., Barnes, M. L., MacBean, N., Fox, A. M., & Litvak, M. E. (2018). Chlorophyll fluorescence better captures seasonal and interannual gross primary productivity dynamics across dryland ecosystems of southwestern North America. *Geophysical Research Letters*, *45*(2), 748–757. https://doi.org/10.1002/2017GL075922

Smith, W. K., Reed, S. C., Cleveland, C. C., Ballantyne, A. P., Anderegg, W. R. L., Wieder, W. R., Liu, Y. Y., & Running, S. W. (2016). Large divergence of satellite and Earth System Model estimates of global terrestrial CO_2 fertilization. *Nature Climate Change*, *6*(3), 306–310. https://doi.org/10.1038/NCLIMATE2879

Somkuti, P., O'Dell, C. W., Crowell, S., Köhler, P., McGarragh, G. R., Cronk, H. Q., & Burgh, E. B. (2021). Solar-induced chlorophyll fluorescence from the geostationary carbon cycle observatory (GeoCarb): An extensive simulation study. *Remote Sensing of Environment*, *263*, 112565. https://doi.org/10.1016/j.rse.2021.112565

Song, L., Guanter, L., Guan, K., You, L., Huete, A., Ju, W., & Zhang, Y. (2018). Satellite sun-induced chlorophyll fluorescence detects early response of winter wheat to heat stress in the Indian indo-Gangetic Plains. *Global Change Biology*, *24*(9), 4023–4037. https://doi.org/10.1111/gcb.14302

Song, Y., Wang, J., & Wang, L. (2020). Satellite solar-induced chlorophyll fluorescence reveals heat stress impacts on wheat yield in India. *Remote Sensing*, *12*(20). https://doi.org/10.3390/rs12203277

Song, Y., Wang, L., & Wang, J. (2021). Improved understanding of the spatially-heterogeneous relationship between satellite solar-induced chlorophyll fluorescence and ecosystem productivity.

Ecological Indicators, *129*, 107949. https://doi.org/10.1016/j.ecolind.2021.107949

Stavros, E. N., Schimel, D., Pavlick, R., Serbin, S., Swann, A., Duncanson, L., Fisher, J. B., Fassnacht, F., Ustin, S., Dubayah, R., Schweiger, A., & Wennberg, P. (2017). ISS observations offer insights into plant function. *Nature Ecology & Evolution*, *1*(7), 0194. https://doi.org/10.1038/s41559-017-0194

Stoy, P. C., El-Madany, T. S., Fisher, J. B., Gentine, P., Gerken, T., Good, S. P., Klosterhalfen, A., Liu, S., Miralles, D. G., Perez-Priego, O., Rigden, A. J., Skaggs, T. H., Wohlfahrt, G., Anderson, R. G., Coenders-Gerrits, A. M. J., Jung, M., Maes, W. H., Mammarella, I., Mauder, M., … Wolf, S. (2019). Reviews and syntheses: Turning the challenges of partitioning ecosystem evaporation and transpiration into opportunities. *Biogeosciences*, *16*(19), 3747–3775. https://doi.org/10.5194/BG-16-3747-2019

Sun, Y., Frankenberg, C., Jung, M., Joiner, J., Guanter, L., Köhler, P., & Magney, T. (2018). Overview of solar-induced chlorophyll fluorescence (SIF) from the orbiting carbon Observatory-2: Retrieval, cross-mission comparison, and global monitoring for GPP. *Remote Sensing of Environment*, *209*, 808–823. https://doi.org/10.1016/J.RSE.2018.02.016

Sun, Y., Frankenberg, C., Wood, J. D., Schimel, D. S., Jung, M., Guanter, L., Drewry, D. T., Verma, M., Porcar-Castell, A., Griffis, T. J., Magney, T. S., Kohler, P., Evans, B., & Yuen, K. (2017). OCO-2 advances photosynthesis observation from space via solar-induced chlorophyll fluorescence. *Science*, *358*(6360), eaam5747. https://doi.org/10.1126/science.aam5747

Sun, Y., Fu, R., Dickinson, R., Joiner, J., Frankenberg, C., Gu, L., Xia, Y., & Fernando, N. (2015). Drought onset mechanisms revealed by satellite solar-induced chlorophyll fluorescence: Insights from two contrasting extreme events. *Journal of Geophysical Research G: Biogeosciences*, *120*(11), 2427–2440.

Sun, Y., Wen, J., Gu, L., Joiner, J., Chang, C. Y.-Y., van der Tol, C., Porcar-Castell, A., Magney, T. S., Wang, L., Hu, L., Rascher, U., Zarco-Tejada, P. J., Barrett, C. B., Lai, J., Han, J., & Luo, Z. (2023). From remotely sensed solar-induced chlorophyll fluorescence to ecosystem structure, function, and service: Part I—Harnessing theory. *Global Change Biology*. https://doi.org/10.1111/gcb.16634

Tagliabue, G., Panigada, C., Celesti, M., Cogliati, S., Colombo, R., Migliavacca, M., Rascher, U., Rocchini, D., Schüttemeyer, D., & Rossini, M. (2020). Sun–induced fluorescence heterogeneity as a measure of functional diversity. *Remote Sensing of Environment*, *247*, 111934. https://doi.org/10.1016/j.rse.2020.111934

Tubuxin, B., Rahimzadeh-Bajgiran, P., Ginnan, Y., Hosoi, F., & Omasa, K. (2015). Estimating chlorophyll content and photochemical yield of photosystem II (ΦPSII) using solar-induced chlorophyll fluorescence measurements at different growing stages of attached leaves. *Journal of Experimental Botany*, *66*(18), 5595–5603. https://doi.org/10.1093/jxb/erv272

Turner, A. J., Köhler, P., Magney, T. S., Frankenberg, C., Fung, I., & Cohen, R. C. (2020). A double peak in the seasonality of California's photosynthesis as observed from space. *Biogeosciences*, *17*(2), 405–422. https://doi.org/10.5194/bg-17-405-2020

van der Tol, C., Berry, J. A., Campbell, P. K. E., & Rascher, U. (2014). Models of fluorescence and photosynthesis for interpreting measurements of solar-induced chlorophyll fluorescence. *Journal of Geophysical Research G: Biogeosciences*, *119*(12), 2312–2327. https://doi.org/10.1002/2014JG002713

van Schaik, E., Kooreman, M. L., Stammes, P., Gijsbert Tilstra, L., Tuinder, O. N. E., Sanders, A. F. J., Verstraeten, W. W., Lang, R., Cacciari, A., Joiner, J., Peters, W., & Folkert Boersma, K. (2020). Improved SIFTER v2 algorithm for long-term GOME-2A satellite retrievals of fluorescence with a correction for instrument degradation. *Atmospheric Measurement Techniques*, *13*(8), 4295–4315. https://doi.org/10.5194/amt-13-4295-2020

Van Wittenberghe, S., Alonso, L., Malenovský, Z., & Moreno, J. (2019). In vivo photoprotection mechanisms observed from leaf spectral absorbance changes showing VIS–NIR slow-induced conformational pigment bed changes. *Photosynthesis Research*, *142*(3), 283–305. https://doi.org/10.1007/s11120-019-00664-3

Van Wittenberghe, S., Laparra, V., García-Plazaola, J. I., Fernández-Marín, B., Porcar-Castell, A., & Moreno, J. (2021). Combined dynamics of the 500–600 nm leaf absorption and chlorophyll fluorescence changes in vivo: Evidence for the multifunctional energy quenching role of xanthophylls. *Biochimica et Biophysica Acta (BBA)—Bioenergetics*, *1862*(2), 148351. https://doi.org/10.1016/j.bbabio.2020.148351

Verrelst, J., Rivera, J. P., van der Tol, C., Magnani, F., Mohammed, G., & Moreno, J. (2015). Global sensitivity analysis of the SCOPE model: What drives simulated canopy-leaving sun-induced fluorescence? *Remote Sens Environment*, *166*, 8–21. https://doi.org/10.1016/j.rse.2015.06.002

von Caemmerer, S. (2000). *Biochemical models of leaf photosynthesis*. In Techniques in Plant Sciences No 2.

Walther, S., Voigt, M., Thum, T., Gonsamo, A., Zhang, Y., Köhler, P., Jung, M., Varlagin, A., & Guanter, L. (2016). Satellite chlorophyll fluorescence measurements reveal large-scale decoupling of photosynthesis and greenness dynamics in boreal evergreen forests. *Global Change Biology*, *22*(9), 2979–2996. https://doi.org/10.1111/gcb.13200

Wang, C., Beringer, J., Hutley, L. B., Cleverly, J., Li, J., Liu, Q., & Sun, Y. (2019). Phenology dynamics of dryland ecosystems along the North Australian tropical transect revealed by satellite solar-induced chlorophyll fluorescence. *Geophysical Research Letters*, *46*(10), 2019GL082716. https://doi.org/10.1029/2019GL082716

Wang, J., Zeng, N., & Wang, M. (2016). Interannual variability of the atmospheric CO_2 growth rate: Roles of precipitation and temperature. *Biogeosciences*, *13*(8), 2339–2352. https://doi.org/10.5194/bg-13-2339-2016

Wang, K., & Dickinson, R. E. (2012). A review of global terrestrial evapotranspiration: Observation, modeling, climatology, and climatic variability. *Reviews of Geophysics*, *50*, RG2005. https://doi.org/10.1029/2011RG000373

Wang, L., Good, S. P., & Caylor, K. K. (2014). Global synthesis of vegetation control on evapotranspiration partitioning. *Geophysical Research Letters*, *41*(19), 6753–6757.

Wang, N., Suomalainen, J., Bartholomeus, H., Kooistra, L., Masiliūnas, D., & Clevers, J. G. P. W. (2021). Diurnal variation of sun-induced chlorophyll fluorescence of agricultural crops observed from a point-based spectrometer on a UAV. *International Journal of Applied Earth Observation and Geoinformation*, *96*, 102276. https://doi.org/10.1016/j.jag.2020.102276

Wang, S., Ju, W., Peñuelas, J., Cescatti, A., Zhou, Y., Fu, Y., Huete, A., Liu, M., & Zhang, Y. (2019). Urban–rural gradients reveal joint control of elevated CO_2 and temperature on extended photosynthetic seasons. *Nature Ecology & Evolution*, *3*(7), 1076–1085. https://doi.org/10.1038/s41559-019-0931-1

Wang, S., Zhang, Y., Ju, W., Chen, J. M., Ciais, P., Cescatti, A., Sardans, J., Janssens, I. A., Wu, M., Berry, J. A., Campbell, E., Fernández-Martínez, M., Alkama, R., Sitch, S., Friedlingstein, P., Smith, W. K., Yuan, W., He, W., Lombardozzi, D., … Peñuelas, J. (2020). Recent global decline of CO_2 fertilization effects on vegetation photosynthesis. *Science*, *370*(6522), 1295–1300. https://doi.org/10.1126/science.abb7772

Wang, S., Zhang, Y., Ju, W., Wu, M., Liu, L., He, W., & Peñuelas, J. (2022). Temporally corrected long-term satellite solar-induced fluorescence leads to improved estimation of global trends in vegetation photosynthesis during 1995–2018. *ISPRS Journal of Photogrammetry and Remote Sensing*, *194*, 222–234. https://doi.org/10.1016/j.isprsjprs.2022.10.018

Wang, X., Biederman, J. A., Knowles, J. F., Scott, R. L., Turner, A. J., Dannenberg, M. P., Köhler, P., Frankenberg, C., Litvak, M. E., Flerchinger, G. N., Law, B. E., Kwon, H., Reed, S. C., Parton, W. J., Barron-Gafford, G. A., & Smith, W. K. (2022). Satellite solar-induced chlorophyll fluorescence and near-infrared reflectance capture complementary aspects of dryland vegetation productivity dynamics. *Remote Sensing of Environment*, *270*, 112858. https://doi.org/10.1016/j.rse.2021.112858

Wang, Y., Suarez, L., Qian, X., Poblete, T., Gonzalez-Dugo, V., Ryu, D., & Zarco-Tejada, P. J. (2021). *Assessing the contribution of airborne-retrieved chlorophyll fluorescence for nitrogen assessment IN almond orchards*. International Geoscience and Remote Sensing Symposium (IGARSS), 5853–5856 https://doi.org/10.1109/IGARSS47720.2021.9554648

Wang, Z., Chlus, A., Geygan, R., Ye, Z., Zheng, T., Singh, A., Couture, J. J., Cavender-Bares, J., Kruger, E. L., & Townsend, P. A. (2020). Foliar functional traits from imaging spectroscopy across biomes in eastern North America. *The New Phytologist*, *228*(2), 494–511. https://doi.org/10.1111/nph.16711

Wang, Z., Townsend, P. A., & Kruger, E. L. (2022). Leaf spectroscopy reveals divergent inter- and intra-species foliar trait covariation and trait-environment relationships across NEON domains. *The New Phytologist*, *235*(3), 923–938. https://doi.org/10.1111/nph.18204

Wehr, R., Munger, J. W., McManus, J. B., Nelson, D. D., Zahniser, M. S., Davidson, E. A., Wofsy, S. C., & Saleska, S. R. (2016a). Seasonality of temperate forest photosynthesis and daytime respiration. *Nature*, *534*(7609), 680–683. https://doi.org/10.1038/nature17966

Wei, Z., Yoshimura, K., Wang, L., Miralles, D. G., Jasechko, S., & Lee, X. (2017). Revisiting the contribution of transpiration to global terrestrial evapotranspiration. *Geophysical Research Letters*, *44*(6), 2792–2801.

Wen, J., Köhler, P., Duveiller, G., Parazoo, N. C., Magney, T. S., Hooker, G., Yu, L., Chang, C. Y., & Sun, Y. (2020). A framework for harmonizing multiple satellite instruments to generate a long-term global high spatial-resolution solar-induced chlorophyll fluorescence (SIF). *Remote Sensing of Environment*, *239*, 111644. https://doi.org/10.1016/j.rse.2020.111644

Whelan, M. E., Lennartz, S. T., Gimeno, T. E., Wehr, R., Wohlfahrt, G., Wang, Y., Kooijmans, L. M. J., Hilton, T. W., Belviso, S., Peylin, P., Commane, R., Sun, W., Chen, H., Kuai, L., Mammarella, I., Maseyk, K., Berkelhammer, M., Li, K.-F., Yakir, D., … Elliott Campbell, J. (2018). Reviews and syntheses: Carbonyl sulfide as a multi-scale tracer for carbon and water cycles. *Biogeosciences*, *15*(12), 3625–3657. https://doi.org/10.5194/bg-15-3625-2018

Wohlfahrt, G., Brilli, F., Hörtnagl, L., Xu, X., Bingemer, H., Hansel, A., & Loreto, F. (2012). Carbonyl sulfide (COS) as a tracer for canopy photosynthesis, transpiration and stomatal conductance: Potential and limitations. *Plant, Cell & Environment*, *35*(4), 657–667. https://doi.org/10.1111/j.1365-3040.2011.02451.x

Wohlfahrt, G., Gerdel, K., Migliavacca, M., Rotenberg, E., Tatarinov, F., Müller, J., Hammerle, A., Julitta, T., Spielmann, F. M., & Yakir, D. (2018). Sun-induced fluorescence and gross primary productivity during a heat wave. *Scientific Reports*, *8*(1), 14169. https://doi.org/10.1038/s41598-018-32602-z

Wolanin, A., Rozanov, V. V., Dinter, T., Noël, S., Vountas, M., Burrows, J. P., & Bracher, A. (2015). Global retrieval of marine and terrestrial chlorophyll fluorescence at its red peak using hyperspectral top of atmosphere radiance measurements: Feasibility study and first results. *Remote Sensing of Environment*, *166*, 243–261. https://doi.org/10.1016/j.rse.2015.05.018

Wong, S. C., Cowan, I. R., & Farquhar, G. D. (1979). Stomatal conductance correlates with photosynthetic capacity. *Nature*, *282*(5737), 424–426.

Wu, G., Guan, K., Jiang, C., Peng, B., Kimm, H., Chen, M., Yang, X., Wang, S., Suyker, A. E., Bernacchi, C. J., Moore, C. E., Zeng, Y., Berry, J. A., & Cendrero-Mateo, M. P. (2020). Radiance-based NIRv as a proxy for GPP of corn and soybean. *Environmental Research Letters*, *15*(3), 034009. https://doi.org/10.1088/1748-9326/AB65CC

Wu, J., Su, Y., Chen, X., Liu, L., Yang, X., Gong, F., Zhang, H., Xiong, X., & Zhang, D. (2021). Leaf shedding of Pan-Asian tropical evergreen forests depends on the synchrony of seasonal variations of rainfall and incoming solar radiation. *Agricultural and Forest Meteorology*, *311*, 108691. https://doi.org/10.1016/j.agrformet.2021.108691

Xu, S., Atherton, J., Riikonen, A., Zhang, C., Oivukkamäki, J., MacArthur, A., Honkavaara, E., Hakala, T., Koivumäki, N., Liu, Z., & Porcar-Castell, A. (2021). Structural and photosynthetic dynamics mediate the response of SIF to water stress in a potato crop. *Remote Sensing of Environment*, *263*, 112555. https://doi.org/10.1016/j.rse.2021.112555

Yang, K., Ryu, Y., Dechant, B., Berry, J. A., Hwang, Y., Jiang, C., Kang, M., Kim, J., Kimm, H., Kornfeld, A., & Yang, X. (2018). Sun-induced chlorophyll fluorescence is more strongly related to absorbed light than to photosynthesis at half-hourly resolution in a rice paddy. *Remote Sensing of Environment*, *216*, 658–673. https://doi.org/10.1016/j.rse.2018.07.008

Yang, J., Tian, H., Pan, S., Chen, G., Zhang, B., & Dangal, S. (2018). Amazon drought and forest response: Largely reduced forest photosynthesis but slightly increased canopy greenness during the extreme drought of 2015/2016. *Global Change Biology*, *24*(5), 1919–1934. https://doi.org/10.1111/gcb.14056

Yang, P., Van Der Tol, C., Campbell, P. K. E., & Middleton, E. M. (2021). Unraveling the physical and physiological basis for the solar-induced chlorophyll fluorescence and photosynthesis relationship using continuous leaf and canopy measurements of a corn crop. *Biogeosciences*, *18*(2), 441–465. https://doi.org/10.5194/BG-18-441-2021

Yang, X., Shi, H., Stovall, A., Guan, K., Miao, G., Zhang, Y., Zhang, Y., Xiao, X., Ryu, Y., & Lee, J. E. (2018). FluoSpec 2—An automated field spectroscopy system to monitor canopy solar-induced fluorescence. *Sensors*, *18*. https://doi.org/10.3390/s18072063

Yang, X., Tang, J., Mustard, J. F., Lee, J.-E., Rossini, M., Joiner, J., Munger, J. W., Kornfeld, A., & Richardson, A. D. (2015). Solar-induced chlorophyll fluorescence that correlates with canopy photosynthesis on diurnal and seasonal scales in a temperate deciduous forest. *Geophysical Research Letters*, *42*(8), 2977–2987. https://doi.org/10.1002/2015GL063201

Yoshida, Y., Joiner, J., Tucker, C., Berry, J., Lee, J. E., Walker, G., Reichle, R., Koster, R., Lyapustin, A., & Wang, Y. (2015). The 2010 Russian drought impact on satellite measurements of solar-induced chlorophyll fluorescence: Insights from modeling and comparisons with parameters derived from satellite reflectances. *Remote Sensing of Environment*, *166*, 163–177.

Yu, L., Wen, J., Chang, C. Y., Frankenberg, C., & Sun, Y. (2019). High-resolution global contiguous SIF of OCO-2. *Geophysical Research Letters*, *46*(3), 1449–1458. https://doi.org/10.1029/2018GL081109

Zarco-Tejada, P. J., Camino, C., Beck, P. S. A., Calderon, R., Hornero, A., Hernández-Clemente, R., Kattenborn, T., Montes-Borrego, M., Susca, L., Morelli, M., Gonzalez-Dugo, V., North, P. R. J., Landa, B. B., Boscia, D., Saponari, M., & Navas-Cortes, J. A. (2018). Previsual symptoms of *Xylella fastidiosa* infection revealed in spectral plant-trait alterations. *Nature Plants*, *4*(7), 432–439. https://doi.org/10.1038/s41477-018-0189-7

Zarco-Tejada, P. J., González-Dugo, M. V., & Fereres, E. (2016). Seasonal stability of chlorophyll fluorescence quantified from airborne hyperspectral imagery as an indicator of net photosynthesis in the context of precision agriculture. *Remote Sensing of Environment*, *179*, 89–103. https://doi.org/10.1016/j.rse.2016.03.024

Zarco-Tejada, P. J., González-Dugo, V., & Berni, J. A. J. (2012). Fluorescence, temperature and narrow-band indices acquired from a UAV platform for water stress detection using a micro-hyperspectral imager and a thermal camera. *Remote Sensing of Environment*, *117*, 322–337. https://doi.org/10.1016/j.rse.2011.10.007

Zarco-Tejada, P. J., Morales, A., Testi, L., & Villalobos, F. J. (2013). Spatio-temporal patterns of chlorophyll fluorescence and physiological and structural indices acquired from hyperspectral imagery as compared with carbon fluxes measured with eddy covariance. *Remote Sensing of Environment*, *133*, 102–115. https://doi.org/10.1016/j.rse.2013.02.003

Zarco-Tejada, P. J., Poblete, T., Camino, C., Gonzalez-Dugo, V., Calderon, R., Hornero, A., Hernandez-Clemente, R., Román-Écija, M., Velasco-Amo, M. P., Landa, B. B., Beck, P. S. A., Saponari, M., Boscia, D., & Navas-Cortes, J. A. (2021). Divergent abiotic spectral pathways unravel pathogen stress signals across species. *Nature Communications*, *12*(1), 1–11. https://doi.org/10.1038/s41467-021-26335-3

Zendonadi Dos Santos, N., Piepho, H.-P., Condorelli, G. E., Licieri Groli, E., Newcomb, M., Ward, R., Tuberosa, R., Maccaferri, M., Fiorani, F., Rascher, U., & Muller, O. (2021). High-throughput field phenotyping reveals genetic variation in photosynthetic traits in durum wheat under drought. *Plant, Cell & Environment*, *44*(9), 2858–2878. https://doi.org/10.1111/pce.14136

Zeng, Z., Piao, S., Li, L. Z. X., Zhou, L., Ciais, P., Wang, T., Li, Y., Lian, X., Wood, E. F., Friedlingstein, P., Mao, J., Estes, L. D., Myneni, R. B., Peng, S., Shi, X., Seneviratne, S. I., & Wang, Y. (2017). Climate mitigation from vegetation biophysical feedbacks during the past three decades. *Nature Climate Change*, *7*(6), 432–436. https://doi.org/10.1038/nclimate3299

Zhang, C., Atherton, J., Peñuelas, J., Filella, I., Kolari, P., Aalto, J., Ruhanen, H., Bäck, J., & Porcar-Castell, A. (2019). Do all chlorophyll fluorescence emission wavelengths capture the spring recovery of photosynthesis in boreal evergreen foliage? *Plant, Cell & Environment*, *42*(12), 3264–3279. https://doi.org/10.1111/pce.13620

Zhang, Y., Commane, R., Zhou, S., Williams, A. P., & Gentine, P. (2020). Light limitation regulates the response of autumn terrestrial carbon uptake to warming. *Nature Climate Change*, *10*(8), 739–743. https://doi.org/10.1038/s41558-020-0806-0

Zhang, Y., Guanter, L., Berry, J. A., Joiner, J., van der Tol, C., Huete, A., Gitelson, A., Voigt, M., & Köhler, P. (2014). Estimation of vegetation photosynthetic capacity from space-based measurements of chlorophyll fluorescence for terrestrial biosphere models. *Global Change Biology*, *20*(12), 3727–3742.

Zhang, Y., Guanter, L., Berry, J. A., van der Tol, C., Yang, X., Tang, J., & Zhang, F. (2016). Model-based analysis of the relationship between sun-induced chlorophyll fluorescence and gross primary production for remote sensing applications. *Remote Sensing of Environment*, *187*, 145–155. https://doi.org/10.1016/j.rse.2016.10.016

Zhang, Y., Joiner, J., Alemohammad, S. H., Zhou, S., & Gentine, P. (2018). A global spatially contiguous solar-induced fluorescence (CSIF) dataset using neural networks. *Biogeosciences*, *15*(19), 5779–5800. https://doi.org/10.5194/bg-15-5779-2018

Zhang, Y., Joiner, J., Gentine, P., & Zhou, S. (2018). Reduced solar-induced chlorophyll fluorescence from GOME-2 during Amazon drought caused by dataset artifacts. *Global Change Biology*, *24*(6), 2229–2230. https://doi.org/10.1111/gcb.14134

Zhang, Y., Parazoo, N. C., Williams, A. P., Zhou, S., & Gentine, P. (2020). Large and projected strengthening moisture limitation on end-of-season photosynthesis. *Proceedings of the National Academy of Sciences of the United States of America*, *117*(17), 9216–9222. https://doi.org/10.1073/pnas.1914436117

Zhang, Y., Song, C., Band, L. E., Sun, G., & Li, J. (2017). Reanalysis of global terrestrial vegetation trends from MODIS products: Browning or greening? *Remote Sens Environment*, *191*, 145–155. https://doi.org/10.1016/j.rse.2016.12.018

Zhang, Z., Zhang, Y., Porcar-Castell, A., Joiner, J., Guanter, L., Yang, X., Migliavacca, M., Ju, W., Sun, Z., Chen, S., Martini, D., Zhang, Q., Li, Z., Cleverly, J., Wang, H., & Goulas, Y. (2020). Reduction of structural impacts and distinction of photosynthetic pathways in a global estimation of GPP from space-borne solar-induced chlorophyll fluorescence. *Remote Sensing of Environment*, *240*, 111722. https://doi.org/10.1016/j.rse.2020.111722

Zhou, K., Zhang, Q., Xiong, L., & Gentine, P. (2022). Estimating evapotranspiration using remotely sensed solar-induced fluorescence measurements. *Agricultural and Forest Meteorology*, *314*, 108800. https://doi.org/10.1016/j.agrformet.2021.108800

Zhu, Z., Zeng, H., Myneni, R. B., Chen, C., Zhao, Q., Zha, J., Zhan, S., & MacLachlan, I. (2021). Comment on "recent global decline of CO fertilization effects on vegetation photosynthesis.". *Science*, *373*(6562), eabg5673. https://doi.org/10.1126/science.abg5673

Zuromski, L. M., Bowling, D. R., Köhler, P., Frankenberg, C., Goulden, M. L., Blanken, P. D., & Lin, J. C. (2018). Solar-induced fluorescence detects interannual variation in gross primary production of coniferous forests in the Western United States. *Geophysical Research Letters*, *45*(14), 7184–7193. https://doi.org/10.1029/2018GL077906

SUPPORTING INFORMATION

Additional supporting information can be found online in the Supporting Information section at the end of this article.

How to cite this article: Sun, Y., Wen, J., Gu, L., Joiner, J., Chang, C. Y., van der Tol, C., Porcar-Castell, A., Magney, T., Wang, L., Hu, L., Rascher, U., Zarco-Tejada, P., Barrett, C. B., Lai, J., Han, J., & Luo, Z. (2023). From remotely-sensed solar-induced chlorophyll fluorescence to ecosystem structure, function, and service: Part II—Harnessing data. *Global Change Biology*, *00*, 1–33. https://doi.org/10.1111/gcb.16646